Technological Instrumentation Interface with Industry and The Medical Sector

Cinzia Da Vià, The University of Manchester, UK
& University of Stony Brook, USA

Some Information about myself

- Professor at The University of Manchester (UK)
- Visiting Professor at the University of Stony Brook, New York, USA
- Member of the ATLAS Collaboration at CERN – LHC
- Chief editor Frontiers in Physics, Radiation Detectors and Imaging
- Co-Chair of the EU-ATTRACT Independent Committee
- IEEE WIE International Committee Member 2017-2022
- Member of the IEEE TAB Program on Climate Change
- Distinguished Lecturer and Organizer of the IEEE NPSS Instrumentation School

Scientific Interests:

- ➢ Radiation Detector development : silicon pixels, 3D silicon detectors, fast timing
- ➢ Radiation effects in silicon, “Lazarus effect”
- ➢ 3D printed detectors, Vertical integrated microsystems
- ➢ Quantum Imaging

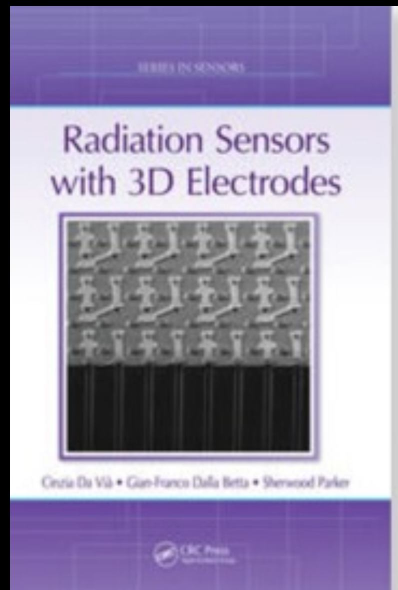

Objectives of these 2h lectures

Cinzia Da Via, The University of Manchester, UK & SUNY USA– 2023

- Synergies between HEP, Medicine and Industry
- Identify the High Energy Physics Instrumentation Assets
- Understand the right requirements for the right applications
    - Medicine but also other fields
- Examples: Accelerators and Detectors
- Summary and a Look at the Future

How things started...

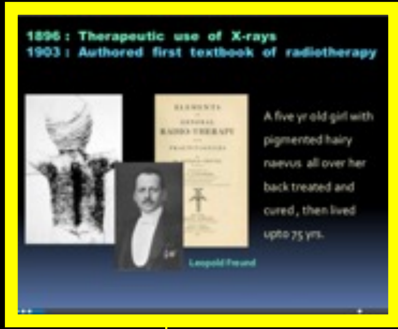

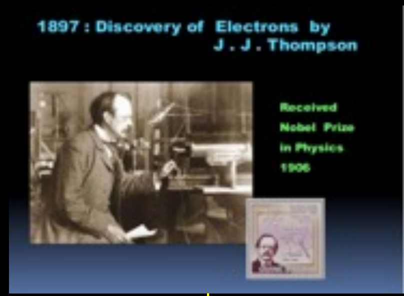

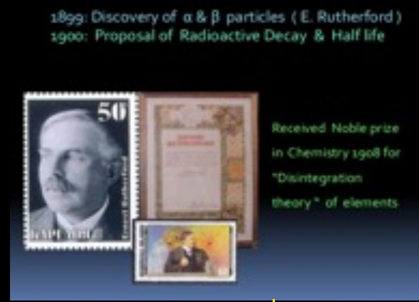

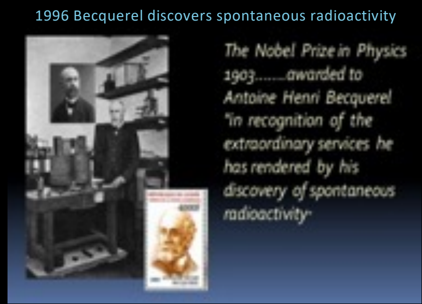

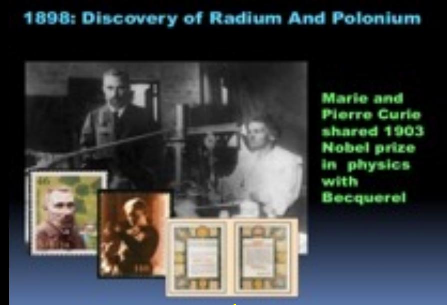

1800es | 1895 | 1896 | 1897 | 1898 | 1899

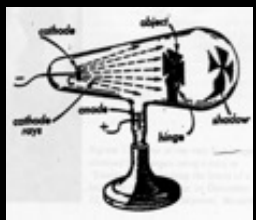

Hittorf-Crookes tube

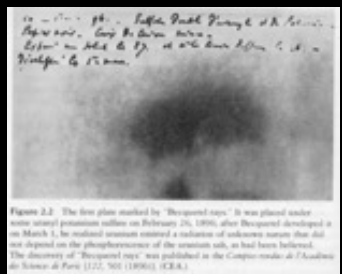

Photographic plate
Used to study "x-rays".. But they deflected with B-field

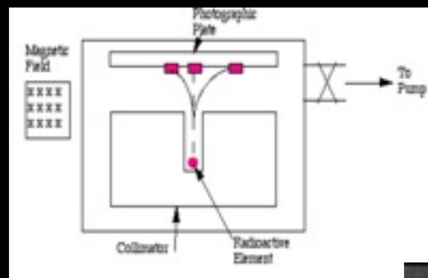

1908-1913
Geiger-Masden Apparatus
Or Rutherford Gold foil
Experiment proved the
atomic structure

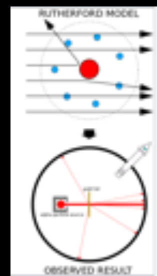

Cathode rays (e^-)
Deflected by B field

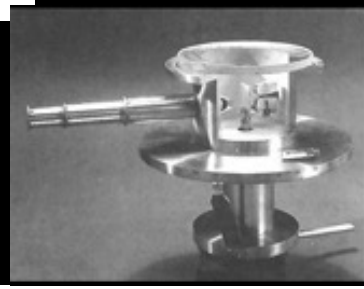

Cinzia Da Via, The University of Manchester, UK & SUNY USA– 2023

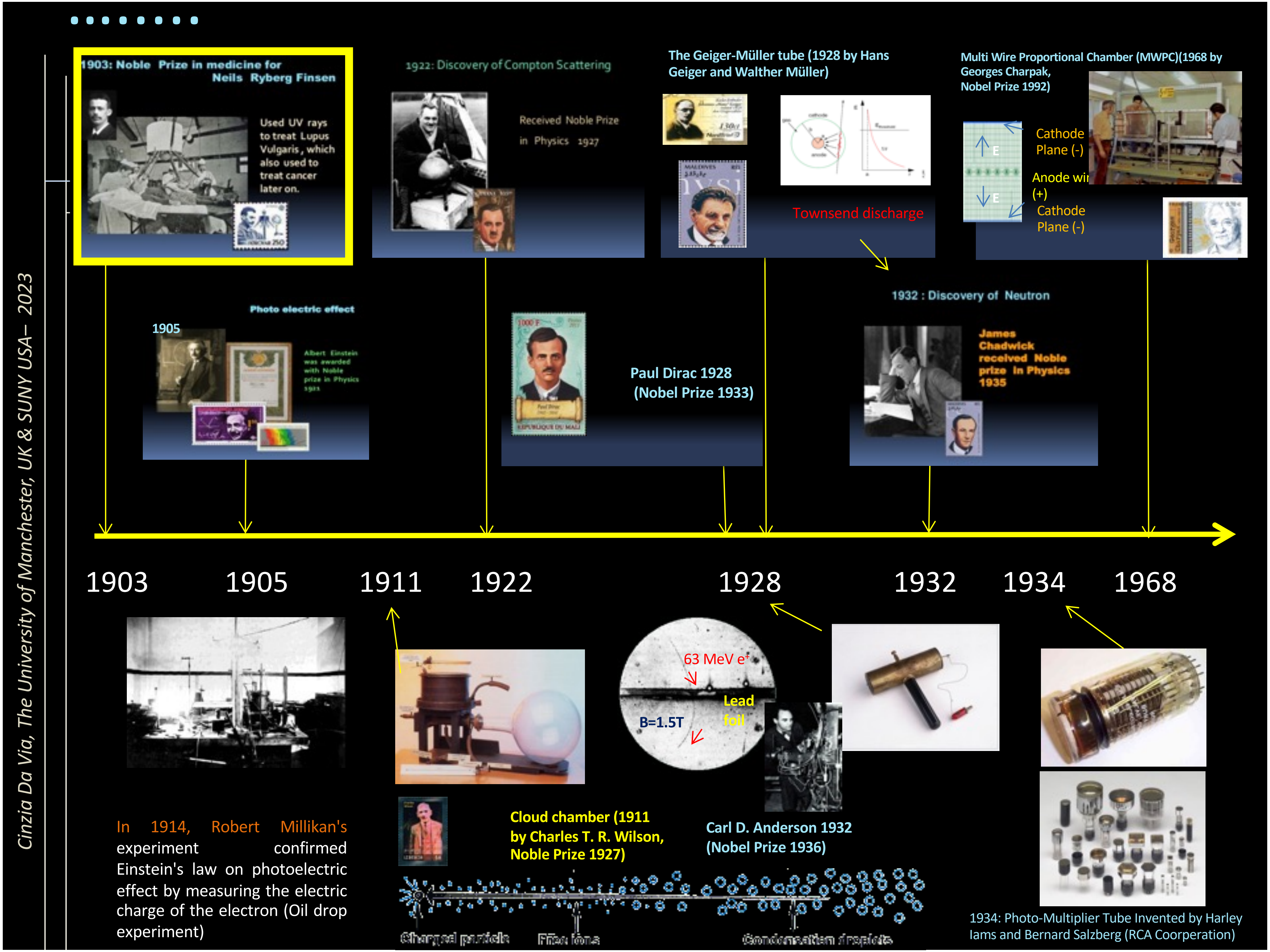

1903: Noble Prize in medicine for Neils Ryberg Finsen
Used UV rays to treat Lupus Vulgaris, which also used to treat cancer later on.
1922: Discovery of Compton Scattering
Received Noble Prize in Physics 1927
The Geiger-Müller tube (1928 by Hans Geiger and Walther Müller)
Townsend discharge
Multi Wire Proportional Chamber (MWPC)(1968 by Georges Charpak, Nobel Prize 1992)
Cathode Plane (-)
Anode wir (+)
Cathode Plane (-)
E
E
Photo electric effect
1905
Albert Einstein was awarded with Noble prize in Physics 1921
Paul Dirac 1928 (Nobel Prize 1933)
1932 : Discovery of Neutron
James Chadwick received Noble prize in Physics 1935
1903
1905
1911
1922
1928
1932
1934
1968
63 MeV e+
Lead foil
B=1.5T
In 1914, Robert Millikan's experiment confirmed Einstein's law on photoelectric effect by measuring the electric charge of the electron (Oil drop experiment)
Cloud chamber (1911 by Charles T. R. Wilson, Noble Prize 1927)
Carl D. Anderson 1932 (Nobel Prize 1936)
Charged particle
Free ions
Condensation droplets
1934: Photo-Multiplier Tube Invented by Harley Iams and Bernard Salzberg (RCA Coorperation)
Cinzia Da Via, The University of Manchester, UK & SUNY USA– 2023

Cinzia Da Via, The University of Manchester, UK & SUNY USA– 2023

The semiconductors revolution

First transistor invented 1947 by William B. Shockley, John Bardeen and Walter Brattain (Nobel Prize 1956)

First semiconductor particle sensor: Pieter Jacobus Van Heerden, *The Crystalcounter: A New Instrument in Nuclear Physics.* University Math Naturwiss, Fak (1945*). CCD Nobel prize Boyle Smith 2009*

Semiconductor a material that has a conductivity between a conductor and an insulator; electricity can pass through it, but not very easily

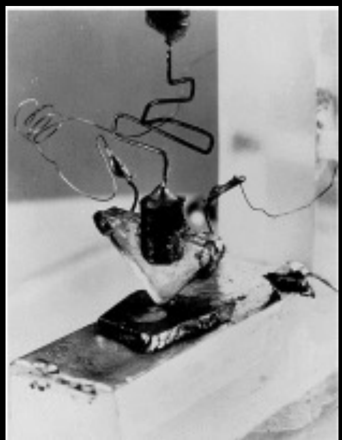

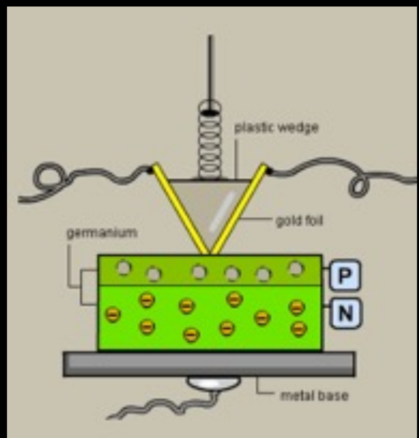

The point contact germanium transistor

p-n junction

Depleted region particle yes/no

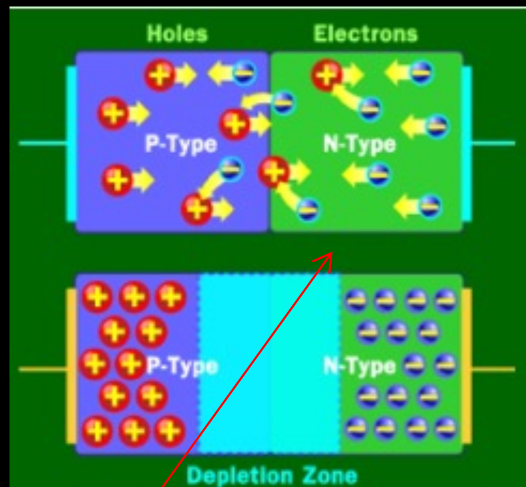

particle

75th Anniversary of the transistor !!!

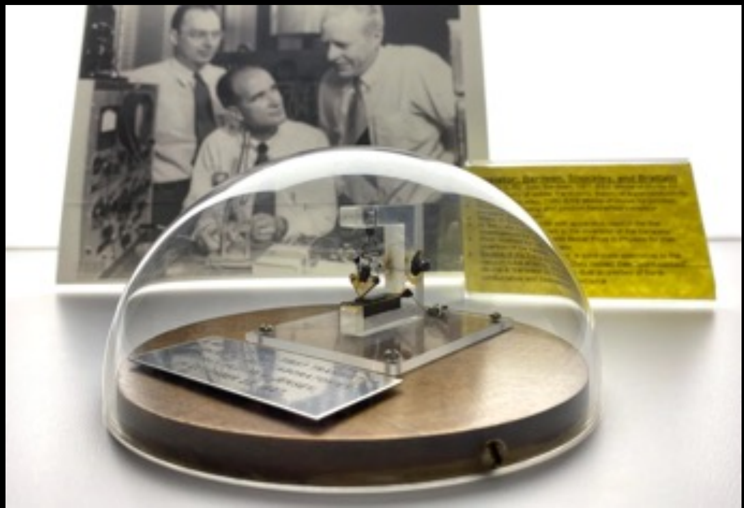

November 1947 – January 1948 were the three magical months that paved the way for modern-day electronics. Walter Brattain and John Bardeen managed to make the first working transistor, now known as the point-contact transistor. The invention was made on December 16, 1947. In January 1948, William Shockley demonstrated the junction transistor.

All three received The Nobel Prize in Physics (1956) and as per Nobel Prize Committee - "In 1947 John Bardeen and Walter Brattain produced a semiconductor amplifier, which was further developed by William Shockley. The component was named a "transistor."

Technology Transfer from the start..

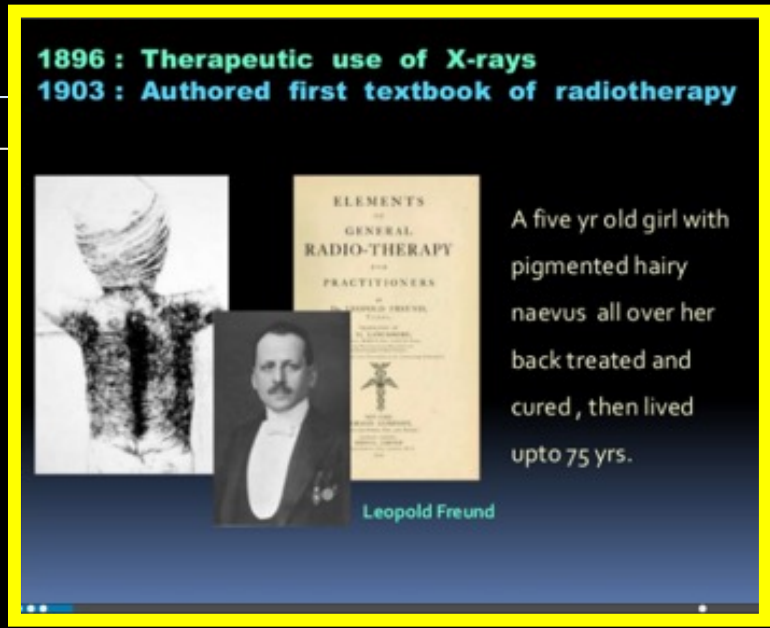

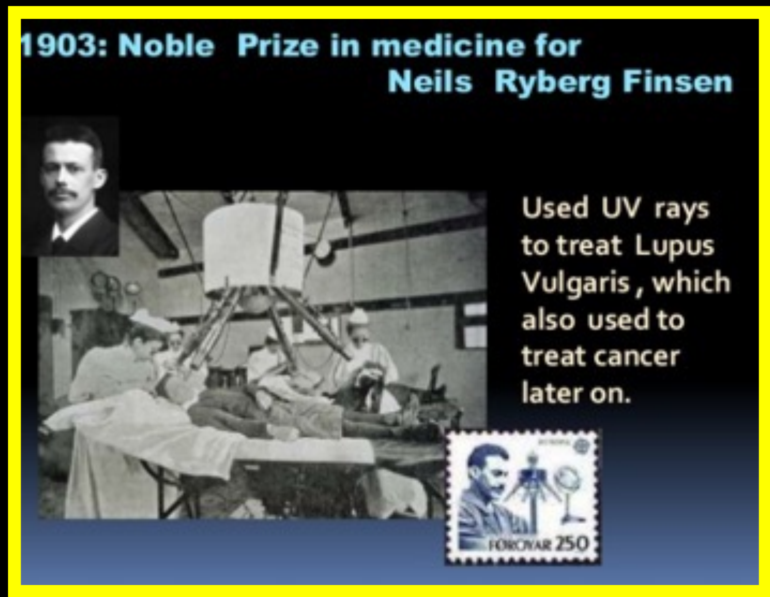

Cinzia Da Via, The University of Manchester, UK & SUNY USA– 2023

1931 : Van de Graaff Generator (MIT)

Harvard Medical School was the first to use his machine clinically to produce X-rays for the treatment of cancerous tumors with radiation in 1937

40 feet high
Electrostatic device
capable of operating
at 5,000,000 volts

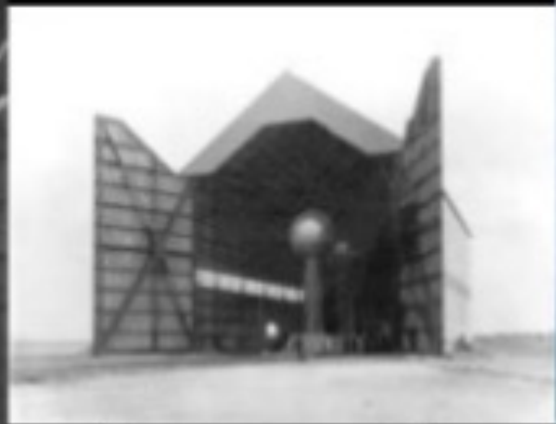

Robert van de Graaff

2 MeV Clinical
Van de Graaff
X-ray machine

Cinzia Da Via, The University of Manchester, UK & SUNY USA– 2023

1953: First Linear Accelerator
1956: First pt treated with LINAC

Henry Kaplan

Gordon Issac,2yr old pt of B/I Retinoblastoma

Multi Wire Proportional Chamber (MWPC)

Extends the concept of the Geiger-Muller to many wires with short distance between two parallel plates

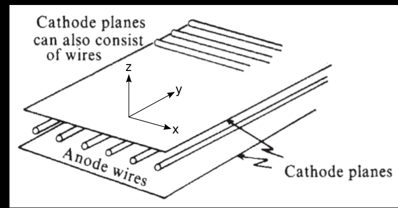

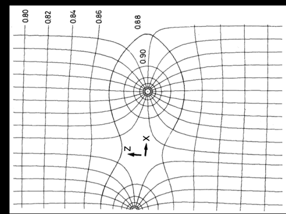

(1968 by Georges Charpak, Nobel Prize 1992)

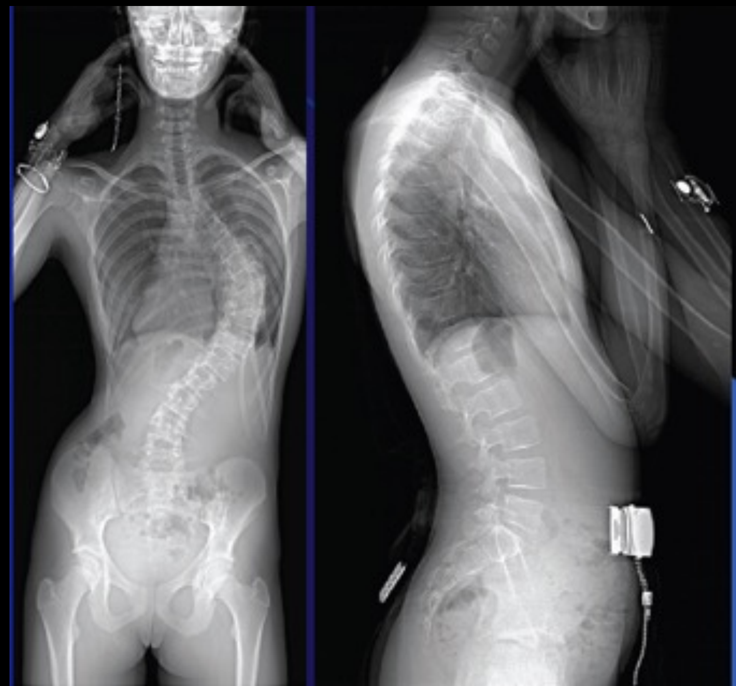

In the 70ties: images with 10 time less dose than traditional radiographic film!

High Energy Physics Instrumentation Assets

Particle Accelerators:
- Vacuum
- Surfaces
- Magnets
- Cooling
- Superconductors

Electrical &Civil Engineering:
- Tunnels
- Infrastructures
- Power distribution
- Large Underground installations

RADIATION HARD

Radiation Detectors:
- Electronics
- Sensors (gas, solid state, scintillators)
- Integration
- Support structures

Data Acquisition Systems:
- Electronics
- Links (electro-optical)
- Big data (storage & distribution)
- Triggering (machine learning, AI)

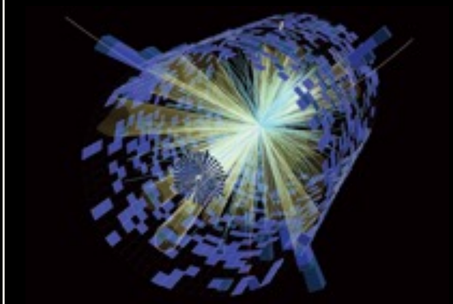

Data analysis & Simulation:
- Theory
- Data libraries
- Software
- Big Data (analysis)

Human Capital:
- Ingenuity
- Large Scale Operations
- Coordination
- Education
- Global Collaboration

Non-HEP Synergies with Particle Accelerators


Synchrotron light sources
50 in the world
- Biology/medicine
- Chemistry
- Material Science
- Technology

Superconducting magnets

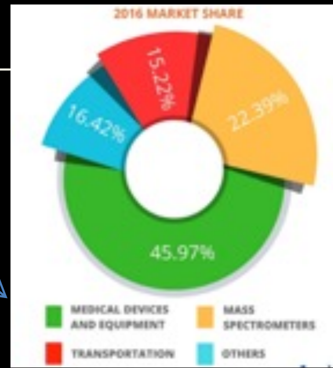

67 working
by 2024
130 operational

Particle therapy

In 2018 50% of cancer patients underwent radiotherapy as part of their treatment. 80% are treated with H-E X-Rays. 200000 patients have been treated with charged hadrons thanks to the improved depth-dose distribution

High Intensity Neutron sources

Fusion Facilities

- JET
- ITER
- DEMO

Ultra vacuum Technology

Cryogenics

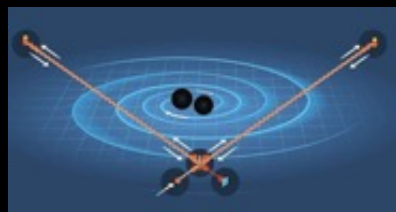

Gravitational waves
Multi-Messenger Astronomy

Surface Coating (Klystrons)
Vacuum Magnetic Birefringence
Axion searches

Cinzia Da Via, The University of Manchester, UK & SUNY USA– 2023

Examples of interface with medicine

Synchrotron light sources

70 in the world

- Biology/medicine
- Chemistry
- Material Science
- Technology

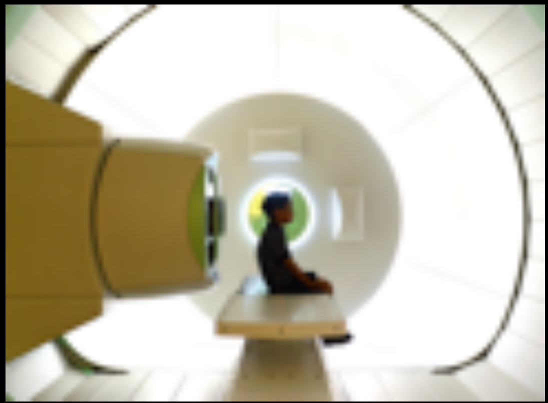

80 working worldwide

Particle therapy

Proton therapy has been used to treat **more than 160,000 people worldwide**. By 2030, it is estimated that between 300,000 and 600,000 patients will have received proton therapy treatment

Superconducting Magnets

- NMR
- MRI
- Nuclear Fusion

Synchrotron light sources

NSLS II Brookhaven National laboratory

Currently 70 in the world

APPLICATIONS IN →

- Biology/medicine
- Chemistry
- Material Science
- Technology
- …….

Cinzia Da Via, The University of Manchester, UK & SUNY USA– 2023

Synchrotron Radiation: Protein crystallography

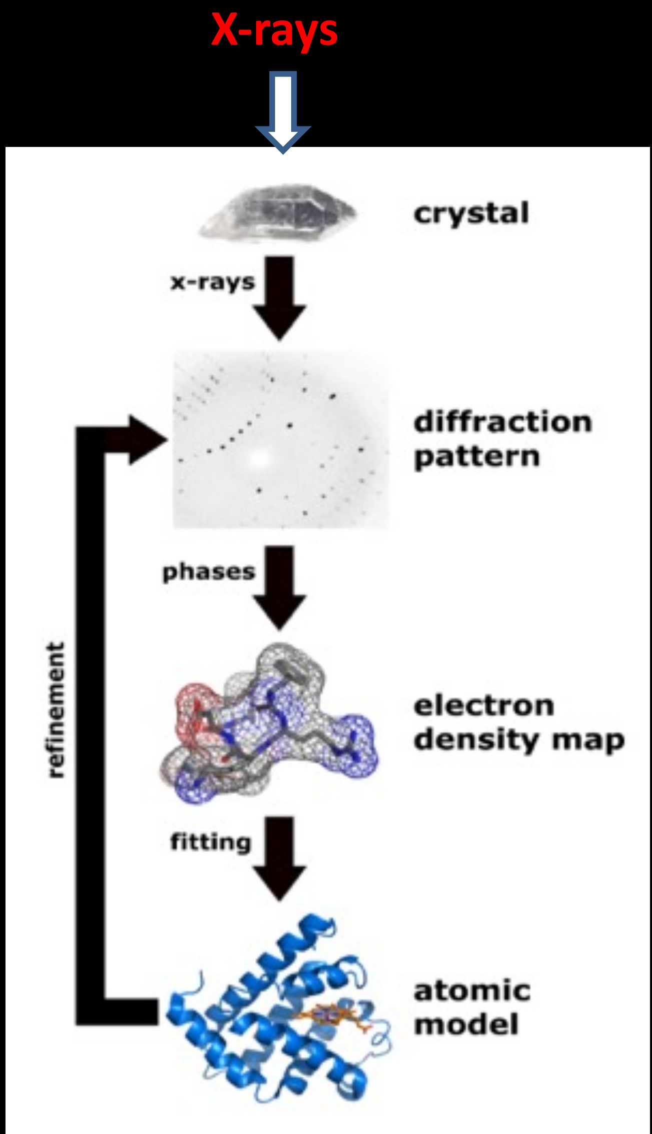

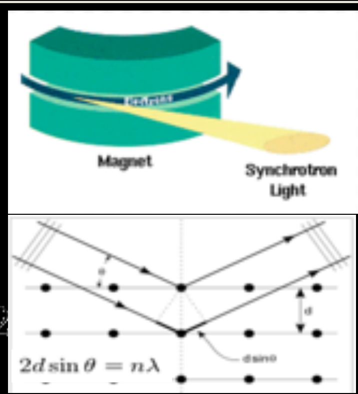

Bragg Law

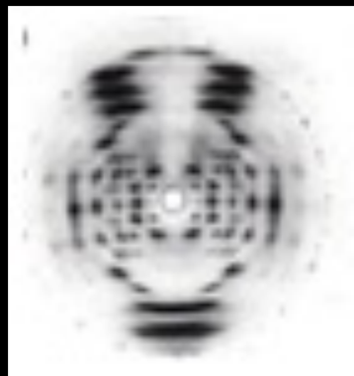

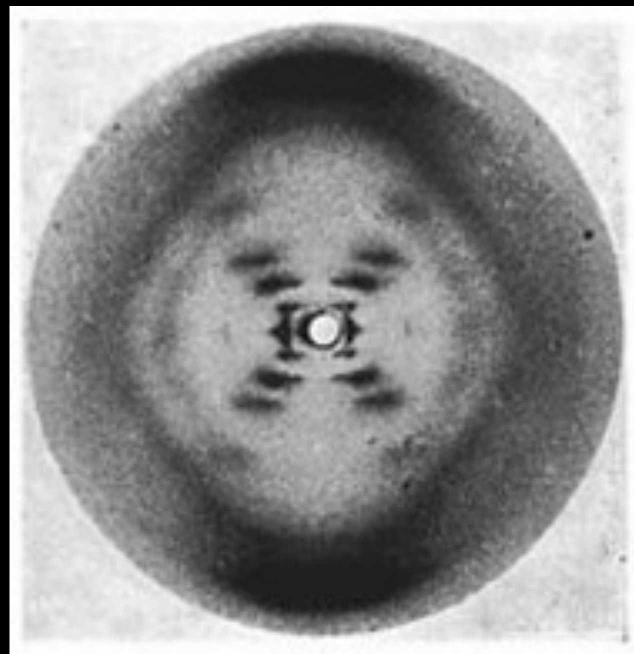

X-ray diffracted Photographic image of the double helix taken in 1952 by Rosalind Franklin and Raymond Gosling. The DNA sample was fibrous DNA

Superconducting magnets: Magnetic Resonance Imaging

The phenomenon of superconductivity was discovered in 1911 by the Dutch physicist **Heike Kamerlingh Onnes** and his by noticing that the **electrical resistance of mercury** goes to zero below 4.2 K (-269°C), followed by other contributions.

Paul Christian Lauterbur and Peter Mansfield received the Nobel Prize in 2003 for their development of MRI

A coil made from superconducting material can produce **stronger magnetic fields** than resistive electromagnets.

The superconducting portions of most current magnets are composed of **niobium-titanium (Type II)**. This material has critical temperature of 10 kelvins and can superconduct at up to about 15 Teslas. More expensive magnets can be made of **niobium-tin** (Nb_3Sn).

CLOSE MRI

OPEN MRI

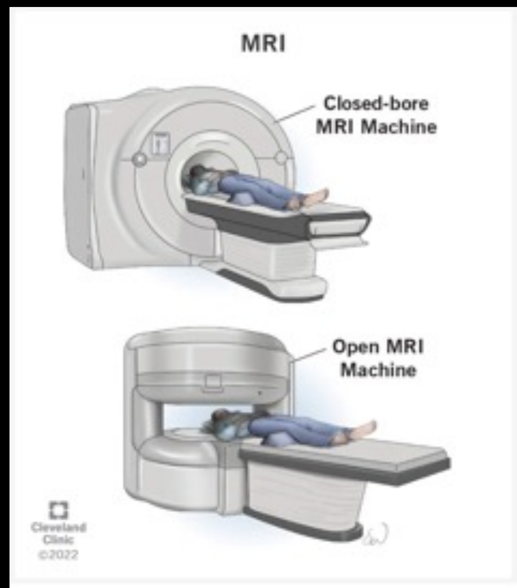

Cinzia Da Via, The University of Manchester, UK & SUNY USA– 2023

Nuclear Magnetic Resonance -definition

The principle of NMR usually involves three sequential steps:

1.The alignment (polarization) of the magnetic nuclear spins in an applied, constant magnetic **field** B_0.

2.The perturbation of this alignment of the nuclear spins by a weak oscillating magnetic **field**, usually referred to as a radio-**frequency** (RF) pulse.

3.Detection and analysis of the electromagnetic waves emitted by the nuclei of the sample as a result of this perturbation.

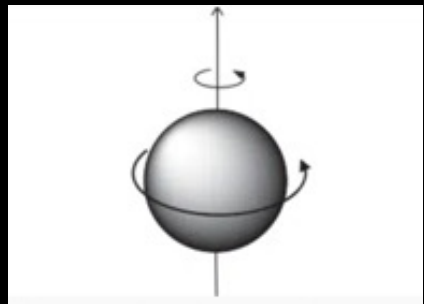

Spinning nucleus along its axis

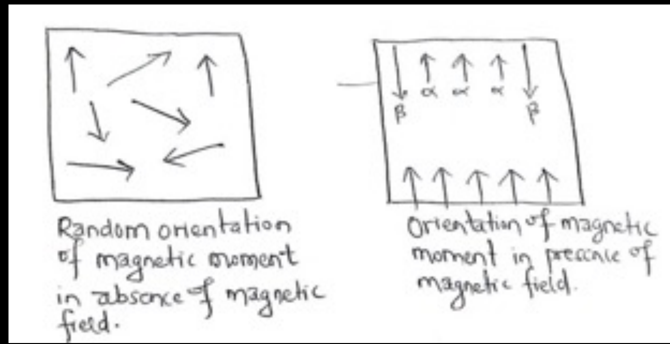

If a nucleus is aligned with the magnetic field, it is said to occupy the **α**-spin state and if it is aligned against the field, it is said to occupy the β-spin state.

The external magnetic field establishes an energy gap between spin states. The magnitude of the energy gap depends on the strength of the external magnetic field.

When the energy between the two energy states lies within the ranges of the radiofrequency radiation then the α-spin state absorbs energy and flips to the β-spin state and the nucleus is said to be in nuclear magnetic resonance.

Cinzia Da Via, The University of Manchester, UK & SUNY USA– 2023

Nuclear Magnetic Resonance for Spectroscopy

When placed in a magnetic field, NMR active nuclei (such as ^{1}H or ^{13}C) absorb electromagnetic radiation at a frequency characteristic of the isotope.

The resonant frequency, energy of the radiation absorbed, and the intensity of the signal are proportional to the strength of the magnetic field.

For example, in a **21 Tesla magnetic field, hydrogen nuclei (protons) resonate at 900 MHz.** It is common to refer to a 21 T magnet as a 900 MHz magnet since hydrogen is the most common nucleus detected, however different nuclei will resonate at different frequencies at this field strength in proportion to their nuclear magnetic moments

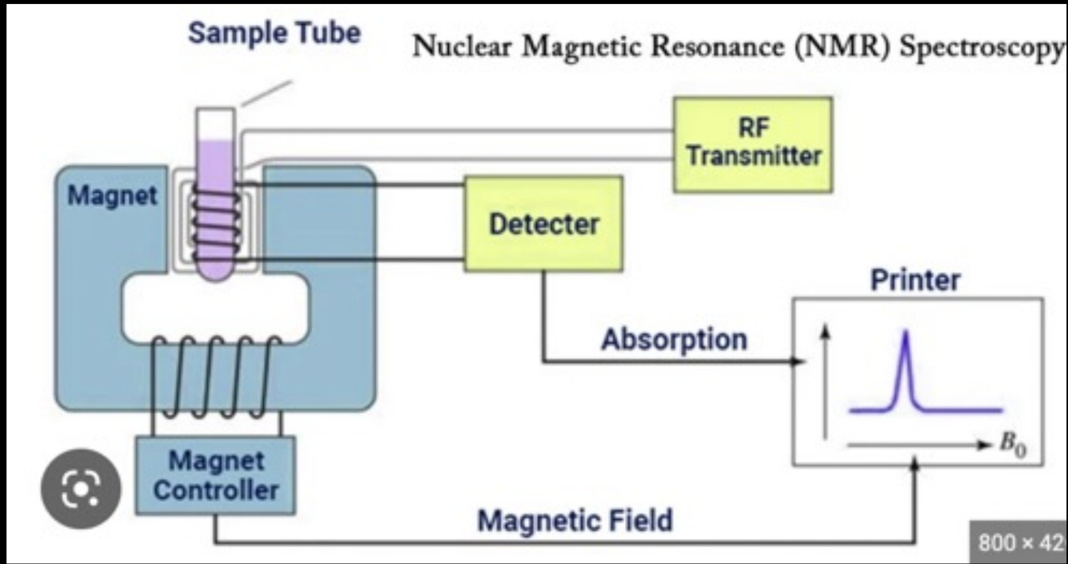

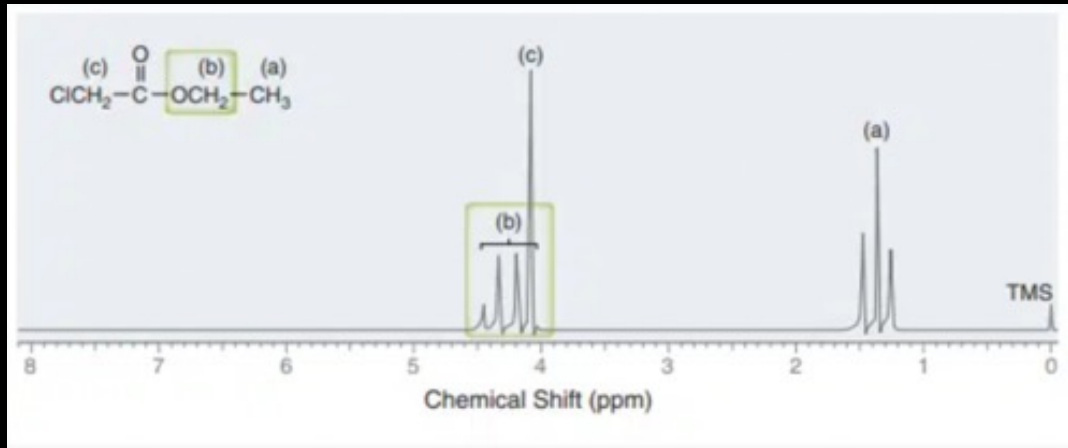

Magnetic Resonance Imaging System -MRI

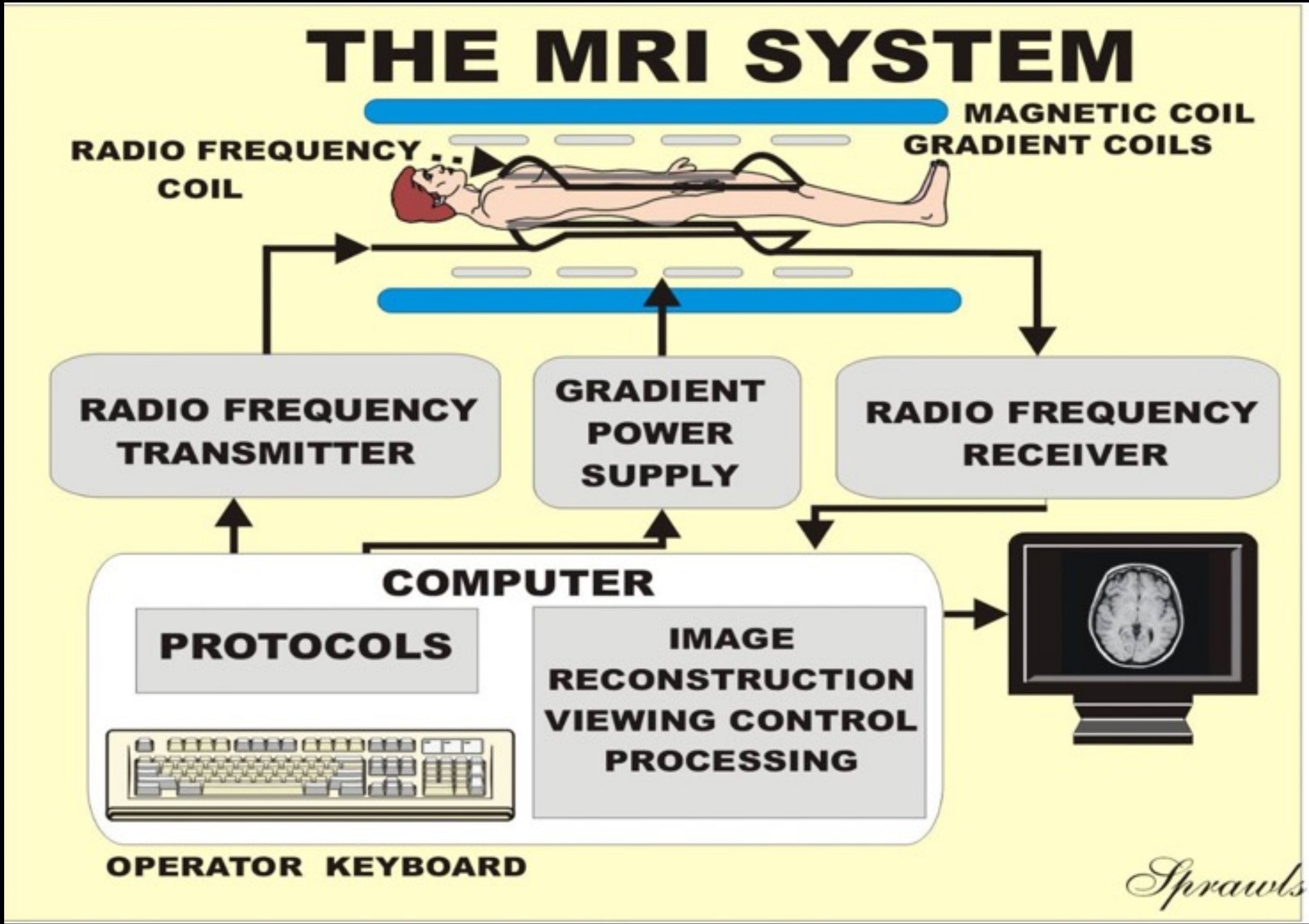

Cinzia Da Via, The University of Manchester, UK & SUNY USA– 2023

MRI Industry

Magnetic Resonance Imaging Systems Market

The global magnetic resonance imaging (MRI) systems market is expected to grow at a CAGR of around 7.80% and the global market value to reach a total value of $5,100 Million approximately in the forecast period 2022-2030.

$5,100 Million	7.80%	Asia pacific	2022-2030
Market Size	CAGR	Dominating Region	Forecast Period

Segmentation

By Type
Open MRI
Close MRI
By Field Strength
High-Field MRI Systems
By Disease Application
Brain
Neurological MRI
By End-Users
Hospitals
Clinics

Key Players

Companies Profiled

- Hitachi
- Siemens AG
- Canon Medical Systems
- GE Healthcare
- Philips
- Toshiba Corporation
- Xingaoyi
- Aurora Imaging Technologies Inc.

Drivers

Market Driving Forces

- The increased number of applications of the MRI technique
- The rising populations and the increasing per capita incomes of people

$$\text{CAGR} = \left(\frac{V_{\text{final}}}{V_{\text{begin}}}\right)^{1/t} - 1$$

CAGR = compound annual growth rate

V_{begin} = beginning value

V_{final} = final value

t = time in years

Compound Annual Growth Rate

The future→"Iseult" project at CEA-Paris-Saclay


CERNCOURIER | Reporting on international high-energy physics

Physics ▾ Technology ▾ Community ▾ In focus Magazine

APPLICATIONS | NEWS

World's most powerful MRI unveiled

1 November 2021

In season On account of its multiple textures and resemblance to brain tissue, a pumpkin was the natural choice to showcase MRI's capabilities at 11.7 T. Credit: CEA

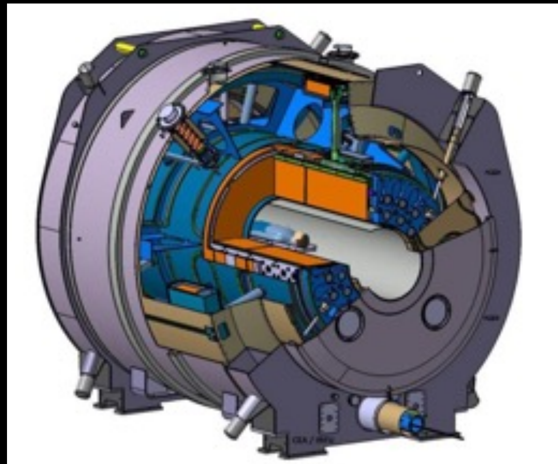

Cross-section of the ISEULT 11.7 T magnet. The superconducting windings are shown in orange, the structure held at 1.8 K in blue, and the cryostat in grey.

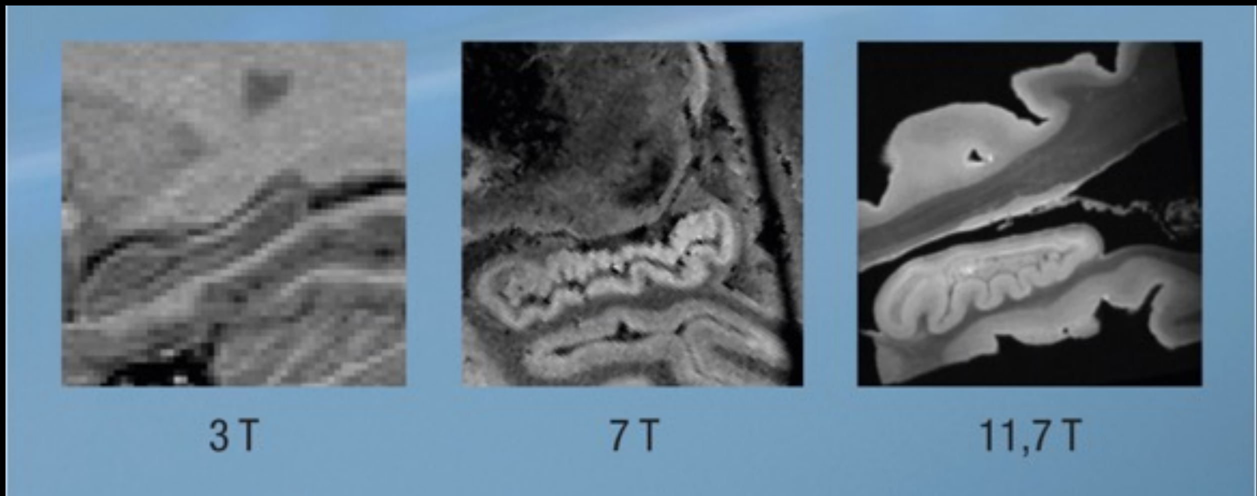

→132 tons superconducting magnet

→solenoid (carrying a current of 1.5 kA)

→produces a field of 11.7 T inside a 0.9 m diameter and 5 m long volume.

→4-times more powerful than typical hospital devices

Accelerators for medicine

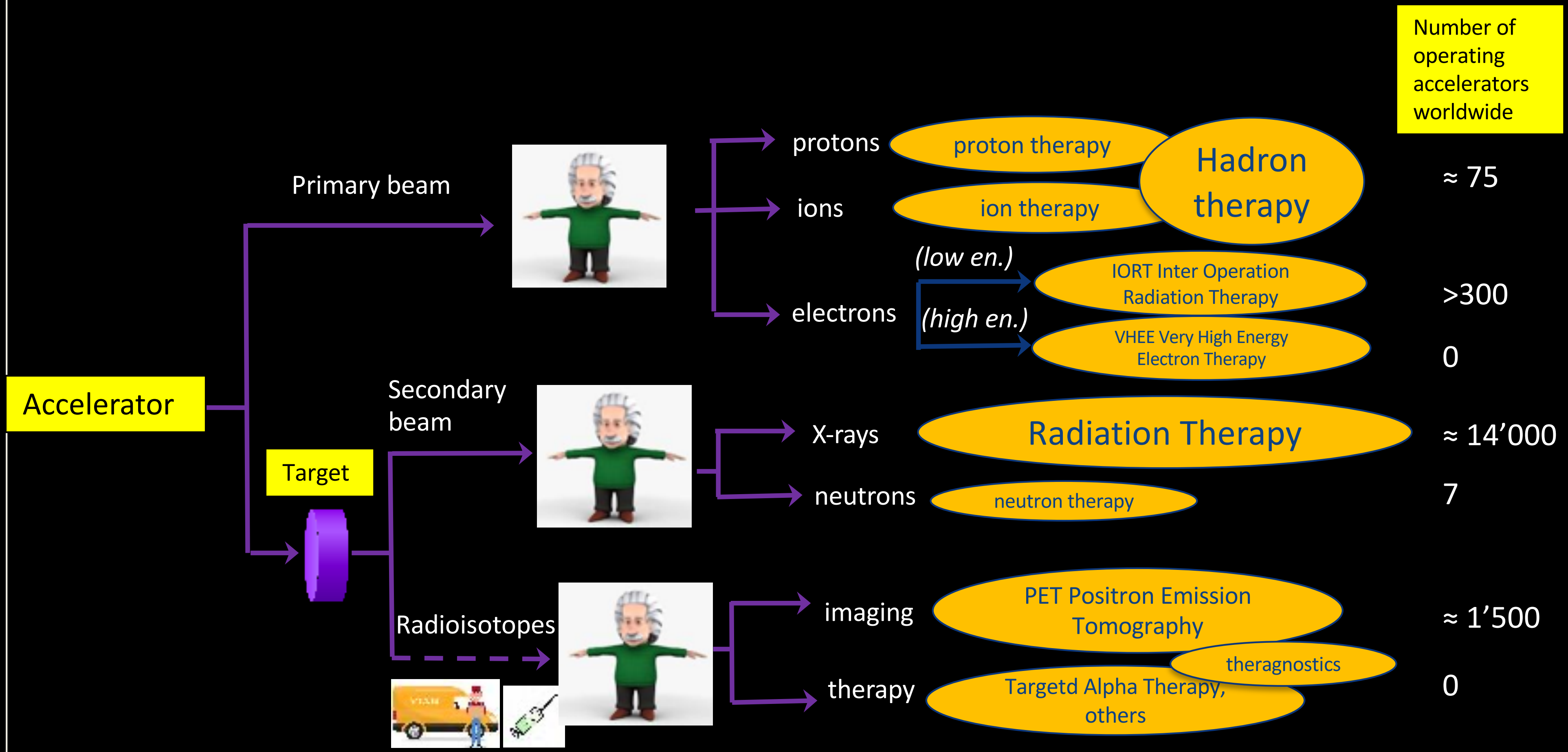

Total: ≈ 16’000 particle accelerators operating for medicine!!!!

Slide from M. Vretener, CERN

Isotopes in Medicine

Slide from P. Le Du

DIAGNOSIS		THERAPY		
in vitro	in vivo	internal		external
		systemic	sources	tele radio
^{14}C ^{3}H ^{125}I others	^{99}Mo-^{99m}Tc ^{201}Tl ^{123}I ^{111}In ^{67}Ga ^{81}Rb-^{81m}Kr others ß+ emitters for PET ^{18}F, ^{11}C, ^{13}N, ^{15}O ^{86}Y, ^{124}I ^{68}Ge-^{68}Ga ^{82}Sr-^{82}Rb	^{131}I, ^{90}Y ^{153}Sm, ^{186}Re ^{188}W-^{188}Re ^{166}Ho, ^{177}Lu, others α-emitters: ^{225}Ac-^{213}Bi ^{211}At, ^{223}Ra ^{149}Tb e^--emitters: ^{125}I	sealed sources ^{192}Ir, ^{182}Ta, ^{137}Cs many others needles for brachytherapy: ^{103}Pd, ^{125}I many others stands ^{32}P and others seeds ^{90}Sr or ^{90}Y, others applicators ^{137}Cs, others	^{60}Co gamma knife ^{137}Cs blood cell irradi-ation

Cinzia Da Via, The University of Manchester, UK & SUNY USA– 2023

Common Diagnosis RadioTracers

Application	Requirement	Isotope
DIAGNOSIS In vivo SPECT	single photons no particles biogenic behavior $T_{½}$ = moderate	^{99m}Tc, ^{123}I, ^{111}In, ^{201}Tl,
DIAGNOSIS in vivo PET	$ß^+$-decay mode biogenic elements $T_{½}$ = short	^{11}C, ^{13}N, ^{15}O, ^{18}F

Slide from P. Le Du

Tracer production situation in Europe

Pays	Réacteur	Puissance (MWth)	Age en 2022 (ans)
Rep. tchèque	LVR15	10	66
Norvège	HBWR	19	62 (arrêté en 2018)
Pays Bas	HFR	45	62
Belgique	BR2	100	62
Pologne	MARIA	30	46
France	OSIRIS	70	(arrêté fin 15)
France	RJH	100	En cours

Slide from P. Le Du

Global Nuclear Medicine/Radiopharmaceuticals Market

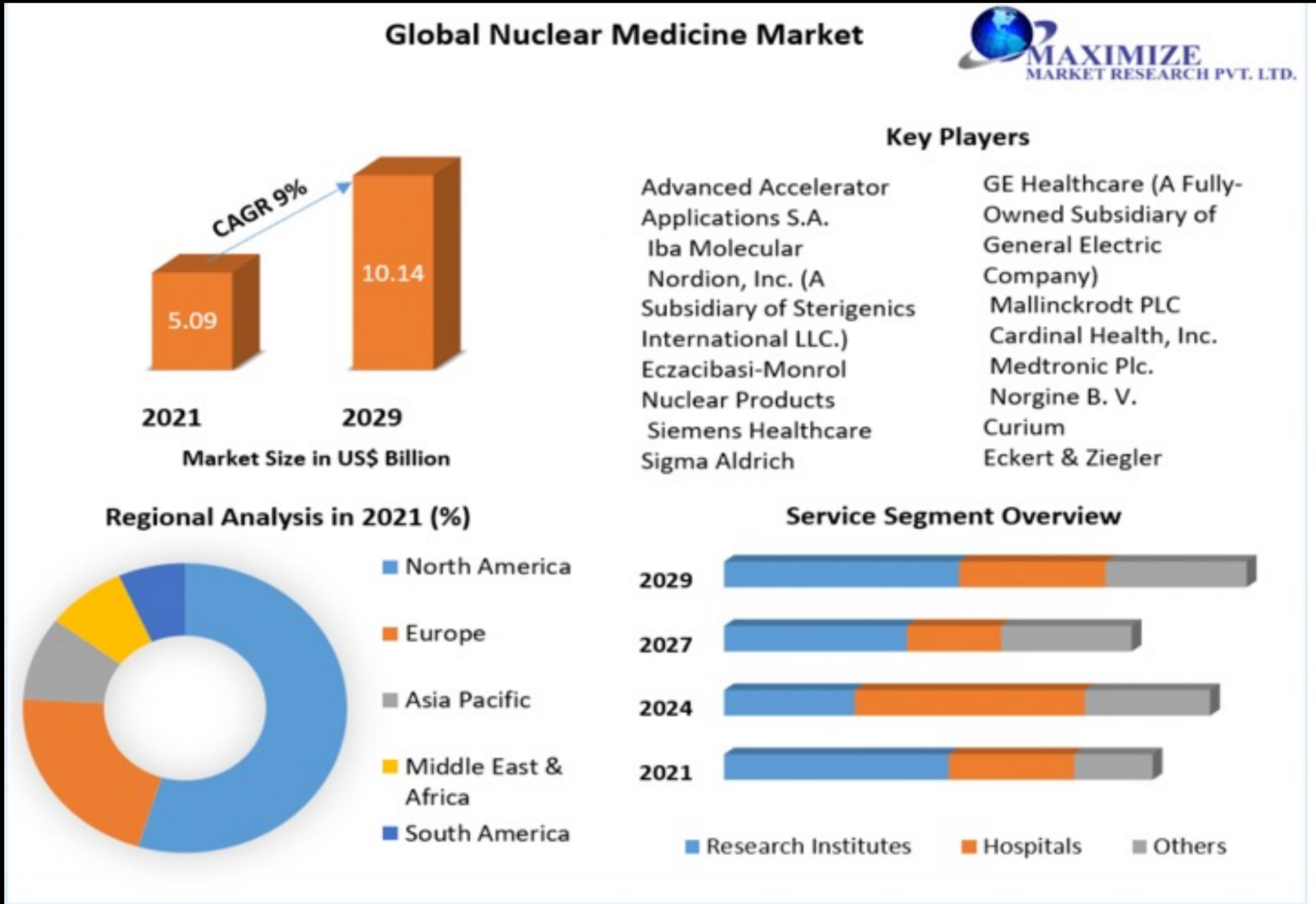

Cinzia Da Via, The University of Manchester, UK & SUNY USA– 2023

Particle Therapy

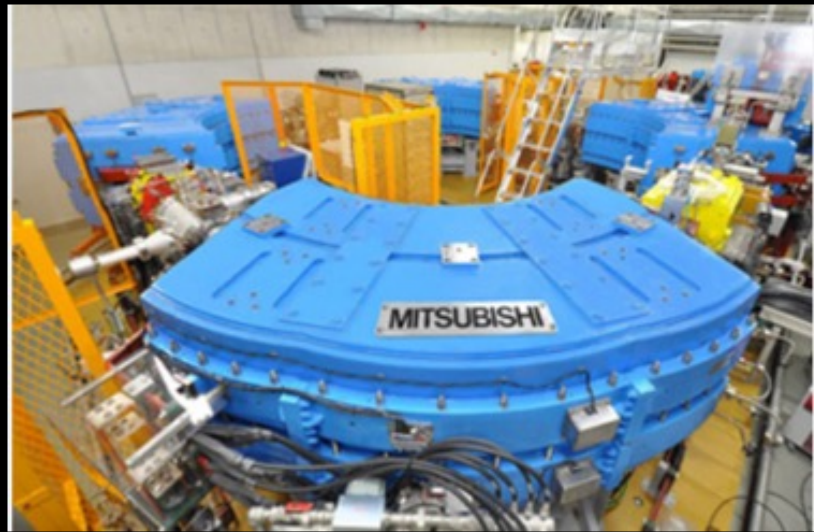

Use Cyclotrons and Synchrotrons Accelerators

Proton therapy has been used to treat **more than 160,000 people worldwide**. By 2030, it is estimated that between 300,000 and 600,000 patients will have received proton therapy treatment

Posted at: Feb 21 2023 7:50PM

Cancer patient from Mumbai treated with proton beam therapy at Apollo Proton Cancer Centre

Mumbai, Feb 21 (UNI) A 62-year-old man from Mumbai who was suffering from lung cancer, has successfully been treated with proton beam therapy (PBT) at Apollo Proton Cancer Centre (APCC), the first and only proton therapy centre in South Asia and the Middle East.

Speaking about the therapy, Dr Srinivas Chilukuri, Radiation Oncologist, Apollo Proton Cancer Centre, Chennai, said, “Proton beam therapy is the most sophisticated form of radiation therapy currently available in the world to treat cancer patients and Apollo hospital is using the same in hundreds of cases."

Proton therapy reduces the immediate and long-term side effects of treatment in many patients, leading to not just an improvement in survival but also survivorship, a release stated here on Tuesday.

In India, the estimated number of cancer cases in 2022 was 14,61,427, and since 2019, 10 patients from Maharashtra had been treated at APCC for thoracic cancers, including lung cancer.

According to the International Association of Cancer Registries (IARC), over 24,000 people die each year as a result of brain tumours. So far, the APCC had treated 336 cases of brain tumours, 45 of which were from Maharashtra.

Due to its effectiveness, proton therapy is being encouragingly adopted for the treatment of various cancers such as brain and spine tumours, skull base tumours, oral cancers, gastro-intestinal cancers, bone and soft tissue tumours, breast cancers, thoracic cancers (lung cancer), genitourinary cancers (prostate cancer) and predominantly in paediatric cancers except for leukaemia, the release added.

UNI JM SS 1944

Cinzia Da Via, The University of Manchester, UK & SUNY USA– 2023

Particle Therapy History

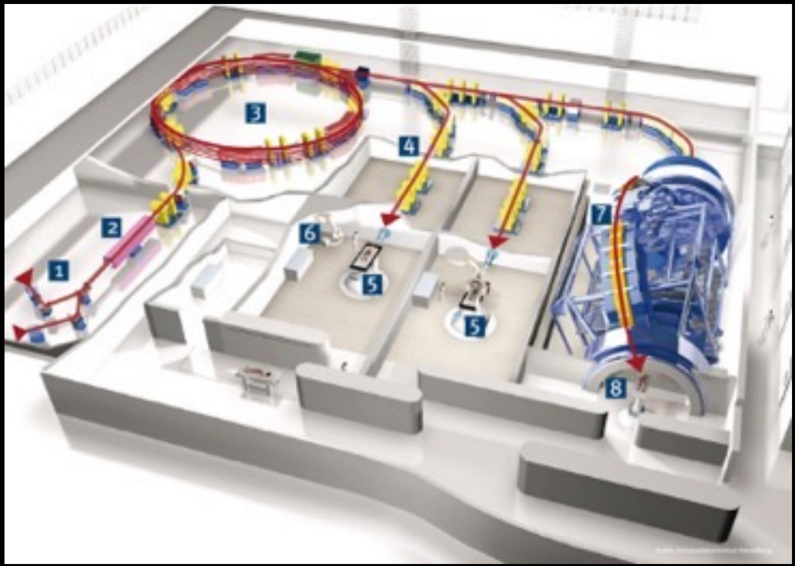

- First experimental treatment in 1954 at Berkeley.
- First hospital-based proton treatment facility in 1993 (Loma Linda, US).
- First treatment facility with carbon ions in 1994 (HIMAC, Japan).
- Treatments in Europe at physics facilities from end of '90s.
- First dedicated European facility for protons and carbon ions in 2009 (Heidelberg).
- From 2006, commercial proton therapy cyclotrons appear on the market (but Siemens gets out of proton/carbon synchrotrons market in 2011).
- Nowadays 3 competing vendors for cyclotrons, one for synchrotrons (all protons).
- 80 working worldwide. More centres are planned in the near future.

Hadron Therapy

Bethe-Bloch equation of ionisation energy loss by charged particles

$$-\frac{dE}{dx} = \frac{4\pi}{m_e c^2} \cdot \frac{nz^2}{\beta^2} \cdot \left(\frac{e^2}{4\pi\varepsilon_0}\right)^2 \cdot \left[\ln\left(\frac{2m_e c^2 \beta^2}{I.(1-\beta^2)}\right) - \beta^2\right]$$

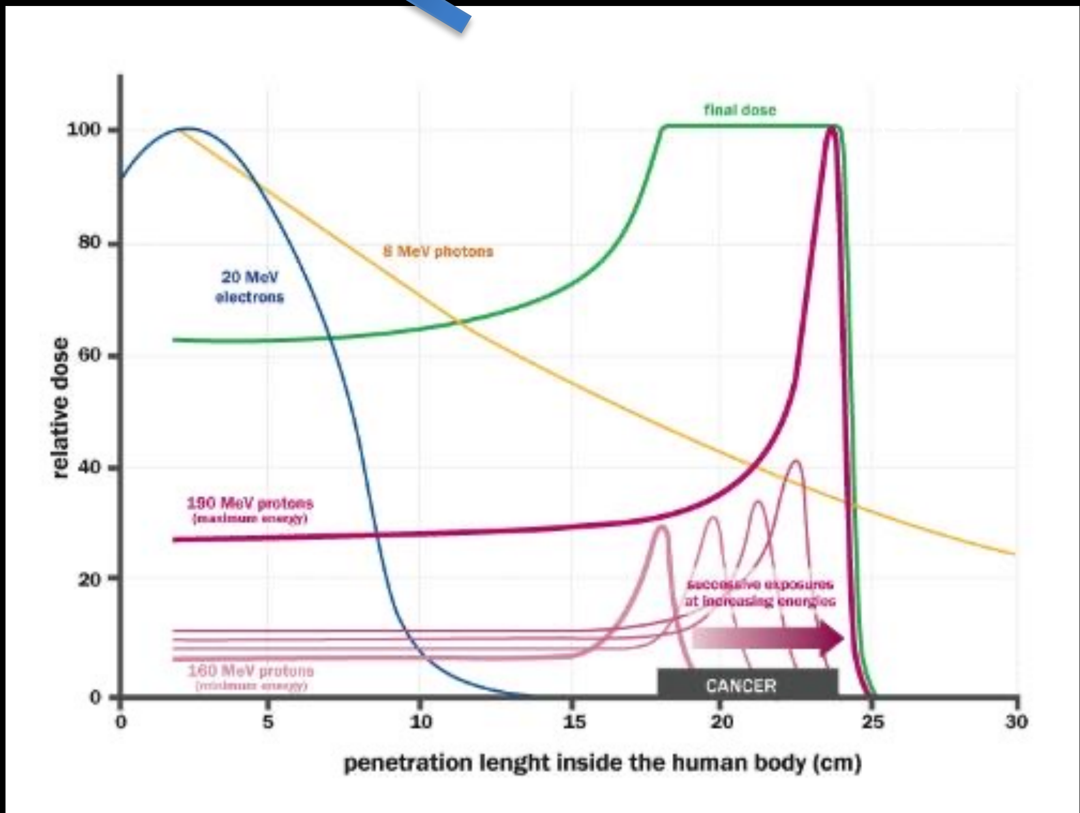

Different from X-rays or electrons, protons (and ions) deposit their energy at a given depth inside the tissues, «Bragg Peak» **minimising the dose to the organs close to the tumour.**

Required **energy (protons) about 230 MeV,** corresponding to 33 cm in water.
Small currents: 10 nA for a typical dose of 1 Gy to 1 liter in 1 minute.

Cinzia Da Via, The University of Manchester, UK & SUNY USA– 2023

Nuclear reactions in hadron therapy

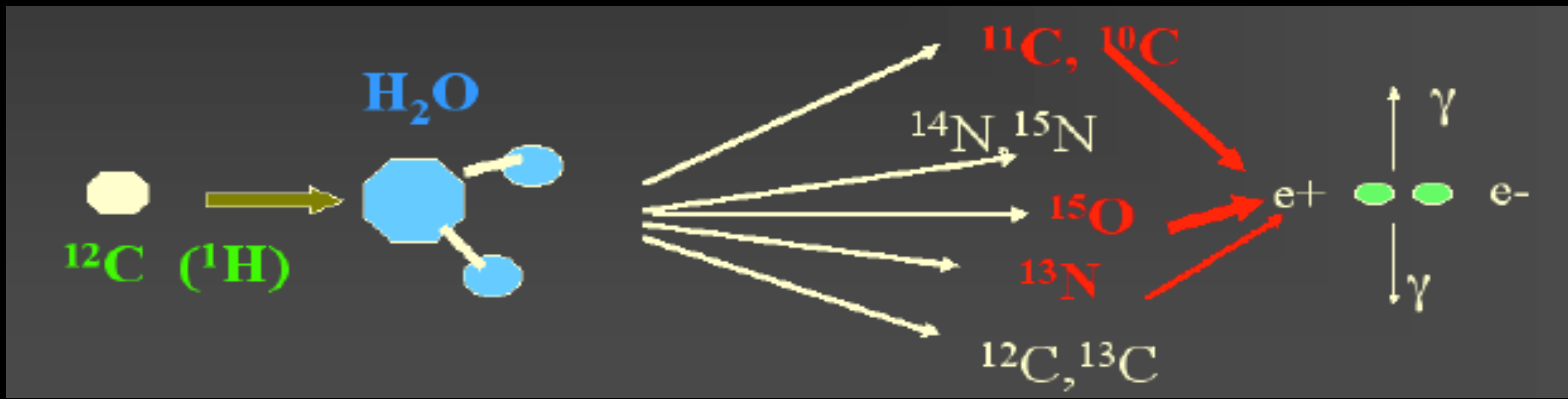

Balance of promptly emitted particles outside the target:

Incident protons: 1.0		($\sim 10^{10}$)
γ-rays:	0.3	($3 \cdot 10^9$)
Neutrons:	0.09	($9 \cdot 10^8$)
Protons:	0.001	($1 \cdot 10^7$)
α-particles:	$2 \cdot 10^{-5}$	($2 \cdot 10^5$)

Relative Biological Effectiveness RBE is the ratio of biological effectiveness of one type of ionising relative to another, given the same amount of absorbed energy

where D_X is a reference absorbed dose of radiation of a standard type X, and D_R is the absorbed dose of radiation of type R that causes the same amount of biological damage

$$RBE = \frac{D_X}{D_R}$$

Cinzia Da Via, The University of Manchester, UK & SUNY USA– 2023

Defining the dosimetry units

Activity = Number of decays per second

– Becquerel Bq : 1 decay / second
– Curie Ci : 37 x 10^9 Bq (37 GBq)

Dose = amount of radiation absorbed in any material

GRAY= absorbed energy / mass unit

– Gy : 1 joule / kilogram = 100 Rad

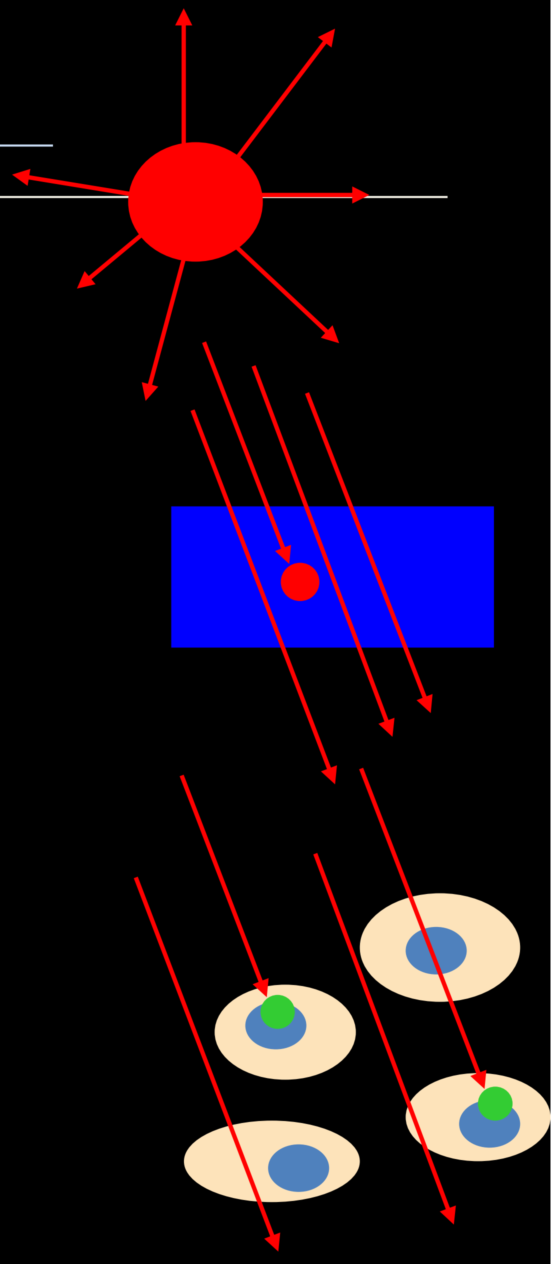

Slide from P. Le Du

Effective dose = estimates biological effect from the absorbed radiation

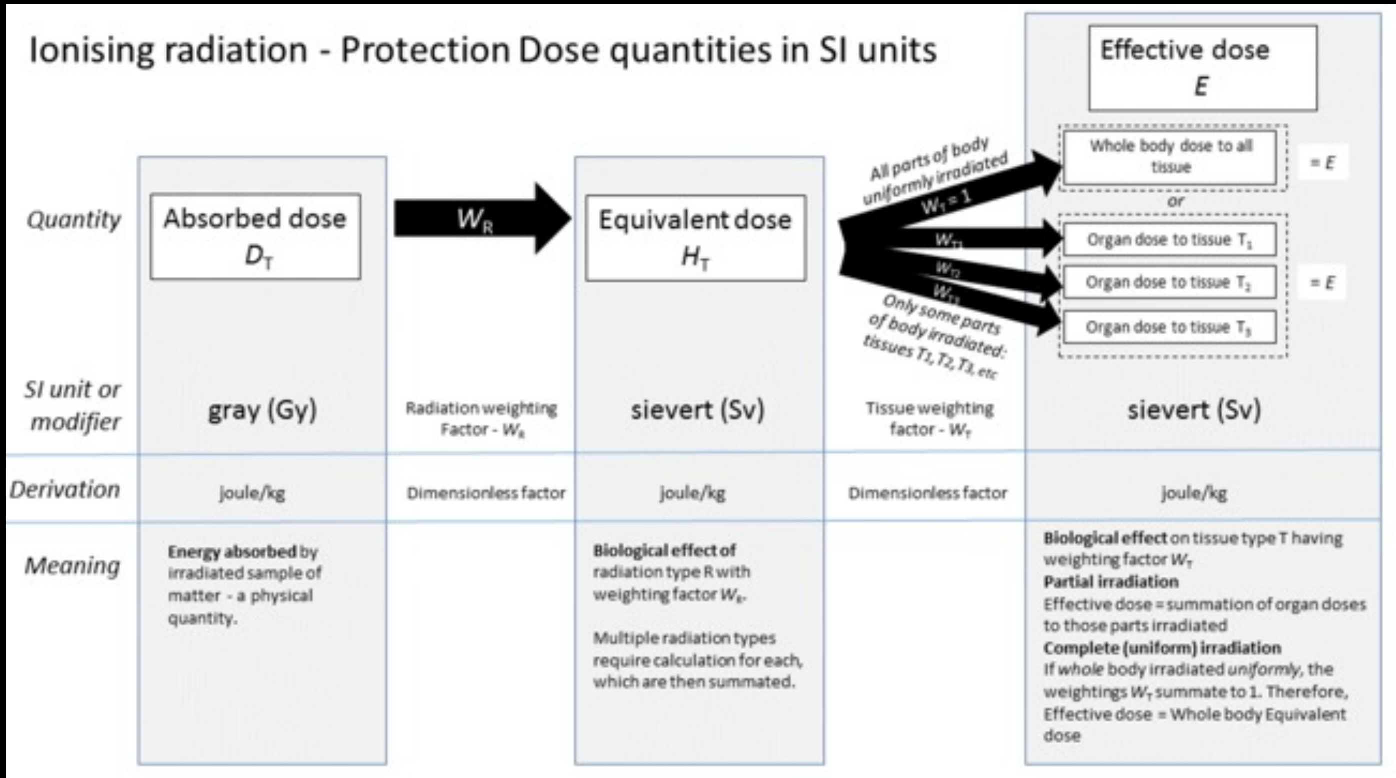

→ indication of global risk

= absorbed dose x WR* x WT**

Particle → WR*= 1 pour RX, beta and gamma, p=5, α=20

Organ → WT** = 0.05 for thyroïd, 0.01 for skin

10.000 mSv : high irradiation / rapid death
1.000 mSv : moderate irradiation / clinical visible signs (burn…)
5 mSv : annual irradiation in regions with (volcanic soil)
2,5 mSv : annual irradiation in Paris
1 mSv : legal limit irradiation in France
1 mSv : average annual medical irradiation in France

Cinzia Da Via, The University of Manchester, UK & SUNY USA– 2023

Precise Bragg Peak Reconstruction: Tracking of the prompt gammas

When the proton Beam hits the target gammas are emitted from nuclear reactions

Prompt gammas are emitted at different Angles and can be counted after collimation

Strong correlation has been measured using Depth Dose distribution and Prompt Gammas

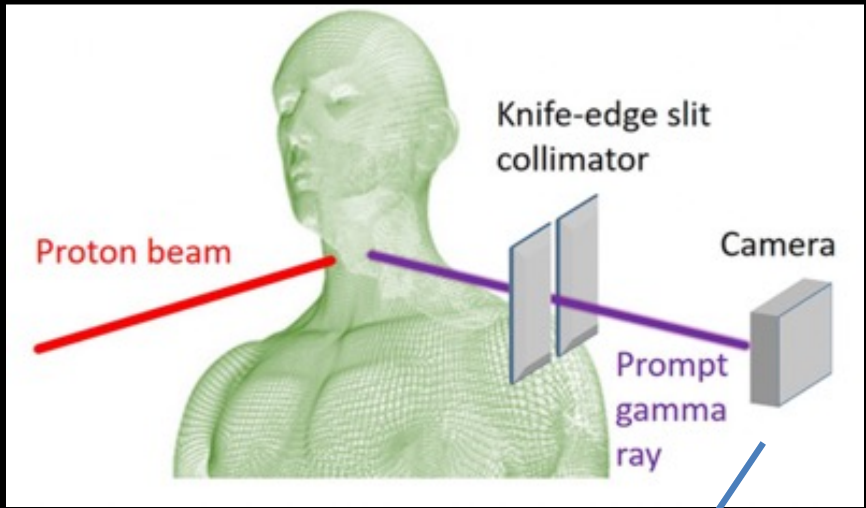

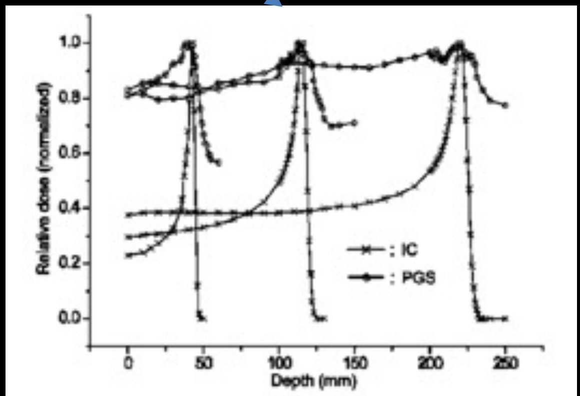

Comparison at 3 different energies

Data from APPLIED PHYSICS LETTERS 89, 183517 2006

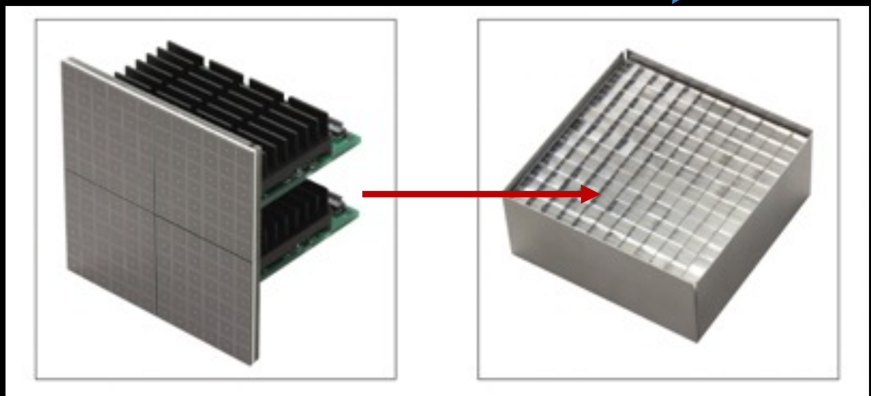

Lyso Crystals and Silicon Photomultipliers

Detectors for Dosimetry in Hadron Therapy

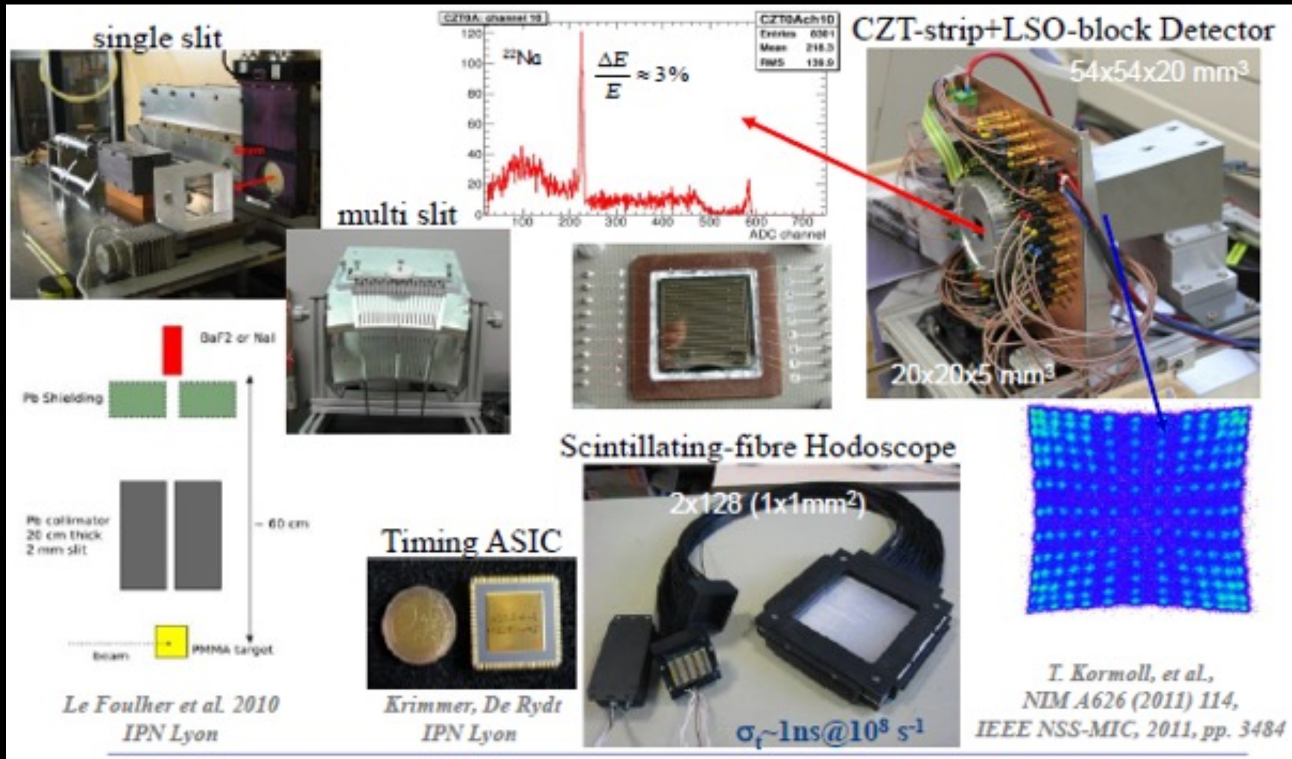

Prompt γ-ray imaging SPECT

TERA

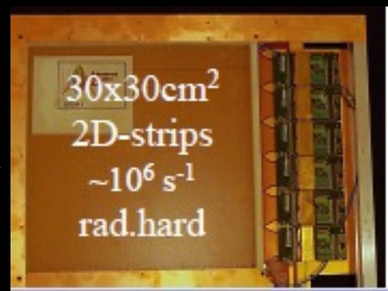

GEM tracker

Interaction-Vertex Imaging

Dosimetry in Hadron therapy: in beam PET

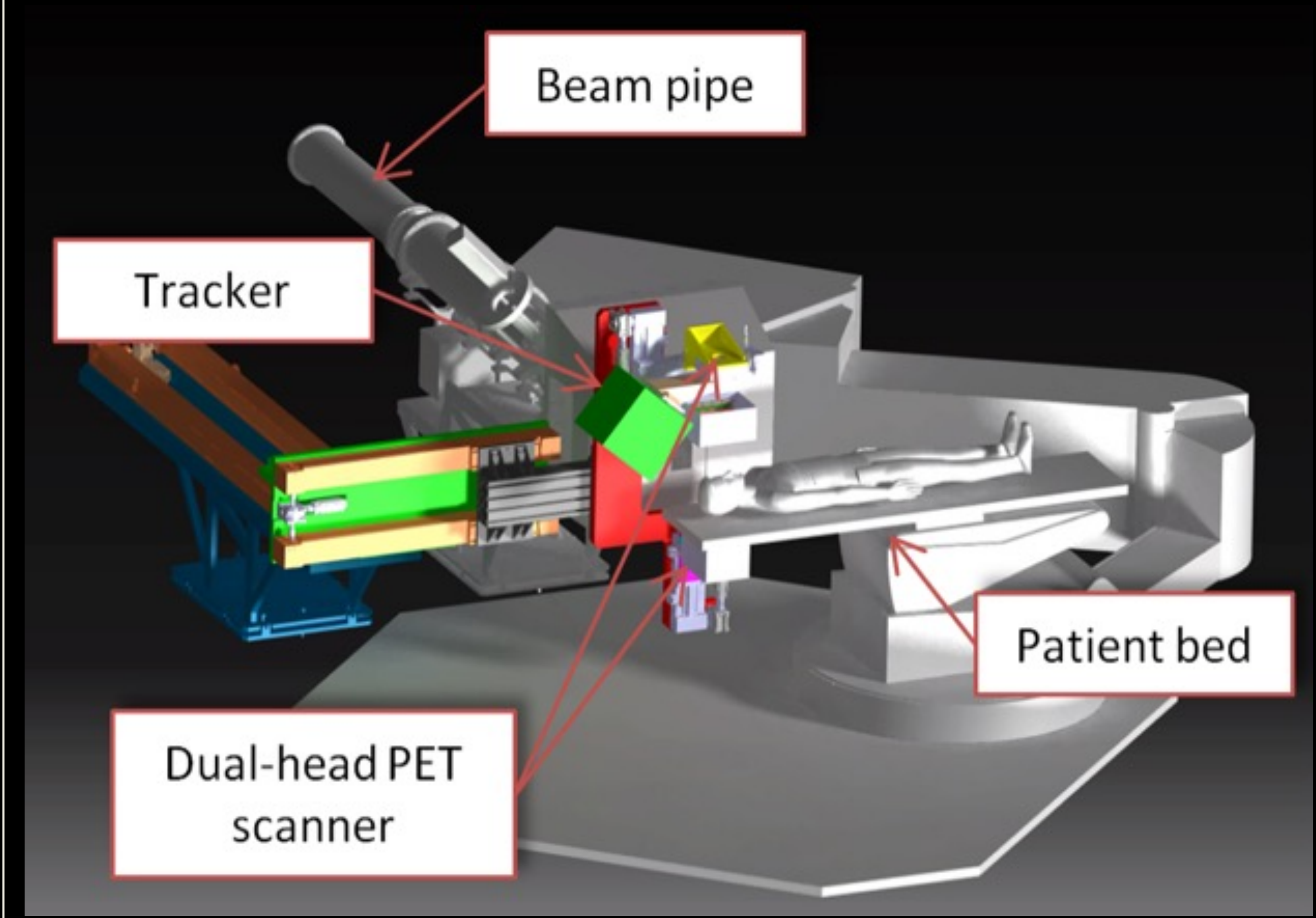

In-beam PET scanner at ^{12}C-therapy unit at GSI

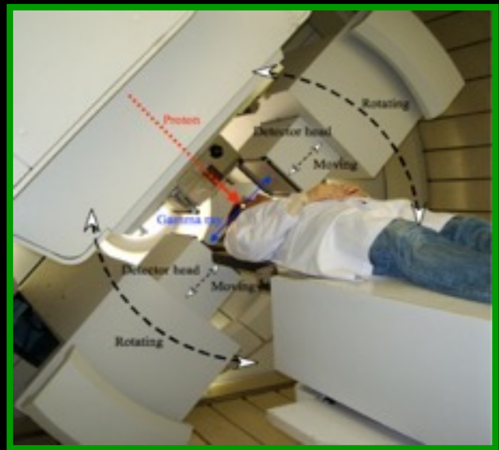

^{1}H-therapy at the National Cancer Center, Kashiwa, Japan

Particle Therapy with Light Ions

Light ions (e.g. Carbon) are more effective than protons or X-rays in attacking cancer.

The particle (or X-ray) breaks the DNA; multiple breaks kill the tumour cell. However, the key mechanism is DNA self-repair by the body cells.

- Protons and X-rays cause single-strand breaks, easy to repair.
- C ions produce a 22 times more ionisations per length generating many double-strand breaks that are much more difficult to repair.

Ions are effective with hypoxic radio-resistant tumours (1 to 3% of cancers), allow for a lower dose thanks to their higher RBE, and have increased dose conformity thanks to less lateral scattering.

So far, 2/3 of cases treated at the mixed facilities (CNAO, etc.) are with carbon.

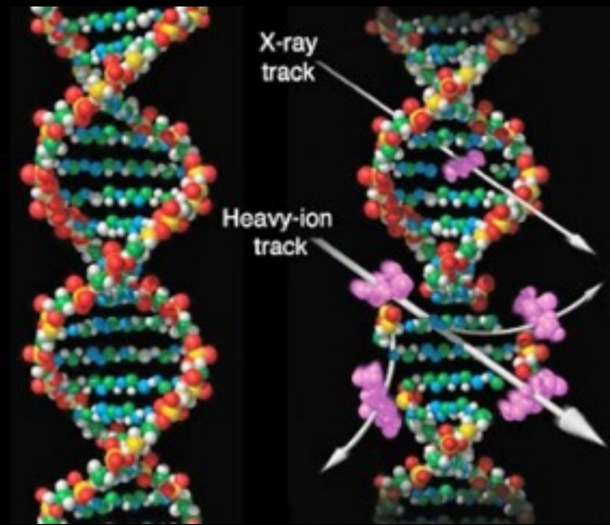

Radio Biological Effectiveness (RBE)
is higher for Carbon than for protons.
1.1 for protons
3 for C ions
(reference is 1 for Co X-rays)

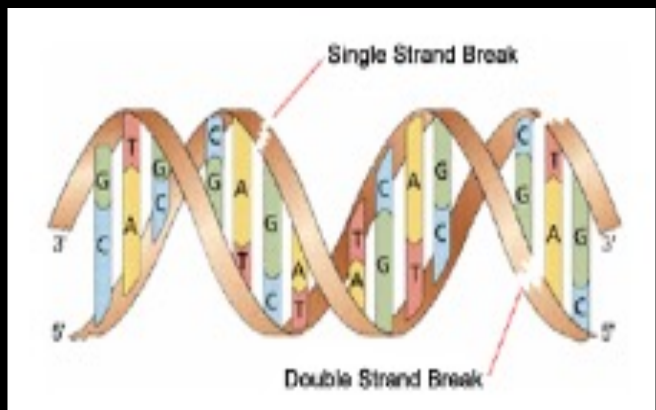

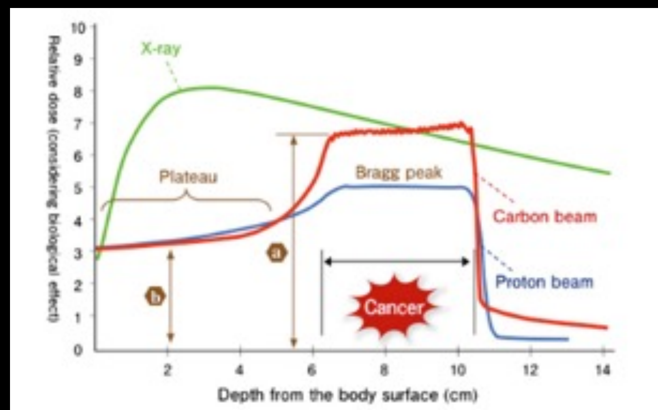

Ion therapy and immunotherapy

Does Heavy Ion Therapy Work Through the Immune System?

Marco Durante, PhD,* David J. Brenner, PhD,† and Silvia C. Formenti, MD†

*Trento Institute for Fundamental Physics and Applications-National Institute for Nuclear Physics, University of Trento, Trento, Italy; †Center for Radiological Research, Columbia University Medical Center, New York, New York; and ‡Department of Radiation Oncology, Weill Cornell Medical College, New York, New York

Received Aug 10, 2016, and in revised form Aug 21, 2016. Accepted for publication Aug 25, 2016.

The «holy grail» of particle therapy

Combination of local therapies with immunotherapy, to convert the individual tumor into an in situ vaccine.

The application of local radiation therapy as an adjuvant to immunotherapy is under active investigation both preclinically and clinically and is currently considered one of the most promising strategies to defeat cancer.

Combining Immunotherapy and Radiotherapy for Cancer Treatment: Current Challenges and Future Directions

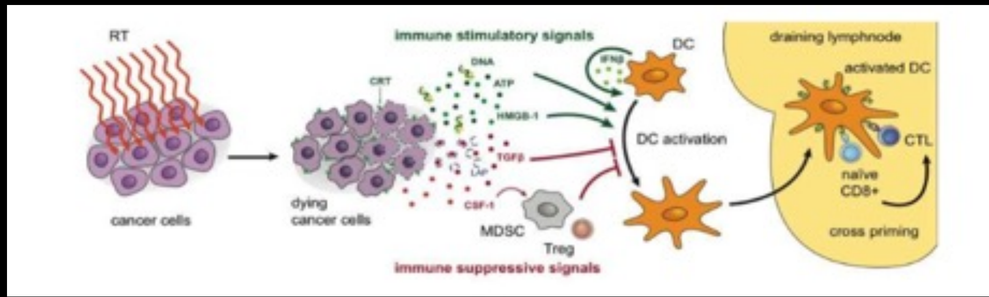

Selection of immunoradiation therapy or standard therapy for patients based on predictive biomarkers.

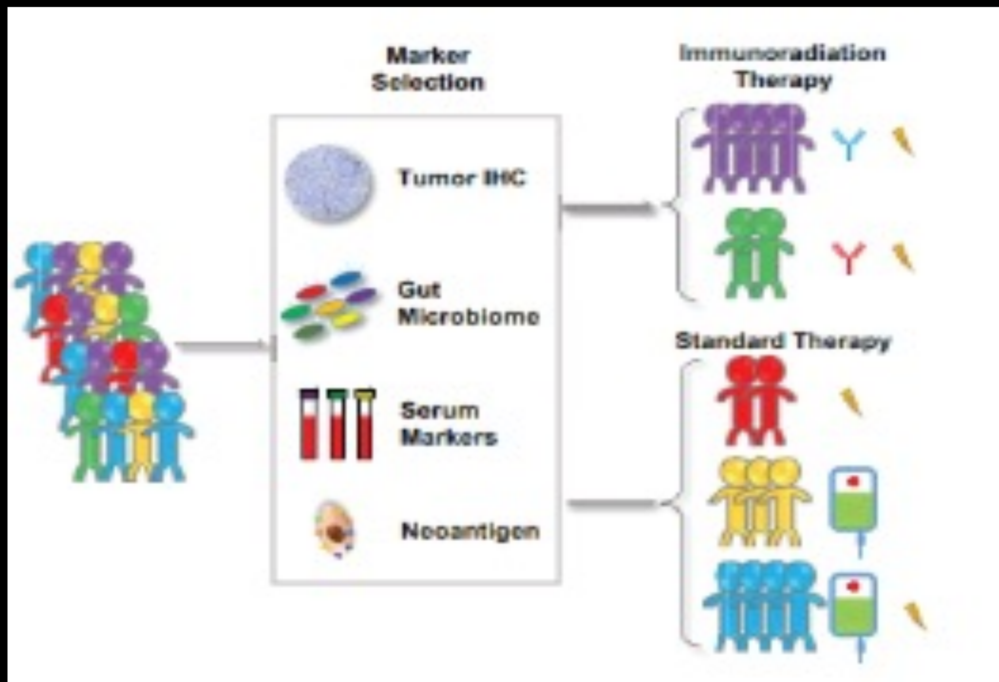

Potential to extend the reach of radiation therapy to diffused tumours and methastasys, responsible for the largest amount of cancer deaths.

Opens the way to personalised treatments, the future of cancer treatment.

International Journal of Radiation Oncology biology • physics

www.redjournal.org

Formenti & Demaria, Lancet Oncol. 2009

FLASH Radiotherapy

https://doi.org/10.3892/ol.2022.13539

FLASH radiotherapy, or **the delivery of ultra-high dose rates of radiation**

(>40 Gy/s)

emerged as a modality of irradiation that enables tumour control to be maintained while reducing toxicity to surrounding non-malignant tissues.

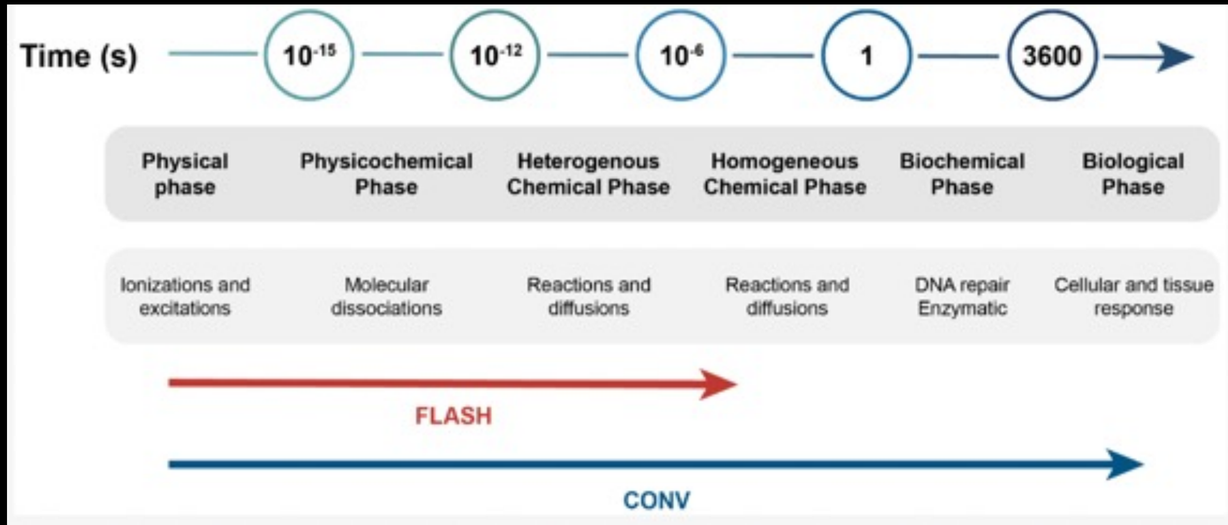

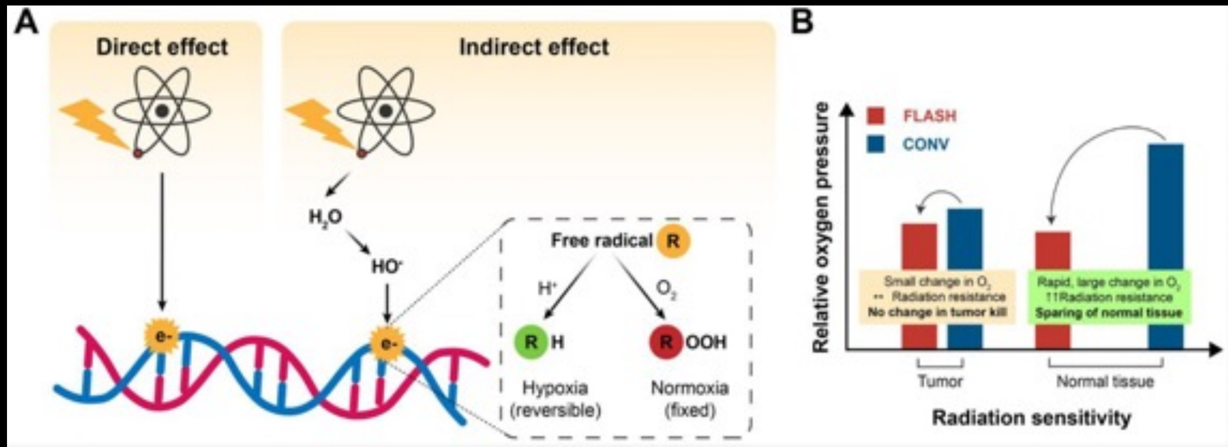

Cinzia Da Via, The University of Manchester, UK & SUNY USA– 2023

Particle Therapy Market

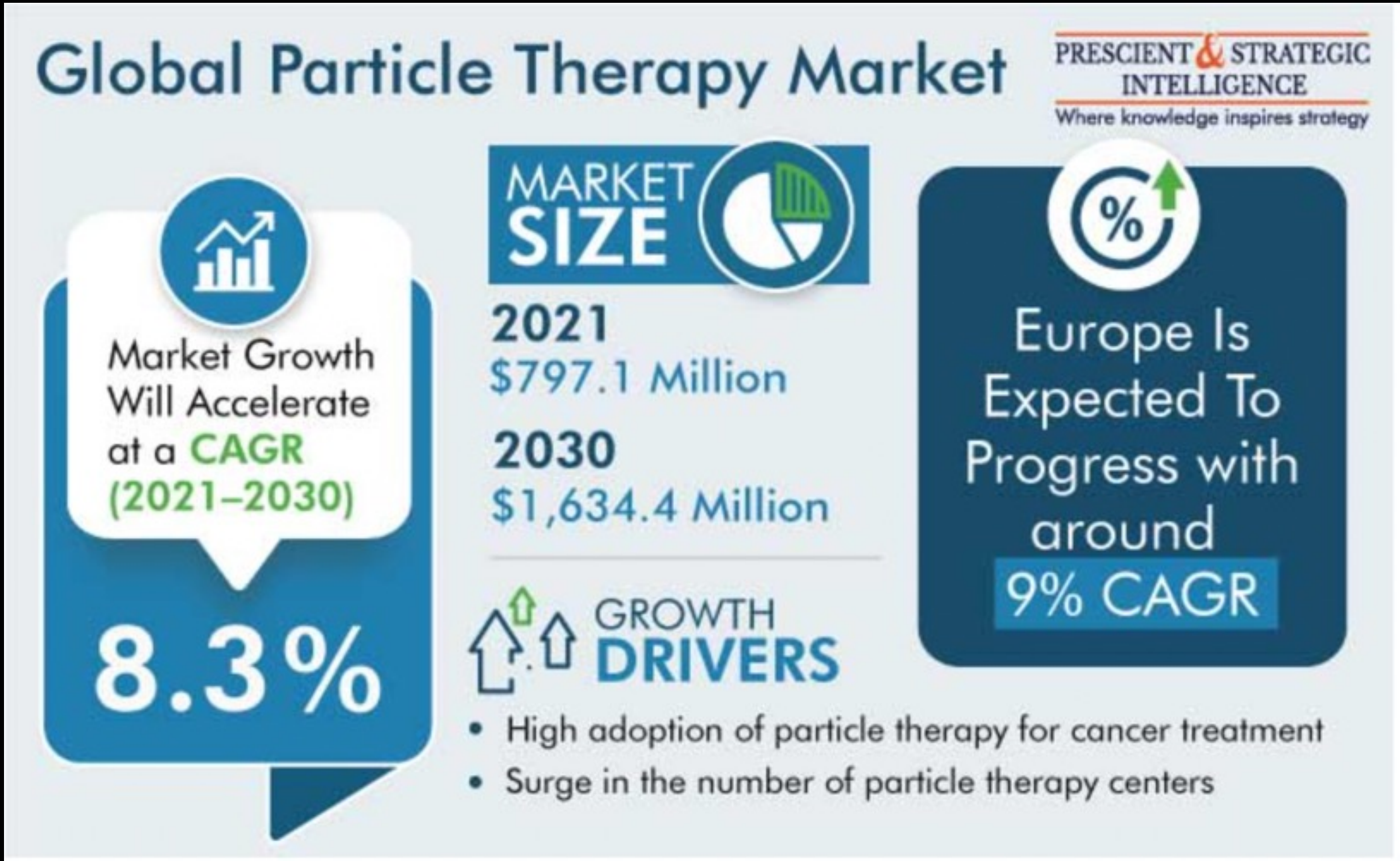

Non-HEP Synergy with Electrical, Material and Civil Engineering

Tunnels for trains
streets etc

Power Systems

Robotics

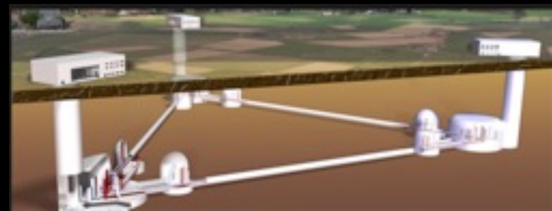

Gravitational Waves
Multi-messengers Astronomy

XXL cavern installations
for Dark Matter
and neutrino searches

Cosmic
rays/AUGER
Radio Astronomy
SKA

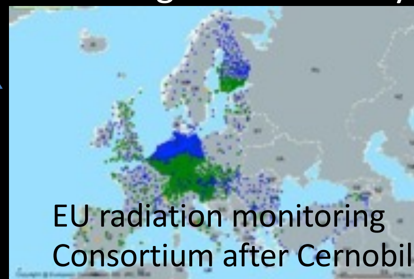

Environmental
monitoring

Non-HEP Synergy with (big) Data Acquisition Systems

Cinzia Da Via, The University of Manchester, UK & SUNY USA– 2023

International Data Corporation (IDC) estimates the amount of data in the world will reach 163 trillion gigabytes by 2025 – Storage and share will be an issue

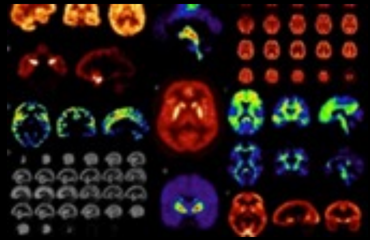

Medicine

Proteomics
Genomics

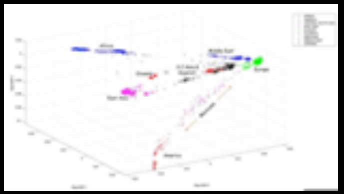

The Swiss Institute of Bioinformatics generates up to 30 Terabites/week in DNA sequencing

Satellites/space

LHC in 2025 2500 petabytes/year (10^{18})

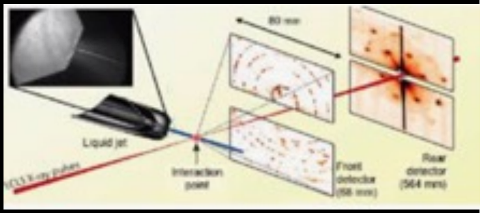

XFELS

Astronomy
Radio-Astronomy
Dark Matter
Gravitational Waves
Multi-messengers

The Blue Brain Project

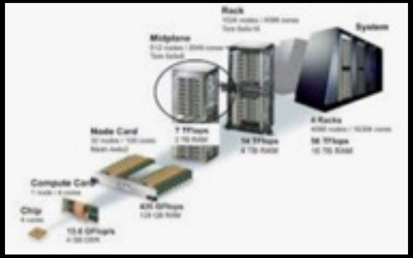

SKA will generate 200 teraflops and storage of about 1.5 petabytes by 2020.
https://www.computerworld.com.au/article/392735ska_telescope_generate_more_data_than_entire_internet_2020/

Non-HEP Synergy with Data Analysis and Simulation

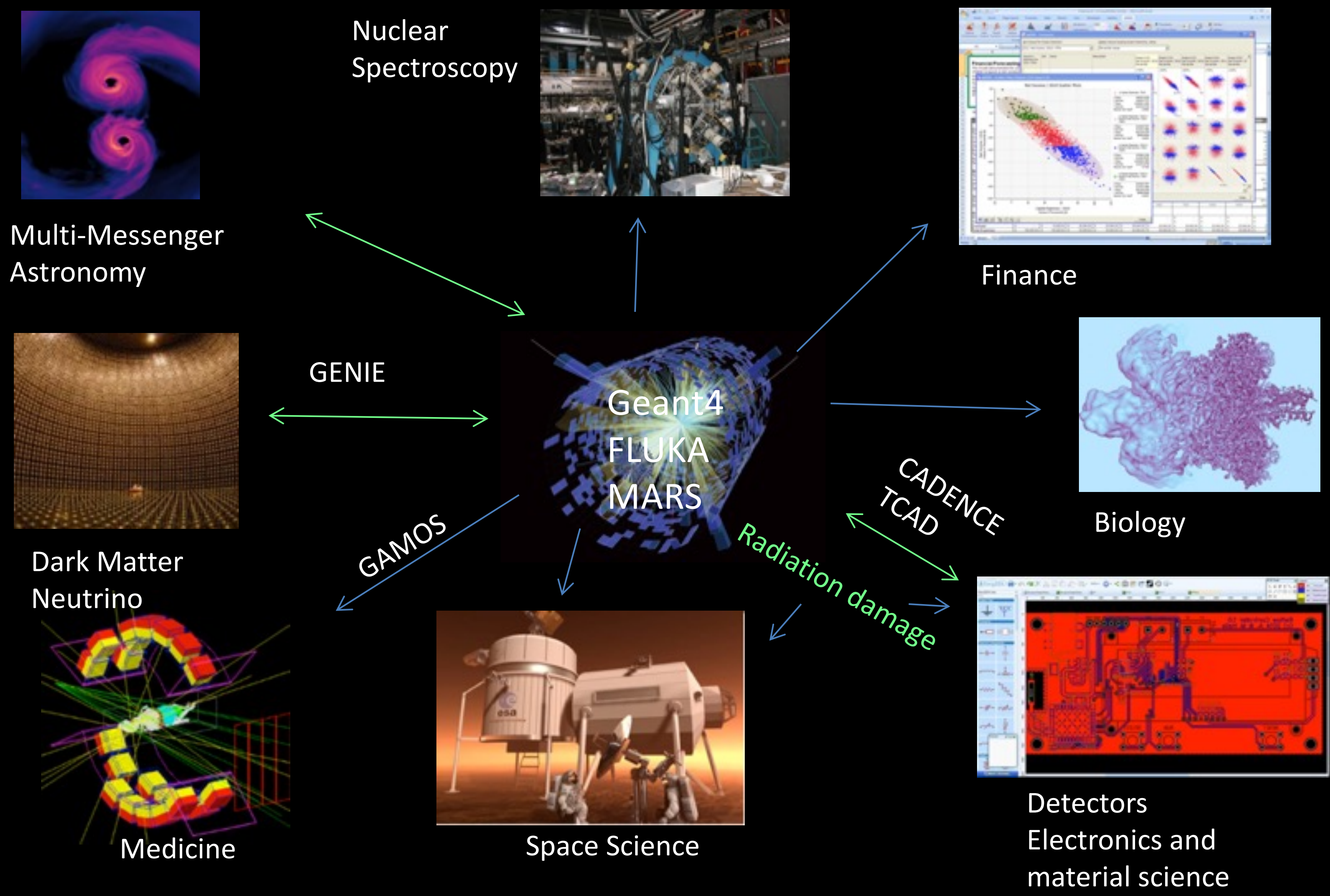

Cinzia Da Via, The University of Manchester, UK & SUNY USA– 2023

Simulation GEANT 4

Higgs event at LHC (CMS)

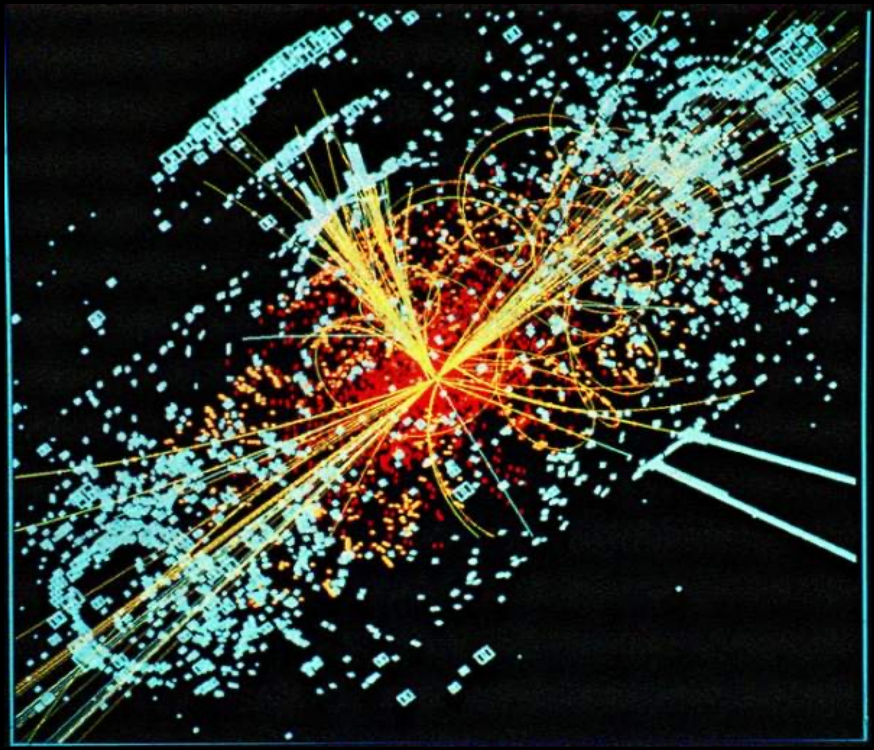

PET with GATE: Geant4 Application for Tomographic Emission

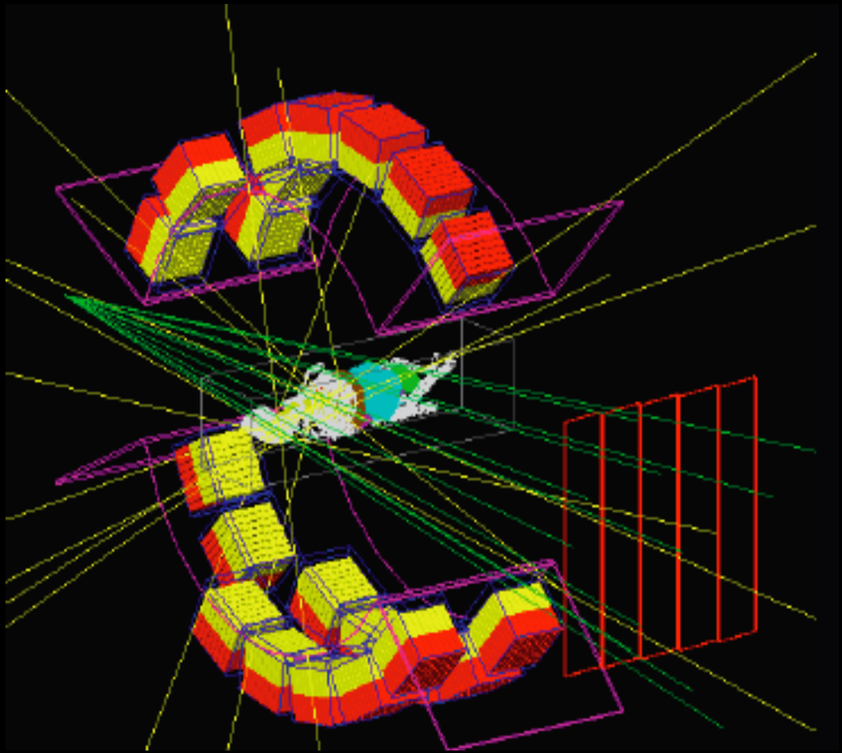

GATE : Geant4 Application for Tomographic Emission

Monte-Carlo simulation allowing to :

✓define geometries
(size, materials,...)
✓ define sources
(geometry, nature, activity)
✓ choice of physical process
(low energy package of G4)
✓ follow track point by point

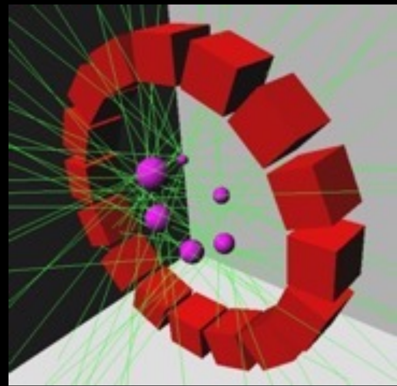

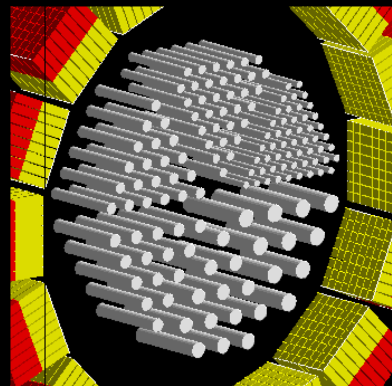

GATE specificities:

✓CERN GEANT4 libraries
✓Time modellign
(sources , movement,random...)
✓Script language(avoid C++)
✓Code interactivity
✓Sharing development

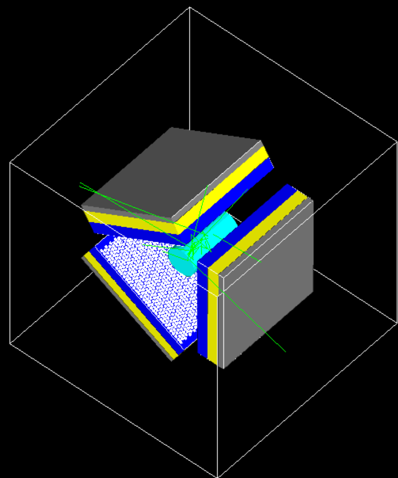

Cinzia Da Via, The University of Manchester, UK & SUNY USA– 2023

AI in GATE (EGEEE)
Enabling GRID for EsciencE

GEANT4 Application to Tomography Emission

- Scientific objectives

  Radiotherapy planning to improve cancer treatment by ionizing radiations illumination of the tumours.

  Therapy planning is computed from pre-treatment MRI scans by accurately locating tumours in 3D and computing radiation doses applied to the patients.

- Method

  GEANT4 base software to model physics of nuclear medicine.

  Use **Monte Carlo simulation** to improve accuracy of computations (as compared to the deterministic classical approach)

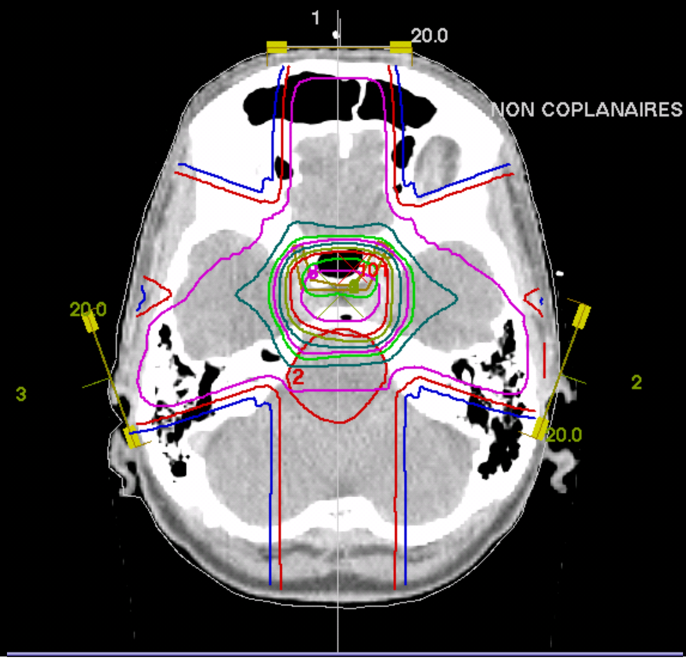

http://www.topasmc.org/

TOPAS is an open-source platform which wraps and extends the Geant4 Simulation Toolkit to make advanced Monte Carlo simulation of all forms of radiotherapy easier to use for medical physicists.

TOPAS can model x-ray and particle therapy treatment heads, model a patient geometry based on CT images, score dose, fluence, etc., save and replay a phase space, provides advanced graphics, and is fully four-dimensional (4D) to handle variations in beam delivery and patient geometry during treatment.

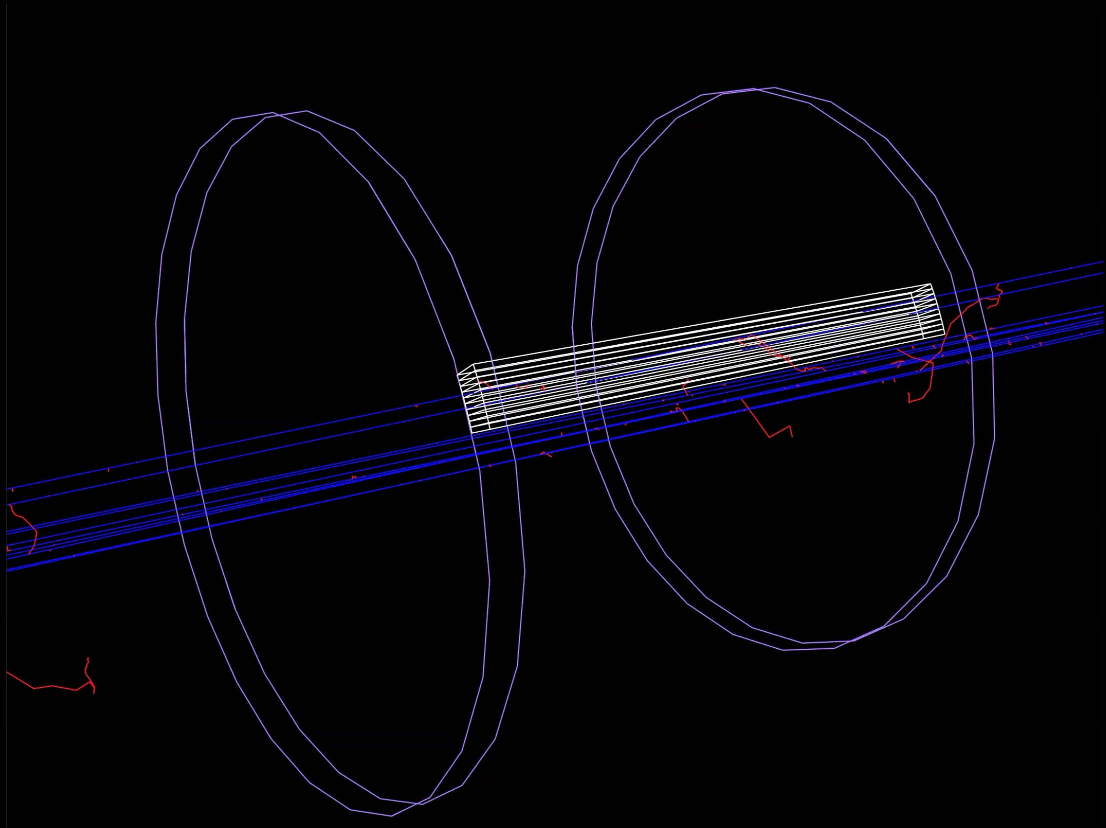

Non-HEP Synergy with Particle Detectors

High Precision Radiation Detection and Imaging – Test Facilities

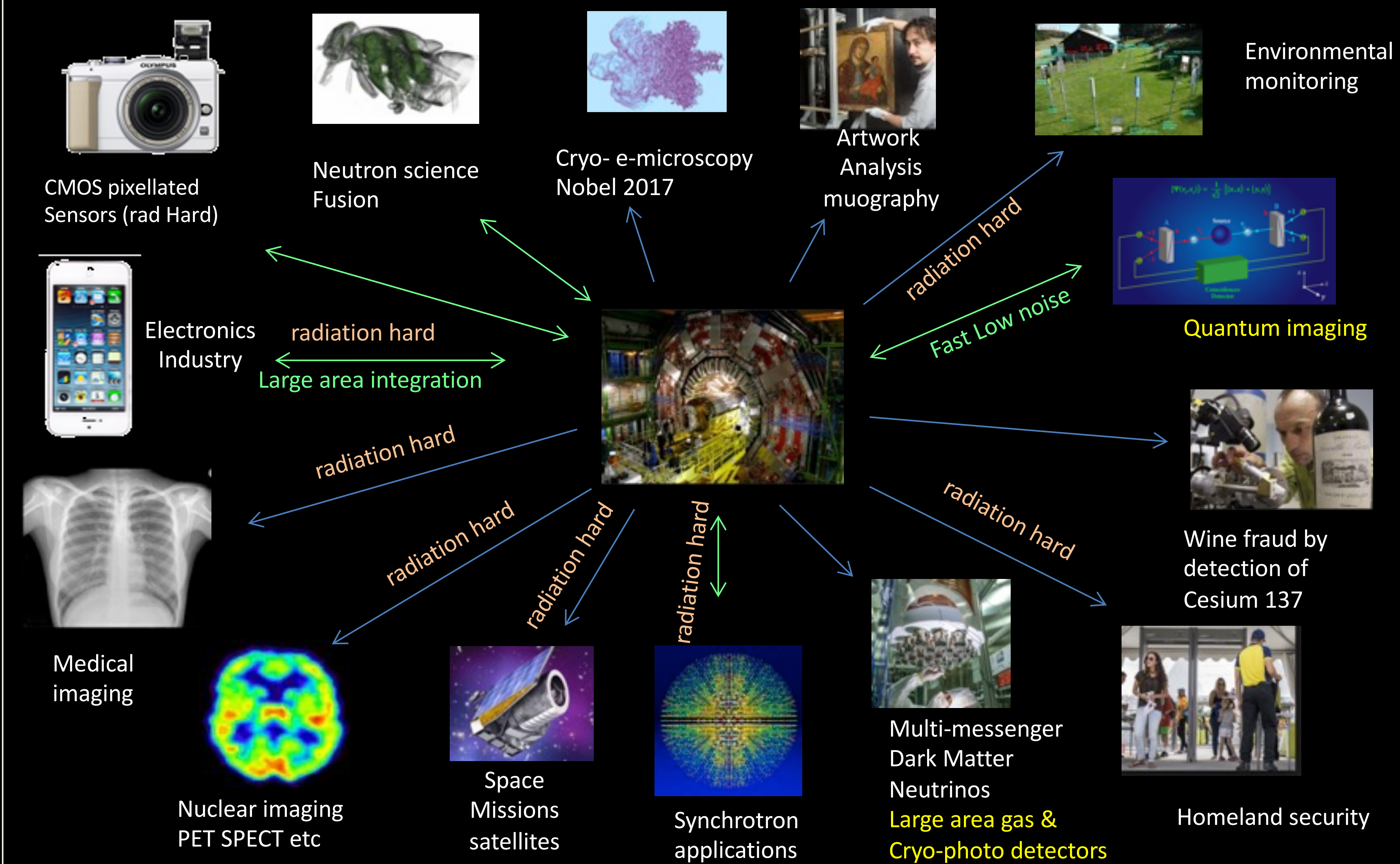

Cinzia Da Via, The University of Manchester, UK & SUNY USA– 2023

Evidence of Converging Detector Requirements and R&D needs among disciplines

ERDIT

European Radiation Detectors and Imaging Technology

	HEP	SYNC	Neutron ESS	Beam monitoring	Astronomy	Hadron Therapy	Medical Imaging Pre-clinical Imaging	Electron Microscopy	Environmental radiation monitoring IAEA
Radiation type	p, n, γ	X-rays	n	p, n, γ, e^-	λ=300nm to 28μm	N, p, γ, light ions (protons to oxygen)	X-rays	e	γ
Max Intensity	12×10^{15} ncm^{-2}	2700 pulses	10^{8} ncm^{-2}	10^{17} ncm^{-2} (p, n) 10MGy (e^-)	from 1 photon/hour/pixel to 1E9 photons/s/pixel	conventional accelerator up to 10^10 ions /s Laser > 10^7/cm2 (ps pulses, low repetition rate ~ 1/s)	CT: 10^9 g/mm²/s, General X-ray: 10^8 g/mm²/s Angiography: 10^8 g/mm²/s Mammography: 10^7 g/mm²/s	20 Mrads	100 μSv/h (~100,000 cts/s)
timing	25ns 10ps	4.5 MHz 10ps	1us	Sub ns	from 2000 frames/s to 1 frame/hour	Up to MHz (singles rate) 10ps	CT: 5000 frames/s General X-ray: - Angiography: 1-60 frames/s Mammography: - 10ps	1000 frames/s	
Pixel size (Min)	50x50 um²	10x10 um²	50x50 um²	50x50 um²	10x10 um²	50x50 um²	CT: 1000 mm General X-ray: 150-200 mm Angiography: 150-200 mm Mammography: 85 mm	10x10 um²	
Spectral resolution	yes	yes	no	yes	no , moderate possible with APD	yes	Today: not used, Future: yes	yes	< 1.5% @ 662 keV
Detector size (max)	2500m² (ILC cal)		80m²	100 cm²	Optical 9Kx9K NIR 4Kx4K	40x40 cm2	CT: 10 x 100 cm² (segmented), General X-ray : 43x43 cm² Angiography: 30x40 cm² Mammography: 24x30 cm²	8k x 8k pixels	6 cm³

Cinzia Da Via, The University of Manchester, UK & SUNY USA– 2023

X-ray energy of the most common medical and biological applications

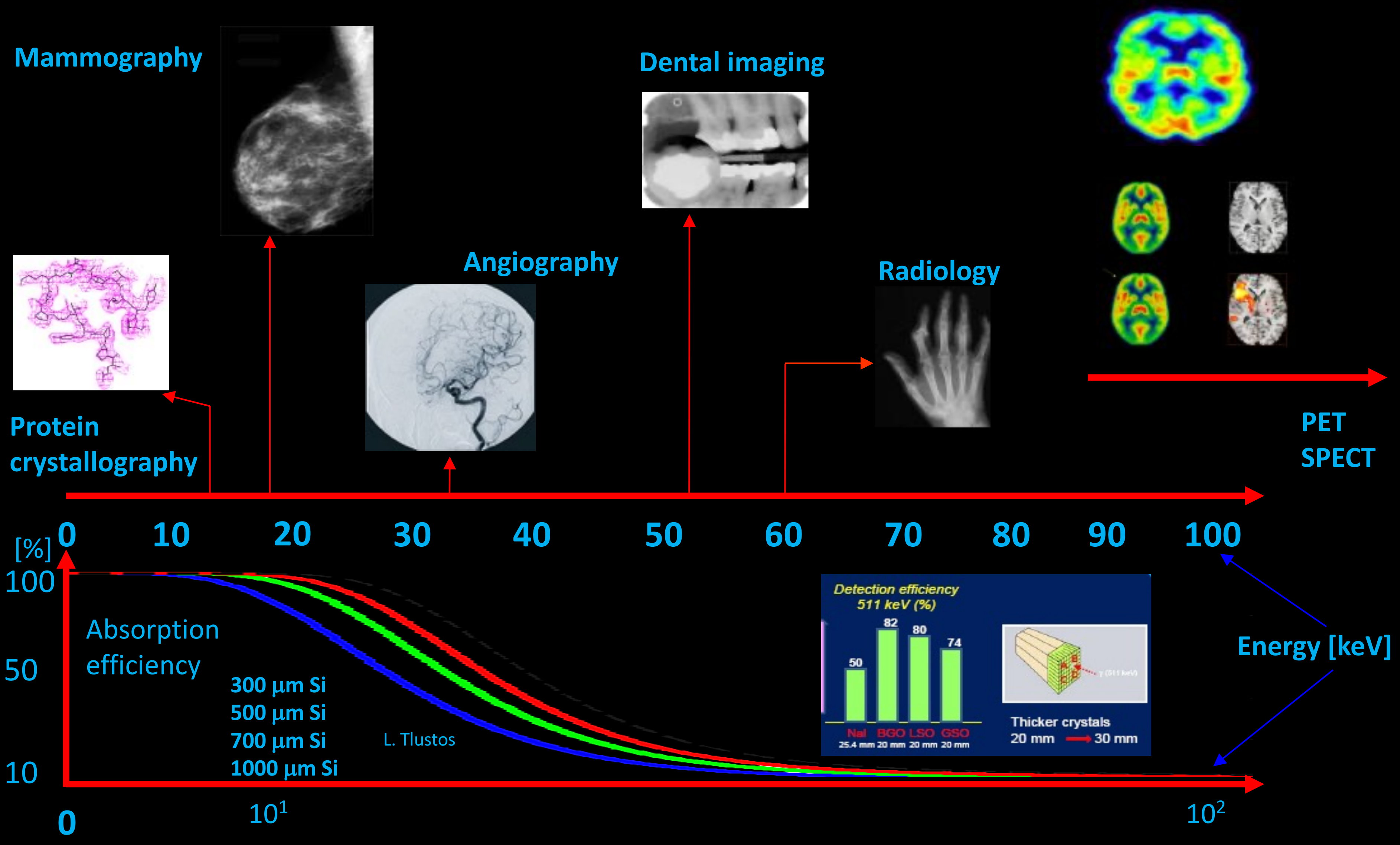

Cinzia Da Via, The University of Manchester, UK & SUNY USA– 2023

C. Da Via' 2007

X-Ray Imaging

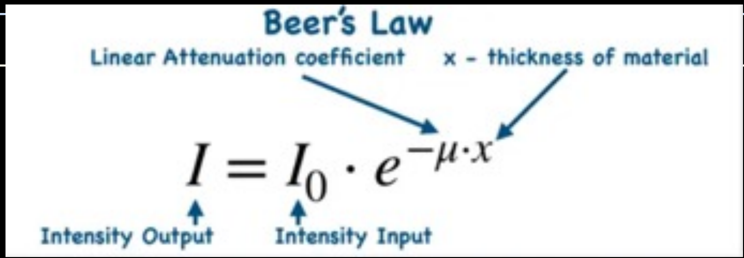

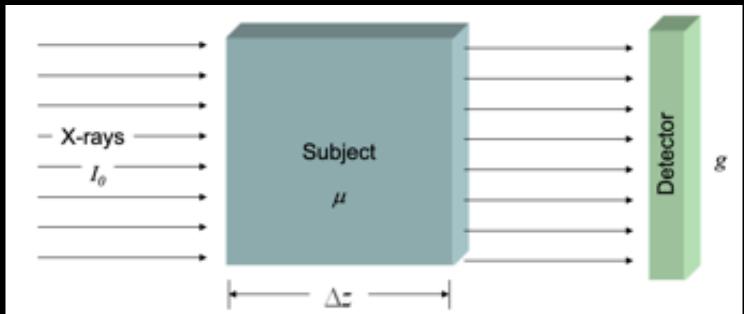

X-ray Absorption depending on material

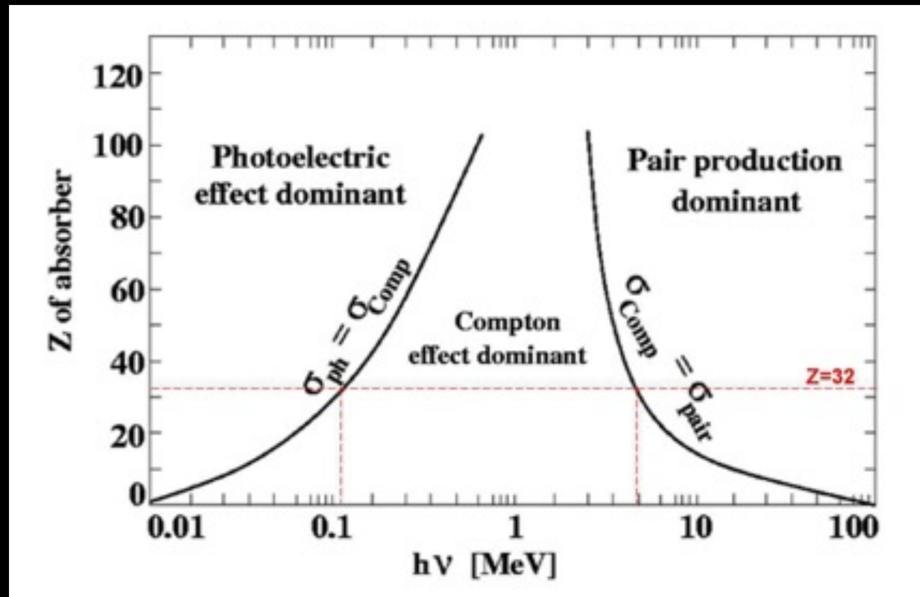

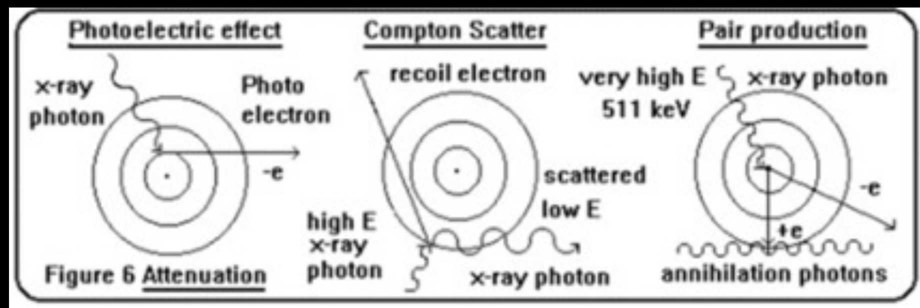

Cinzia Da Via, The University of Manchester, UK & SUNY USA– 2023

Modern X-ray Radiology: EID vs ERPCD

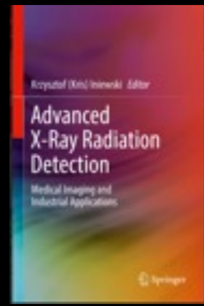

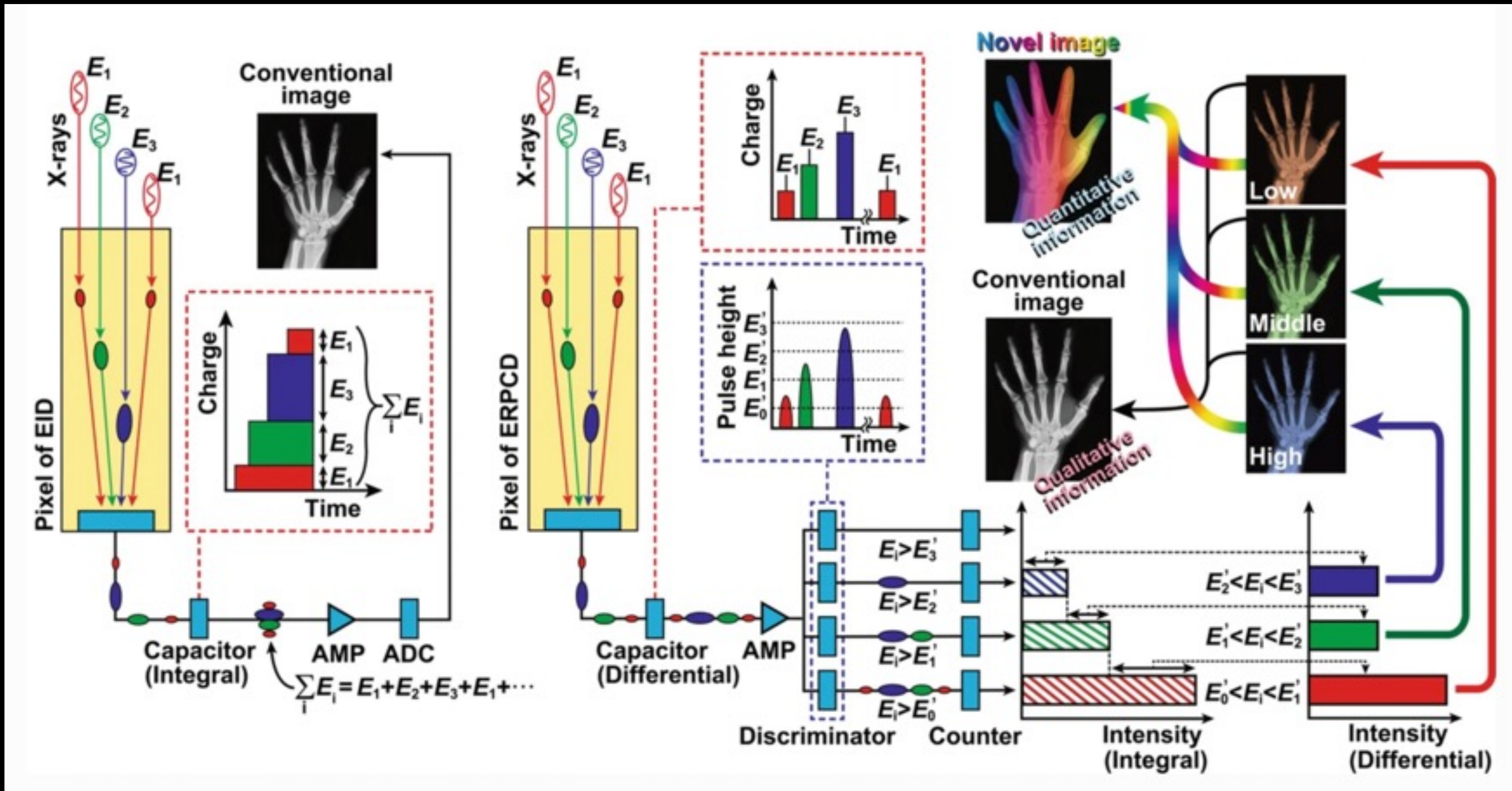

Comparison between **Energy Integrating Detector (EID)** and **Energy-Resolving Photon-Counting Detector (ERPCD).** The EID generates images with information related to the sum of the energies. On the other hand, the ERPCD can analyse each X-ray energy – so a spectral analysis of the image

Multiple-contrast X-ray radiographs

https://doi.org/10.1038/s41598-020-70363-w

(a) Conventional radiograph image of a human hand.
(b) Bone
(c) Soft-tissue-equivalence image
(d) Bone-tissue-overlay image generated by superposing the two basis component images. In the overlay image, the bone-components are coloured in blu.

Radiography requires good contrast, resolution, S/N

Organ	dose skin mGy	effective dose mSv
Thorax, face	0,2 - 0,5	0,015 - 0,15
Lumbar region	4 - 28	1,5
Urography	40 - 60	3
Brain scan	7 - 78	1
Whole Body scan	30 - 60	4 - 10
Mammography	7 - 25	0,5 - 1

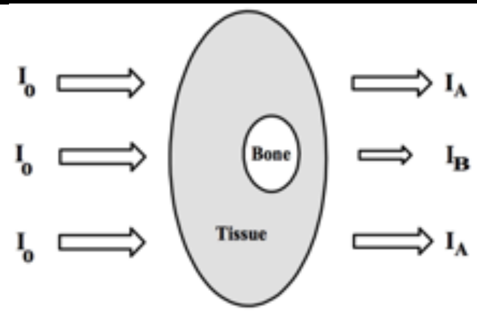

The objective of the new technologies is to increase precision and reduce the dose

Optimum image quality has adequate resolution and contrast, and a low noise level

This image has high spatial resolution and low noise, but it has almost zero contrast.

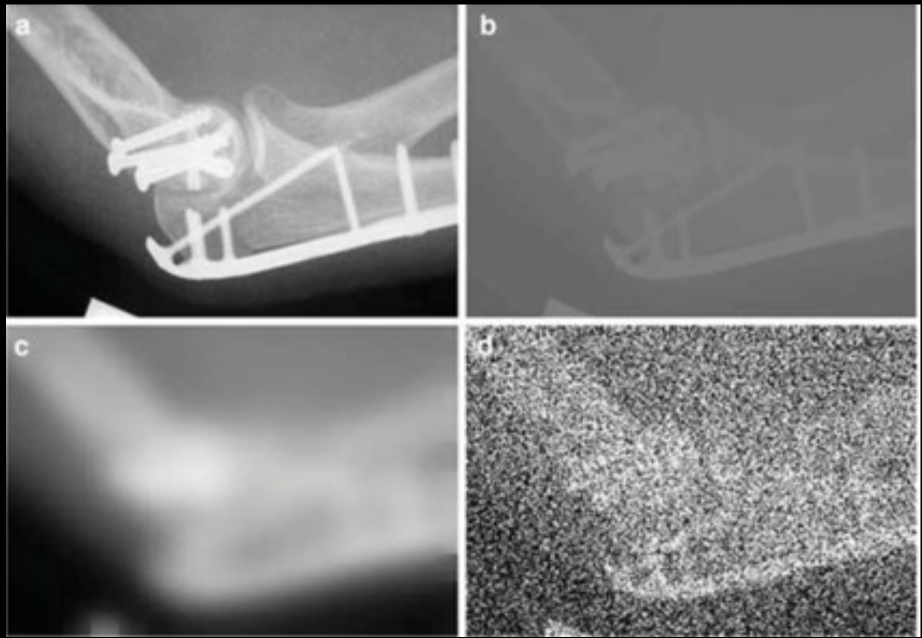

This mage has low noise and high contrast, but very poor spatial resolution.

This image has high spatial resolution but very high noise level which destroyed the image contrast

Cinzia Da Via, The University of Manchester, UK & SUNY USA– 2023

Cinzia Da Via, The University of Manchester, UK & SUNY USA– 2023

Direct / indirect conversion

The target is to reduce the dose to the patient!

Scintillator
Gadox, YAG CsI
(high Z)

Photodiode/ CCD

electronics

electronics

Sampled image

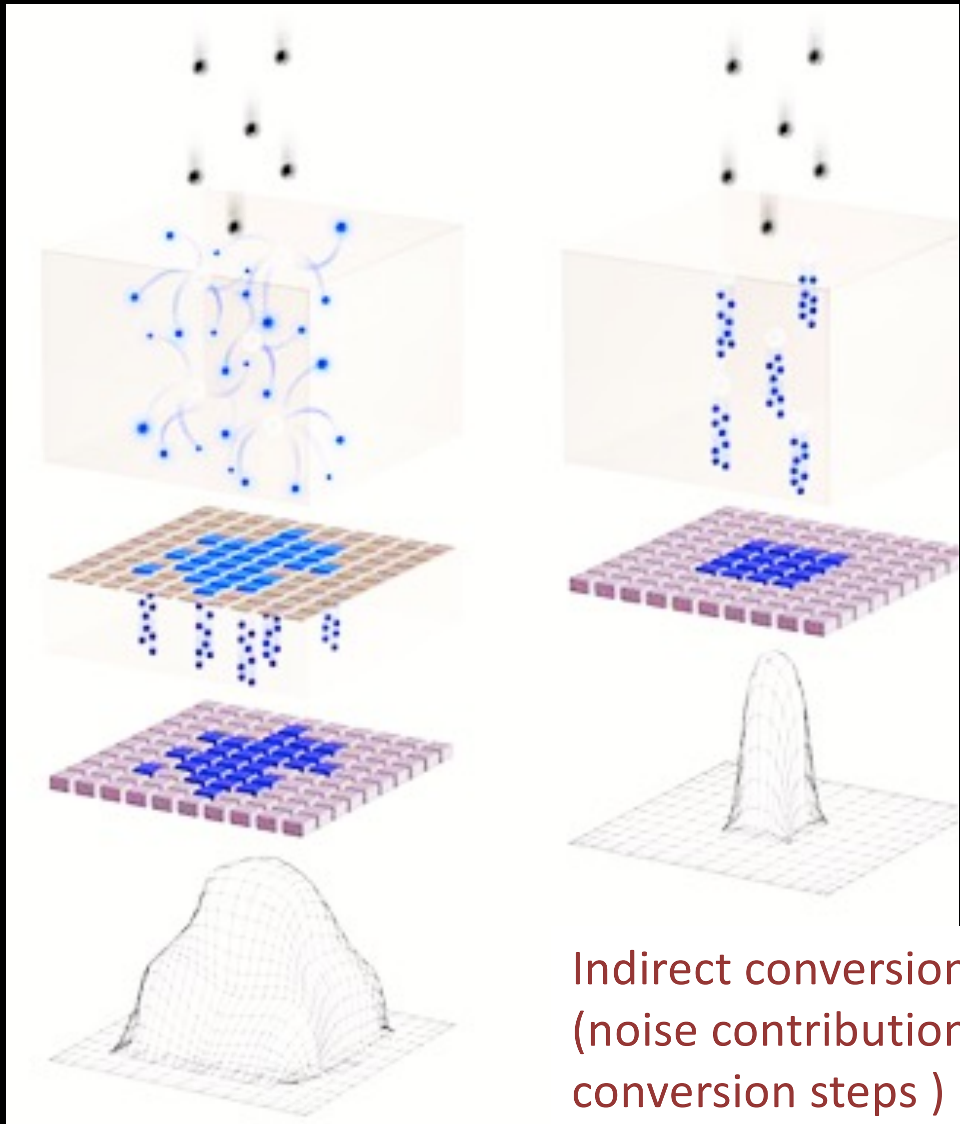

X-rays

Direct conversion
Si, Ge, CdTe,
GaAs, Se

Sampled image

Indirect conversion implies lower DQE (noise contribution from the two conversion steps)

High Z Materials for direct conversion

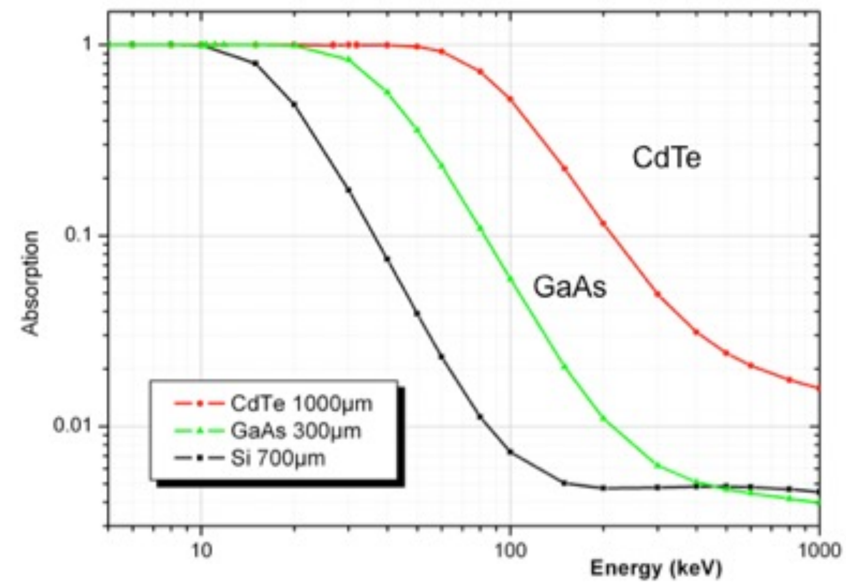

Absorption

@ 40keV:

Si: 7.5%

GaAs: 55%

CdTe: 100%

@ 60keV:

Si: 2.2%

GaAs: 22%

CdTe: 90%

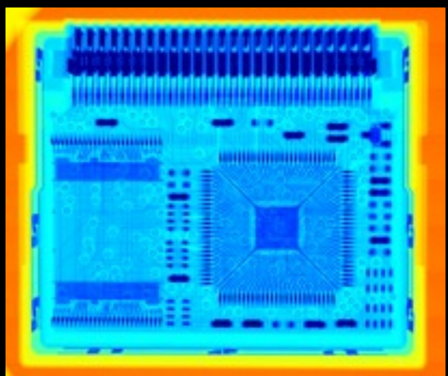

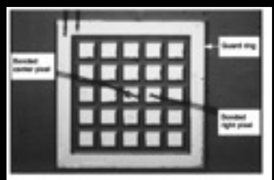

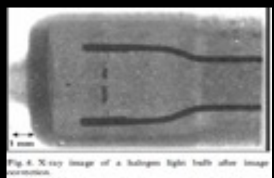

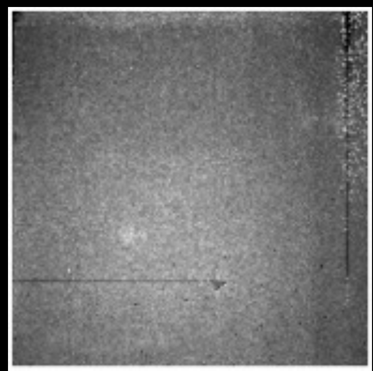

MPX3 CdTe 1mm – SPM 55µm

Cinzia Da Via, The University of Manchester, UK & SUNY USA– 2023

Timepix3 hybrid detector

https://www.researchgate.net/publication/341026498

GaAs -90 KeV
350um thick

Features

•Pixel size 55µm x 55µm
•256 x 256 pixels
•Timepix3 is suitable for readout of both semiconductor detectors and gas-filled detectors
•Single thresholds per pixel each with 4 bits of local adjustment

•Two main measurement modes:

•(1) simultaneous 10 bit ToT and 18 bit TOA and
• (2) 10 bit event counting and 14 bit integral TOT

•TOT monotonic for large positive charges
•Fast TOA for time stamping with a precision of 1.56 ns
•Data driven readout: dead time free, for a maximum hit rate of 40 Mhits/s/cm^2
•Shutdown/wake-up features for power pulsing tests on a full system
•3-side buttable (with a single 1.2mm dead edge)
•TSV ready

Applications

•X-rays imaging
•Particle track reconstruction.
•Timepix3 is suitable for readout of both semiconductor detectors and gas-filled detector

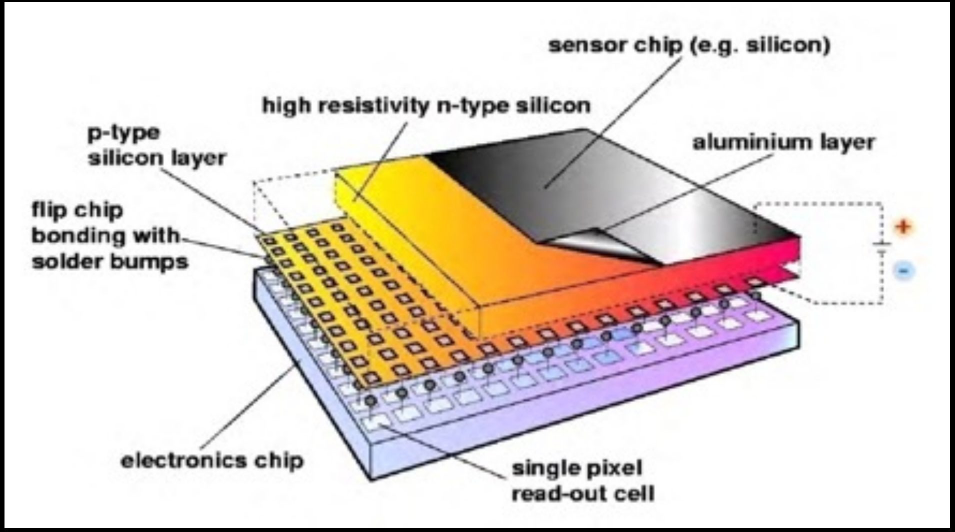

Particle signatures with the Timepixel detector

α | 5 KeV X-rays | 2MeV electrons

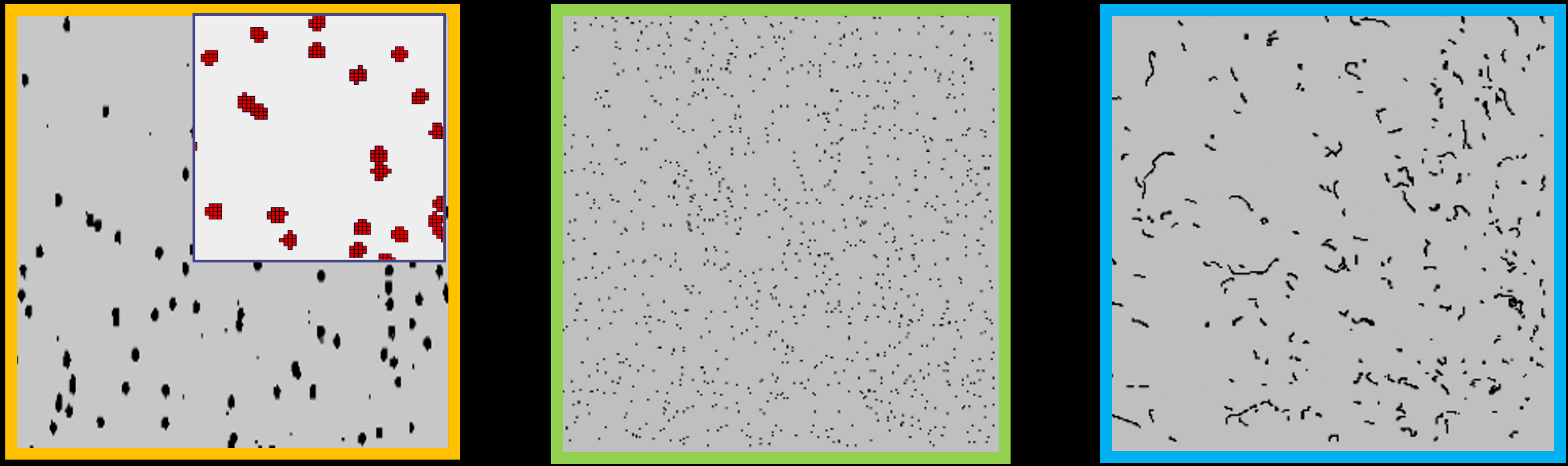

- ^{241}Am alpha source gives clusters of ~5x5 pixels measured with the MEDIPIX-USB device and a 300 µm thick silicon sensor. The clusters are shown in detail in the inlet. The cluster sizes depend on particle energy and threshold setting.
- Signature of X-rays from a ^{55}Fe X-ray source. Photons yield single pixel hits or hits on 2 adjacent pixels due to charge sharing.
- A ^{90}Sr beta source produces curved tracks in the silicon detector.
- A pixel counter is used just to say "YES" if individual quantum of radiation generates in the pixel a charge above the pre-selected threshold

Medipix and Timepix : 55x55um^2 256 x 256 pixels

https://medipix.web.cern.ch

Space weather and dosimetry

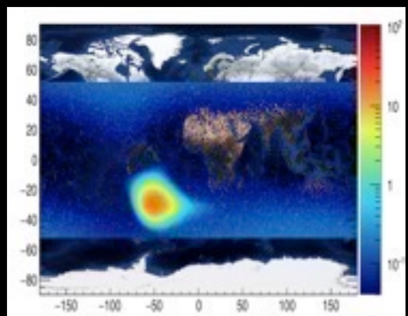

Mixed field radiation monitoring and dosimetry

NASA/Univ. Houston/IEAP Prague

Cultural heritage studies

Investigation of art using colour X-ray imaging

InsightArt, Prague

Medical colour X-ray imaging

World first colour X-ray image of a living human

- Clearer images
- Lower dose
- Material separation

MARS Bioimaging, NZ

Pixels Sensors in High Energy Physics

Radiation Hardness
hybrid

Granularity, low mass
monolithic

3D sensors

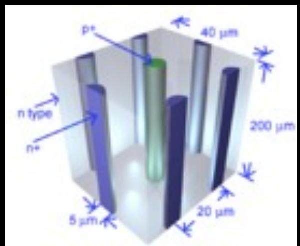

diamond

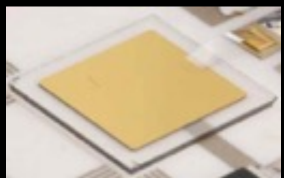

n-in-n, n-in-p-
planar

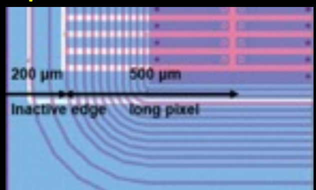

CCD

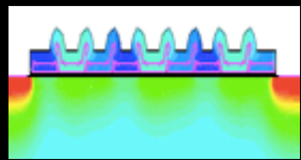

Mimosa

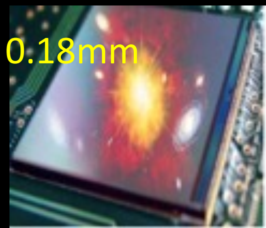

HV-MAPS

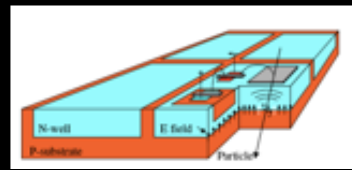

DEPFET

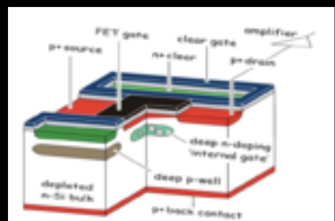

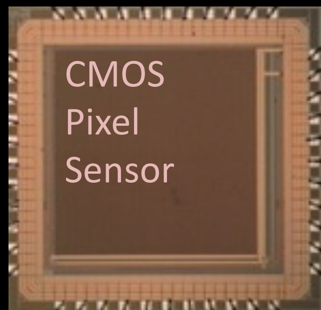

deepNwell

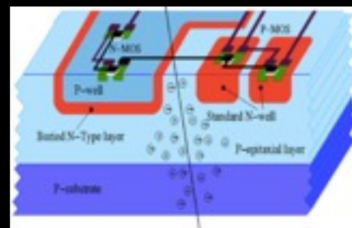

SOI

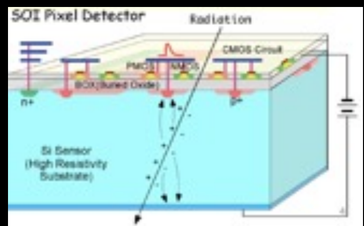

INMAPS

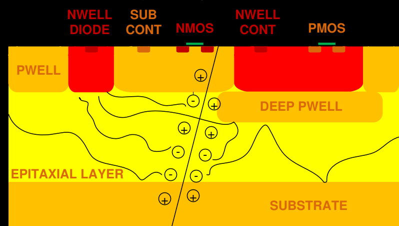

LePiX

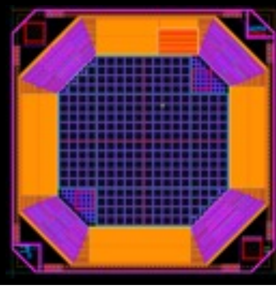

Cinzia Da Via, The University of Manchester, UK & SUNY USA– 2023

Indirect Conversion: Scintillators and Silicon Photomultipliers (SiPm, GM-APD, MPPC…)

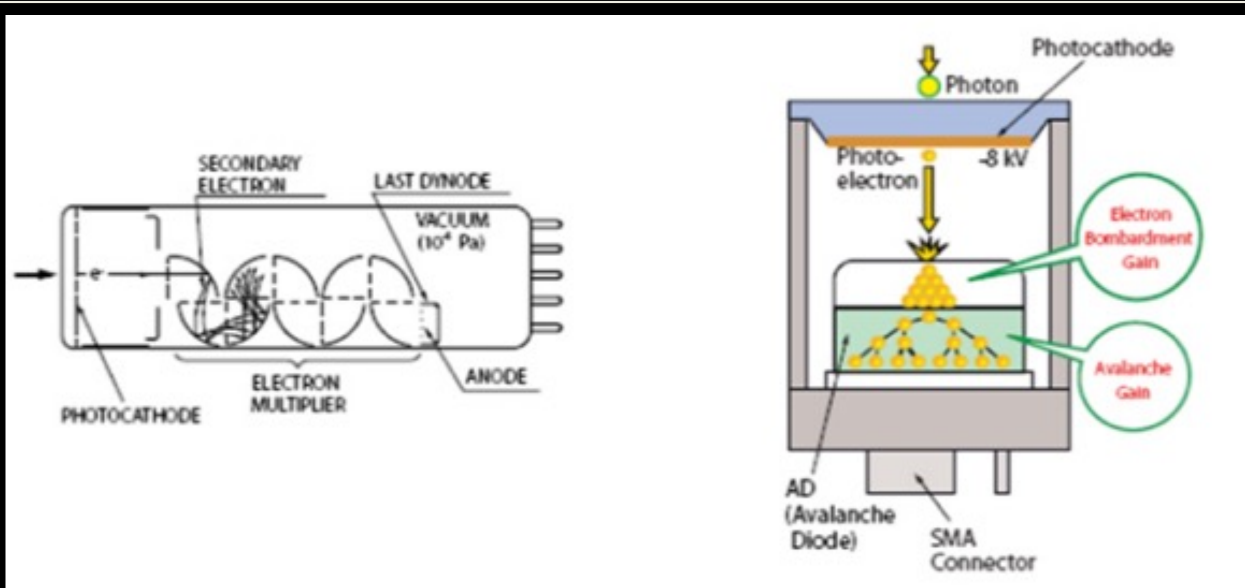

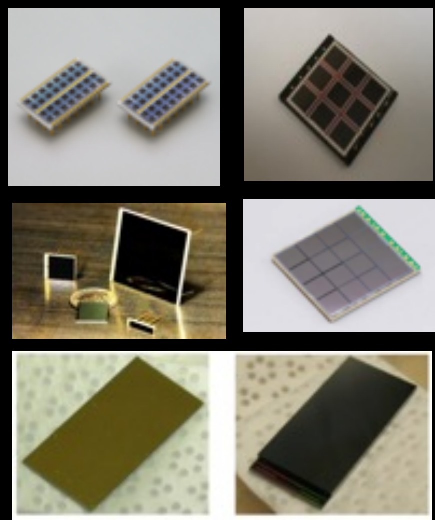

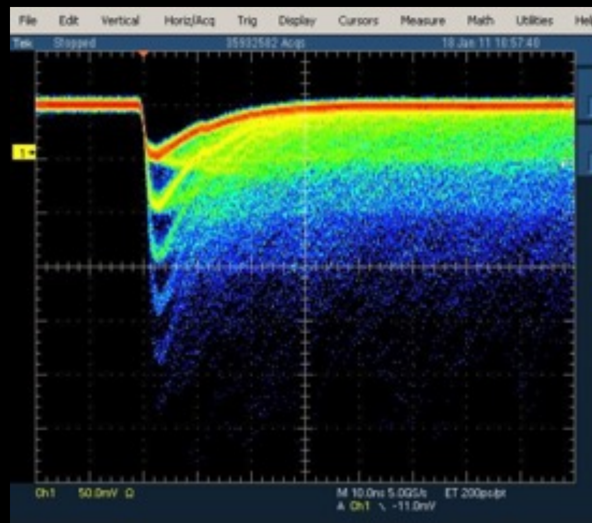

Cinzia Da Via, The University of Manchester, UK & SUNY USA– 2023

Gaseous Pixel Detectors + Medipix

H. van der Graaf (Nikhef) TIPP2011

Gaseous Pixel detector (GridPix) is a MEMS made Micromegas like structure on a CMOS readout chip

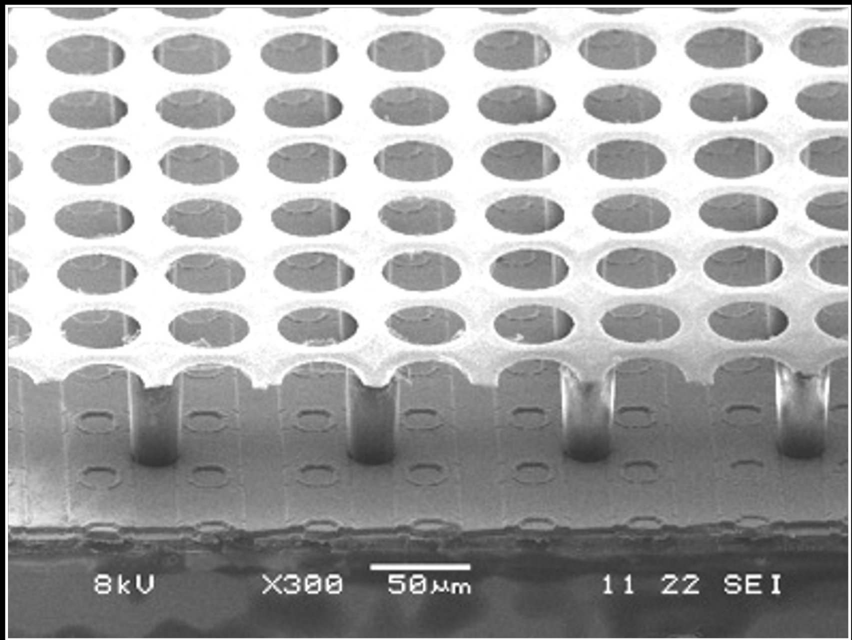

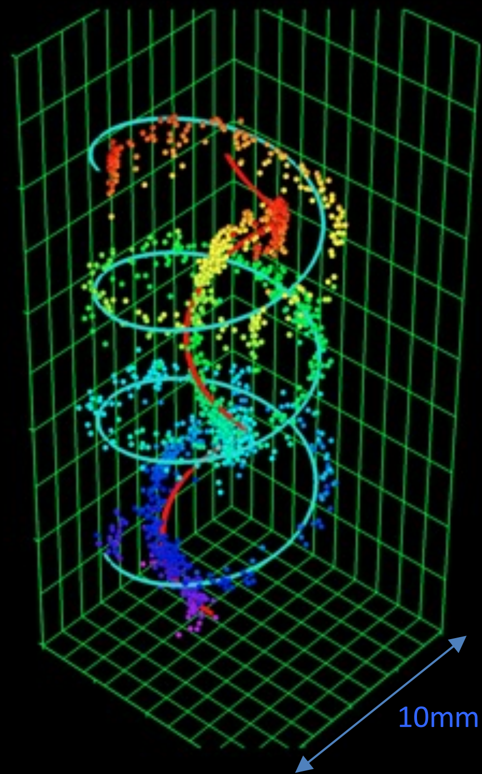

^{90}Sr electrons in 0.2 T B-field

Performance :

- position resolution:15 µm
-single electron efficiency: > 90 %
- track detection efficiency: 99.6 %;

µ-TPC operation with TimePix chip

Silicon for Synchrotron and low X-ray energy Applications

Single photon Counting — Charge Integration

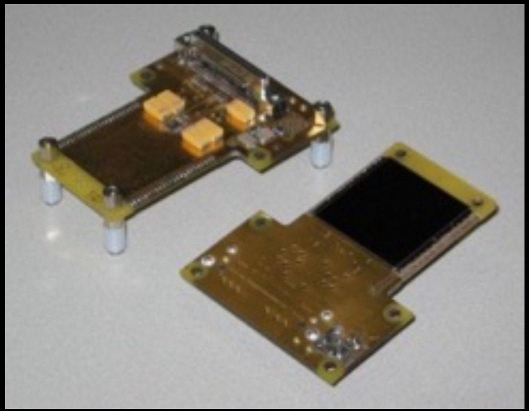

Medipix2 Quad
Pixels: 512 x 512
Pixel size: 55 x 55 mm^2
Area: 3 x 3 cm^2

Medipix

pixellated hybrid detector (Si, GaAs, CdTe, 3D thickness: 300/700/1000mm

Gotthard

AGIPD

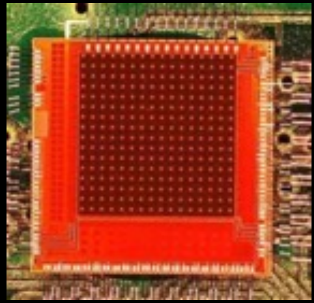

Mithen II

Eiger

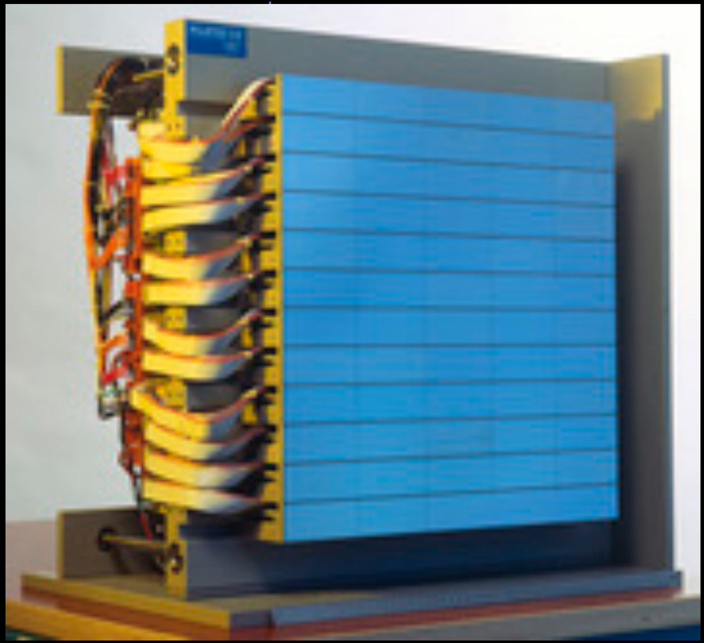

The PILATUS 6M,

424 x 435 mm2 with 170 × 170 μm^2 (2463 x 2527) 6 million pixels, has been developed at PSI and commercialized by the company Dectris for synchrotron imaging

Mammography, digital breast tomosynthesis (DBT), also known as 3D mammography

Digital Mammograms have a pixel size of around 50–100 microns DMs tend to be very large images, ranging from 2300 × 1800 pixels (of dimension 100 microns) to 4096 × 5625 pixels (of dimension 54 micron)

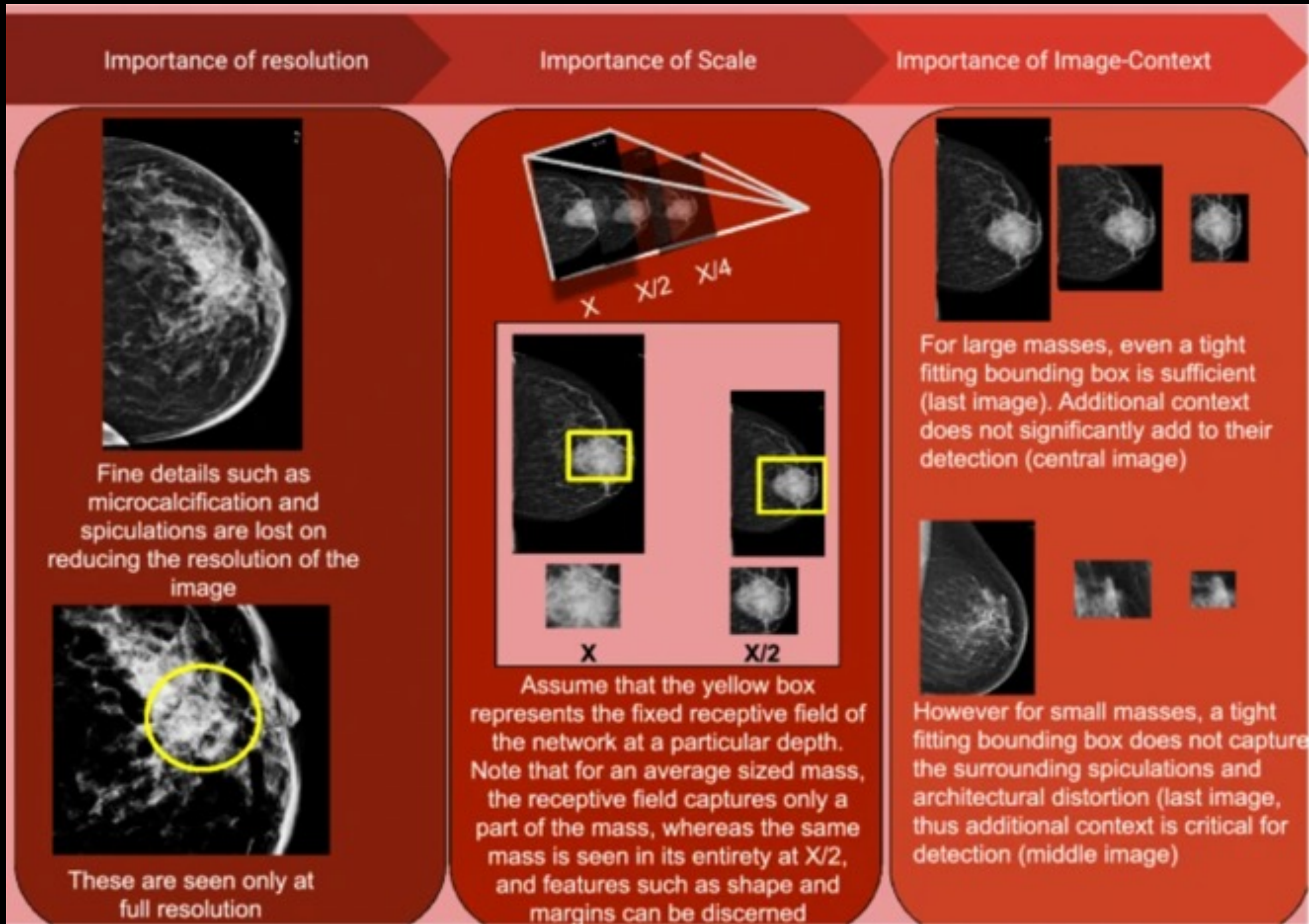

Cinzia Da Via, The University of Manchester, UK & SUNY USA– 2023

Digital radiography with MWPC in the 1970ies

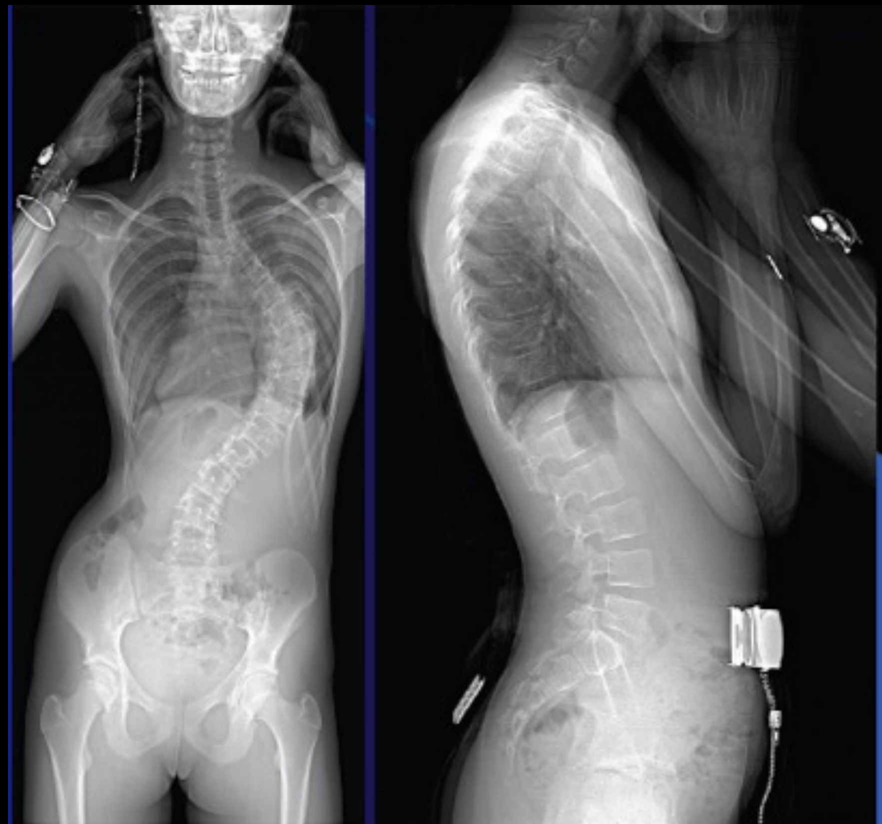

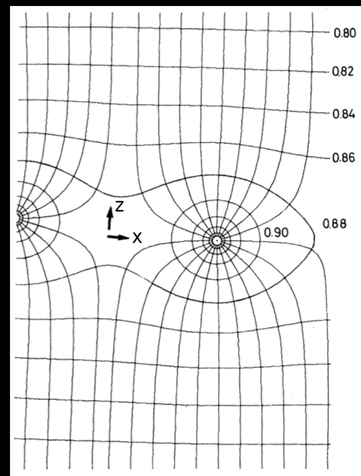

with 10 time less dose than traditional radiographic film!

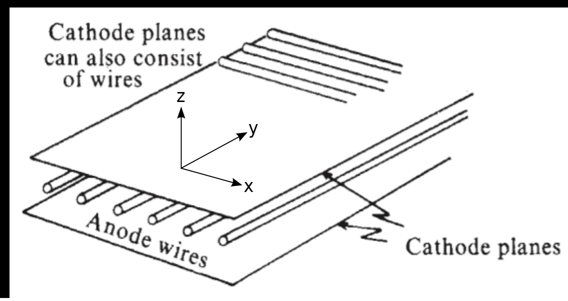

Cinzia Da Via, The University of Manchester, UK & SUNY USA– 2023

Computed Tomography

Spatial resolution and speed

- 64 … 320 detector rows
- Slice thickness 0.33 … 0.6 mm
- Tube rotation time 0.3 s
  - Organ in a sec
  - Whole body < 10 sec
- dual source (180° → 90°)
- Volume coverage with one rotation: 4 … 16 cm

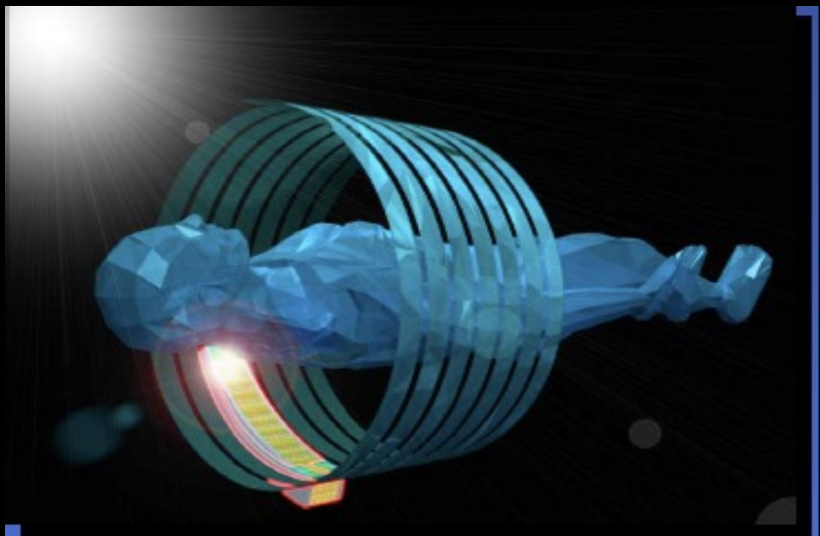

Cinzia Da Via, The University of Manchester, UK & SUNY USA– 2023

Computed Tomography Image reconstruction

- Take 1D profiles or 2D projection at discrete angle around the object
- Assume that each measured point = sum of actvity elements along the Line of Response (LOR)
- Rotate and repeat
- Still a lot of radiation full body CT = 4-10 mSv (depending organ)
- Standard radiography = 0.1 mSv

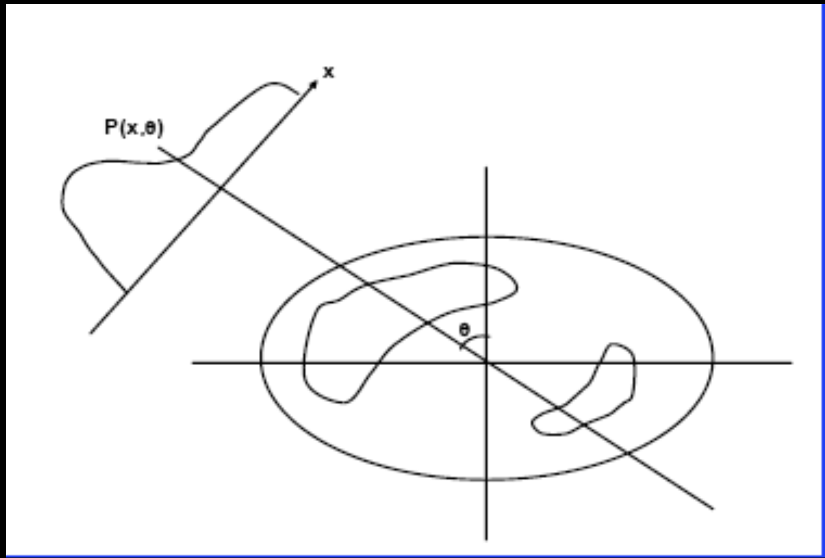

Raw data can be displayed 'sinograms'
Then data are riconctructed

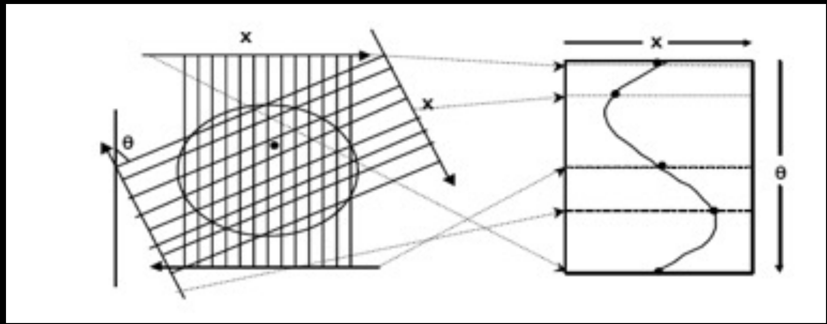

Nuclear Medicine: SPECT

Single Photon Emission Computed Tomography

Radiotracers are organ specific

Tracer	Physical half-life	Photon energy (Kev)	Application/Purpose
Tl-201	73 h	X : 10, 69-83 γ : 135, 167	Myocardial perfusion
Tc-99m sestamibi	6 h	X : 18-21 γ : 140	Myocardial perfusion, Tumor imaging
Tc-99m tetrofosmin	6 h	X : 18-21 γ : 140	Myocardial perfusion
I-123 MIBG	13.2 h	X : 4, 27-31 γ : 159	Myocardial sympathetic nerve imaging
I-123 BMIPP	13.2 h	X : 4, 27-31 γ : 159	Ischemic memory imaging

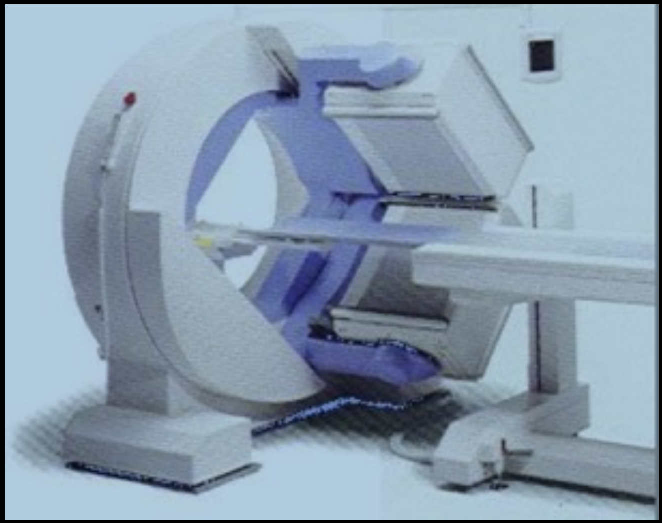

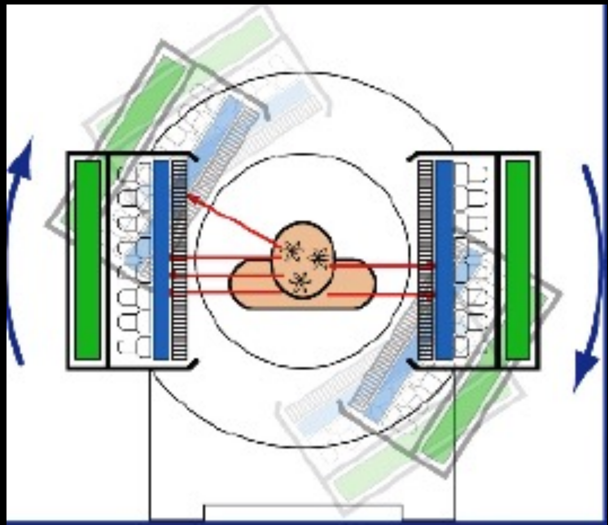

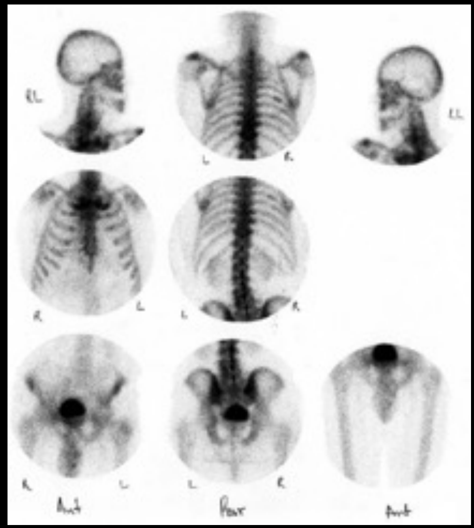

Cinzia Da Via, The University of Manchester, UK & SUNY USA– 2023

Positron Emission Tomography

$$A(t) = A(0)e^{-t(\ln 2/\tau)}$$

Radioactive decay : Afte time t, the activity left, A(t), is proportional to the initial number, A(0), and an exponential term involving the half-life, τ, of the nuclide. ^{18}F, which has a half-life of 109 minutes

Radioactive rates or activity are measured in units of Becquerel (1 Bq = 1 decay/second) in the SI system or the traditional Curie (1 Ci = 3.7·1010 decays/sec). A common scale factor used in the clinic is 1 mCi = 37 MBq.

In β+ (positron) decay a nuclide transforms one of its core protons (p) into a neutron (n) and emits a positron (β+) and a neutrino (ν): p → n + β+ + ν. The average positron range in matter depends on the positron's energy and material characteristics, such as the density and the atomic number. For ^{18}F-FDG, positron ranges are rather short, typically less than a millimeter.

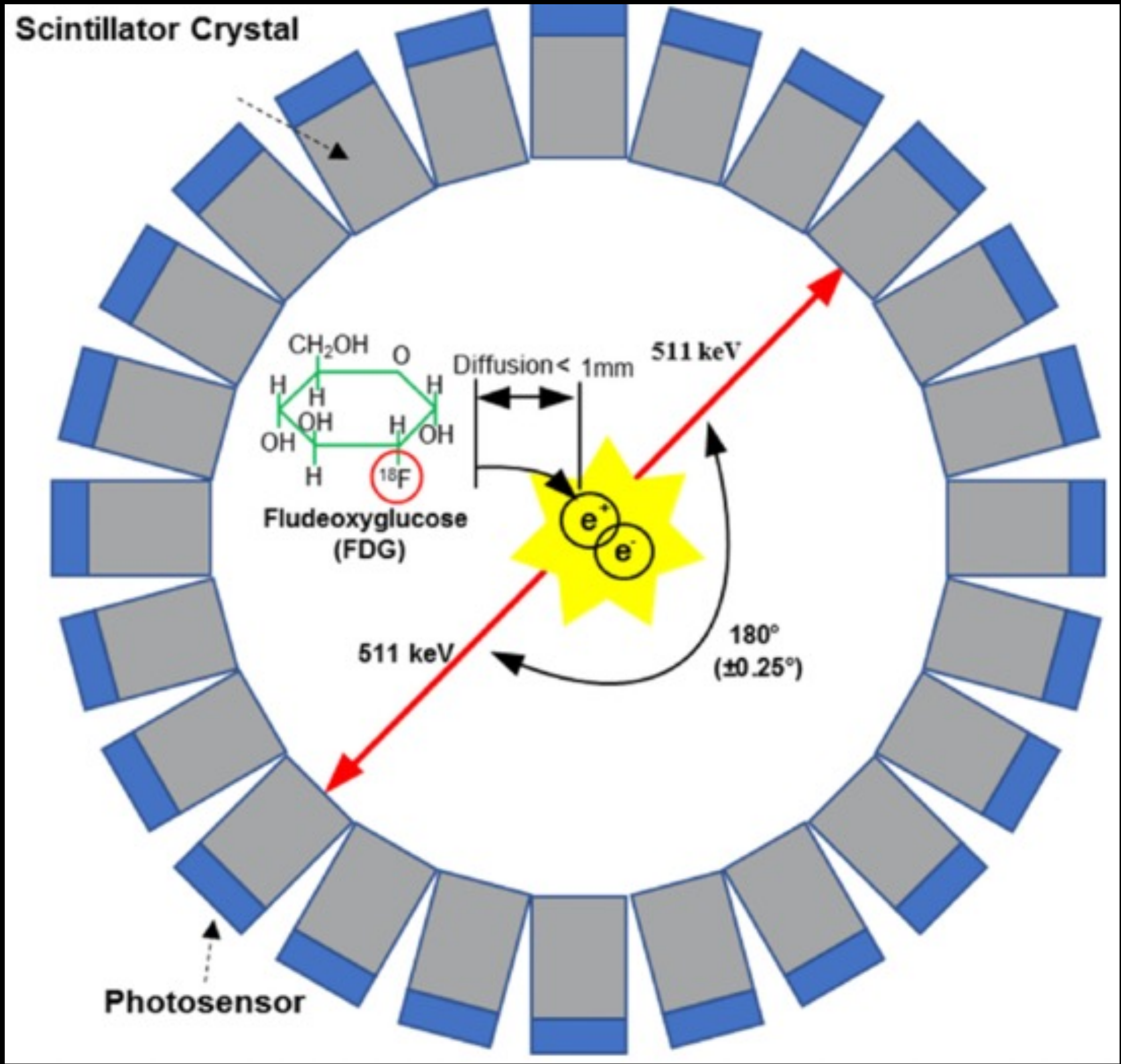

Cinzia Da Via, The University of Manchester, UK & SUNY USA– 2023

PET SCAN Sequence

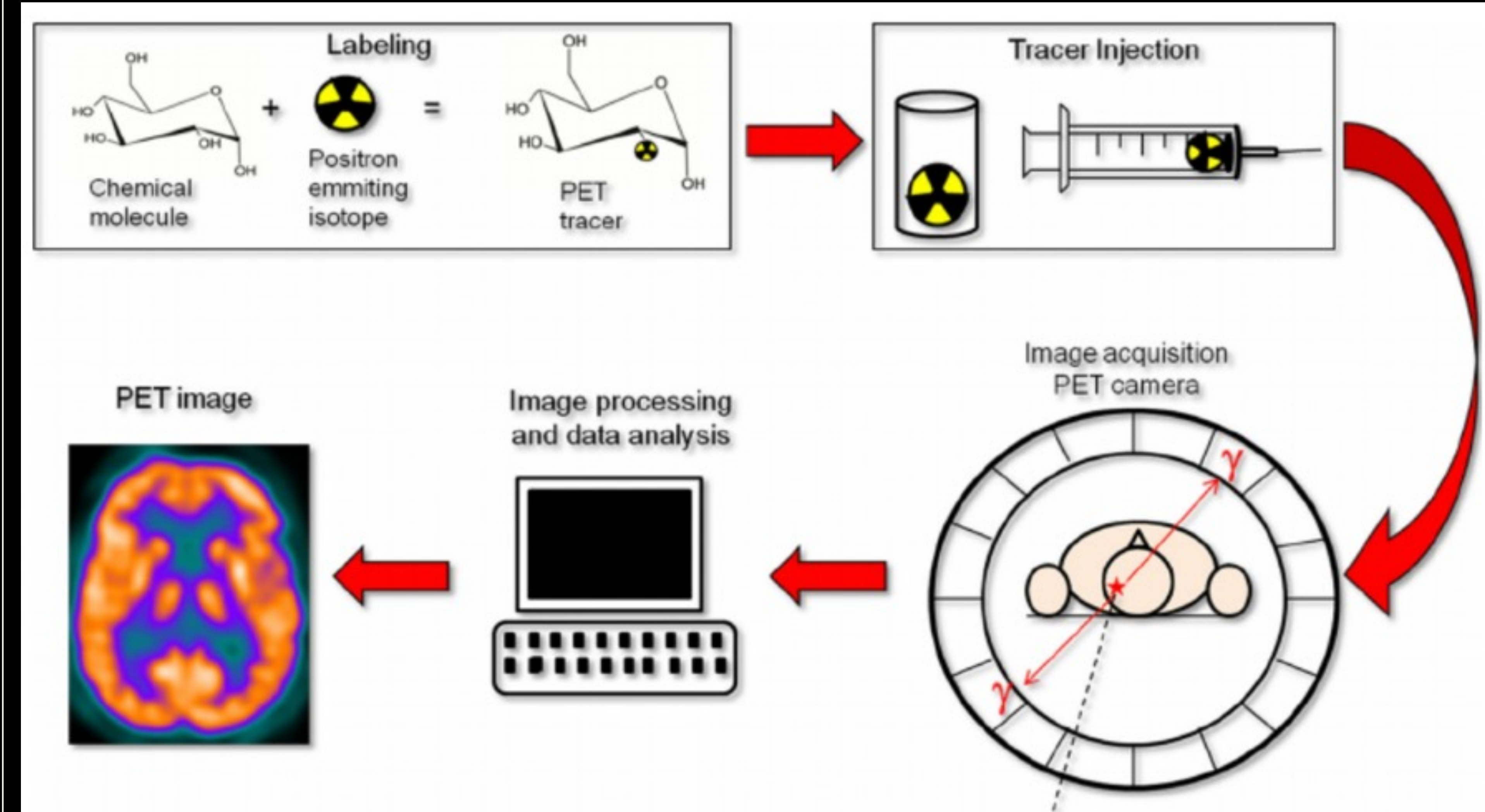

Historic Evolution of PET I

1977

First Steps
Townsend & Jeavons

First mouse imaging with ^{18}F

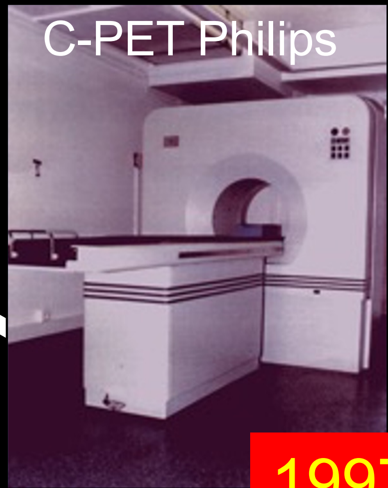

1997

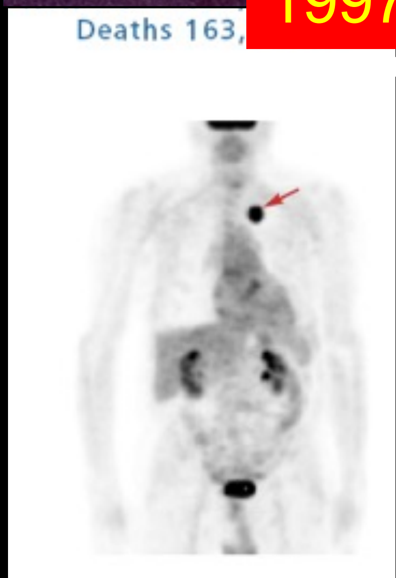

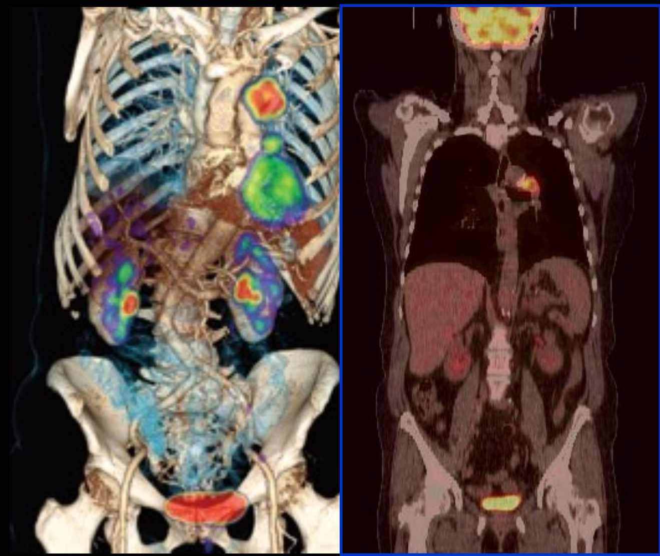

Biograph PET + X ray-CT

Cinzia Da Via, The University of Manchester, UK & SUNY USA– 2023

Historic Evolution of PET II

2017

TDM/PET-TOF (250 psec)

TOF= Time of Flight

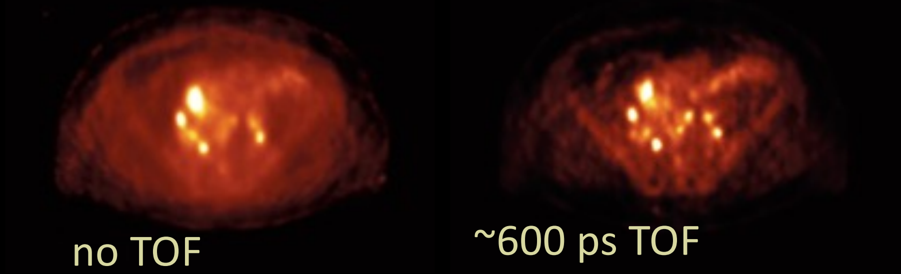

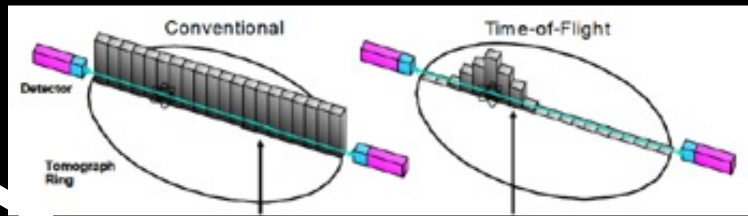

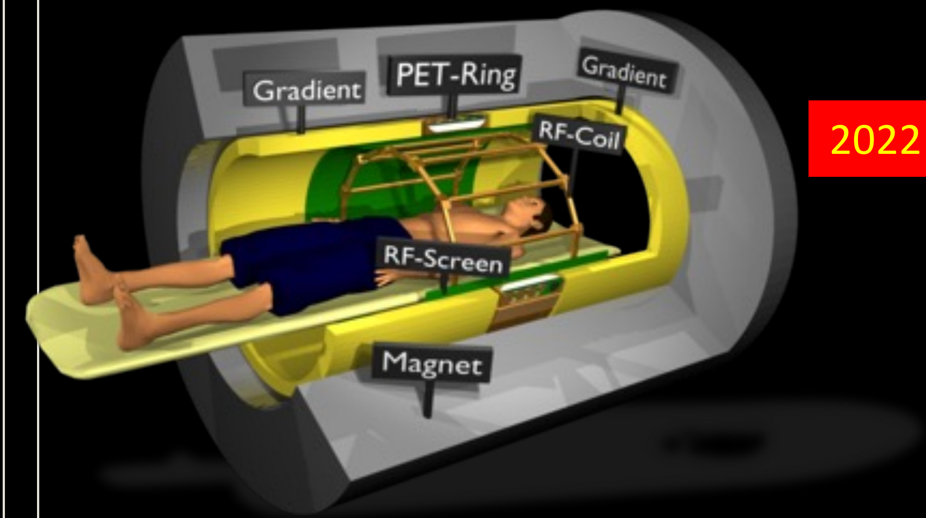

2022

Sucima PET-MRI EU project

~200-ps TOF PET Siemens Biograph Vision 600

Historic Evolution of PET III

2022

CRT = Laboratory 30ps
→ 10 to 1 psec 3 min scan
SNR, Direct imaging Multi-photon imaging, Positronium imaging
Scintillation, Cerenkov, Metascintillators, Photonics
AI vs TOF, COSTS

2027 ?

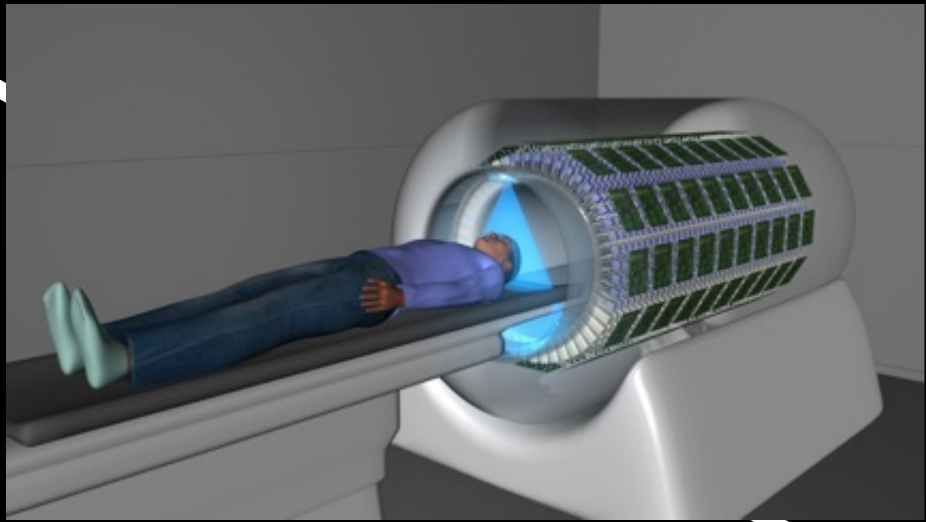

Iseult Project: 11.7T Whole-Body MRI

Explorer total body project

Cinzia Da Via, The University of Manchester, UK & SUNY USA– 2023

Cinzia Da Via, The University of Manchester, UK & SUNY USA– 2023

Total Body PET

Vandenberghe et al. EJNMMI Physics (2020) 7:35
https://doi.org/10.1186/s40658-020-00290-2

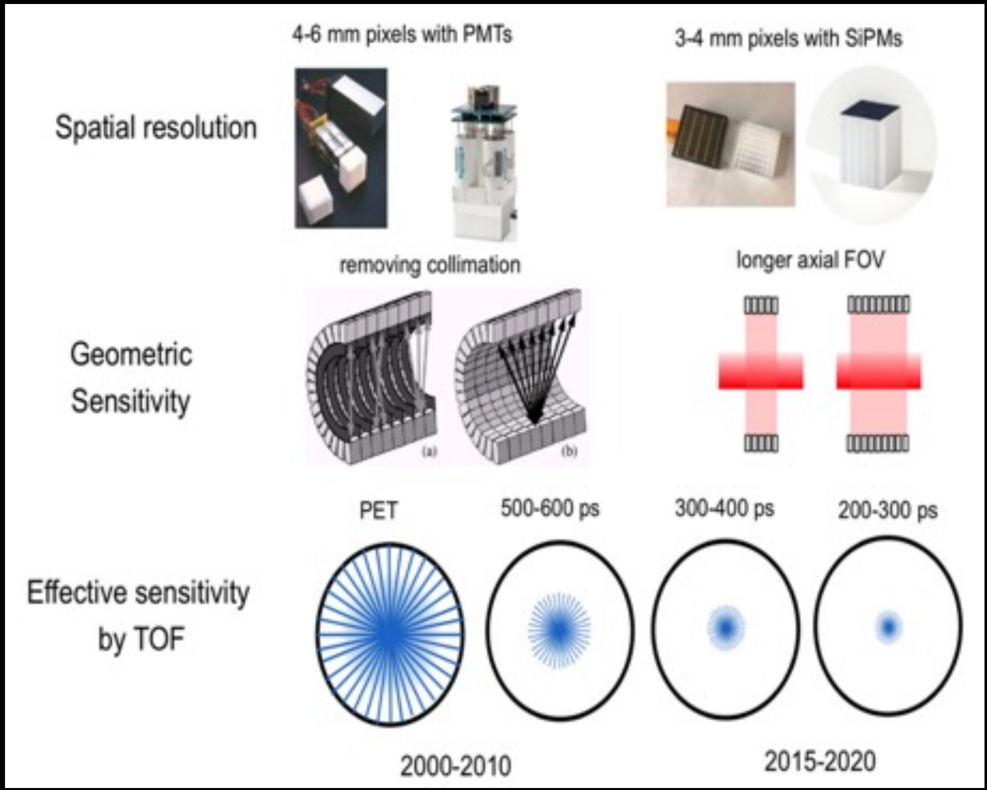

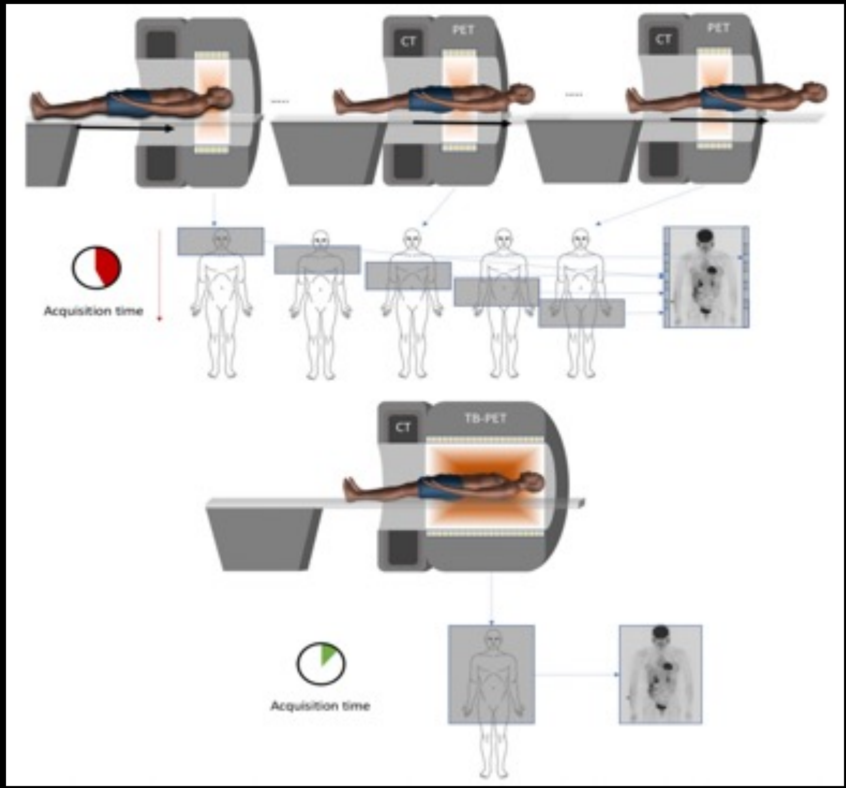

Key Advantages of this design:

1. The detection efficiency of photon pairs emitted from a certain point already in the FOV is increased by the larger solid angle (longer axial extent).
2. A much larger fraction of the patient is seen in one bed position, so more FOV is covered in the same time frame.

Total Body PET sensitivity

Vandenberghe et al. EJNMMI Physics (2020) 7:35
https://doi.org/10.1186/s40658-020-00290-2

$$S = \int_{z=0}^{z=AFOV/2} dz \left[\int_{\theta_{\min}(z)}^{\theta_{\max}(z)} (\epsilon_{\det}(\theta) \cdot Att(\theta))^2 \cdot \sin\theta d\theta \right] \cdot \epsilon_{sel}^2 / L_{patient}$$

The whole-body sensitivity S, defined as the ratio of the registration rate of image forming events (the true coincidences) to the total activity of 511 keV photon pairs created inside the patient, depends on the photons' attenuation in the body (Att), as well as detection (det) and selection (sel) efficiencies

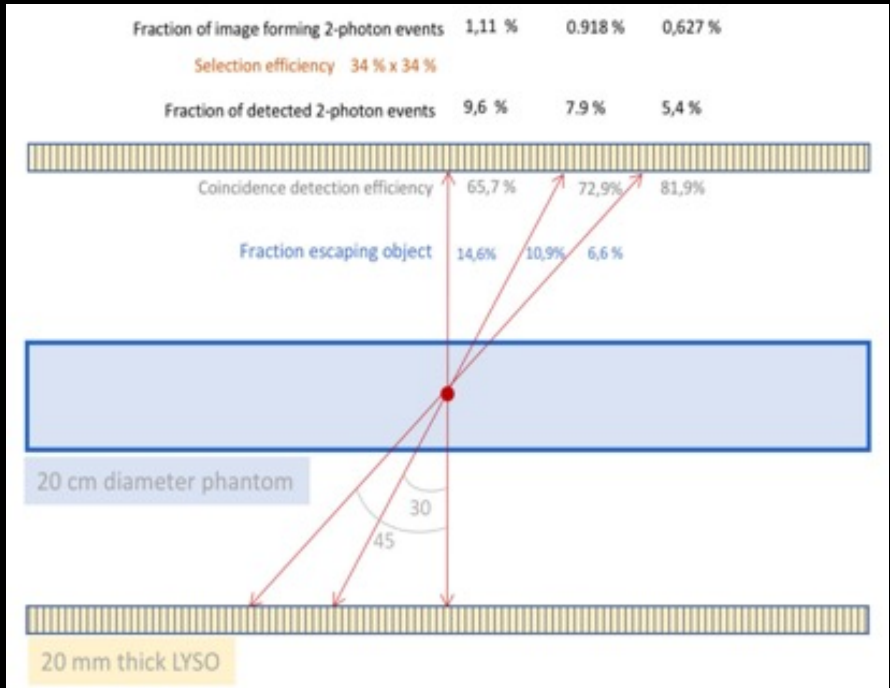

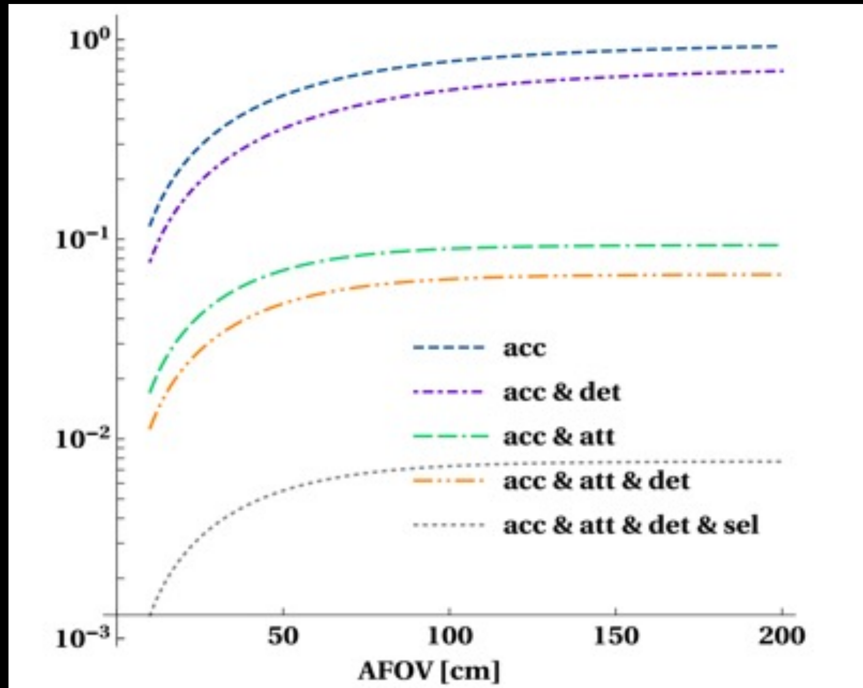

The fraction of detected two-photon events for a central point source taking into account the detector acceptance (Acc), detection with 20-mm-thick LYSO crystals (Acc & Det), attenuation caused by a 20-cm phantom (Acc & Att) as well as (Acc & Att & Det) and selection of event forming events (Acc & Att & Det & Sel). The y-axis displays fraction with maximum value equal to 1

3 Photons PET

2005 Phys. Med. Biol. 50 5679

the relatively rare (about 0.5% in water) three-photon positron annihilations (Ore and Powell 1949, De Benedetti and Siegel 1954) can also be used for imaging.

By detecting the positions and energies of the three photons, one can easily locate the point where the annihilation occurred. Thus the amount of information obtained from a single event is higher than for a 2γ pair, where localization is along a line.

The rate of 3γ decay is not only proportional to concentration of activity but is also sensitive to the local physical and chemical environments, notably the presence of oxygen.

This is due to formation of positronium: a positron–electron bound state, which behaves as an active chemical particle. **75% of the positronium is formed as an ortho-positronium, triplet state which in vacuum annihilates only into 3γ with a relatively long lifetime of 142 ns,**

while the remaining 25% form a para-positronium rapidly decaying into 2γ (half-life 0.125 ns).

In matter interaction processes, in general called quenching, that lead to 2γ annihilations are usually much faster, reducing the fraction of three-photon annihilations.

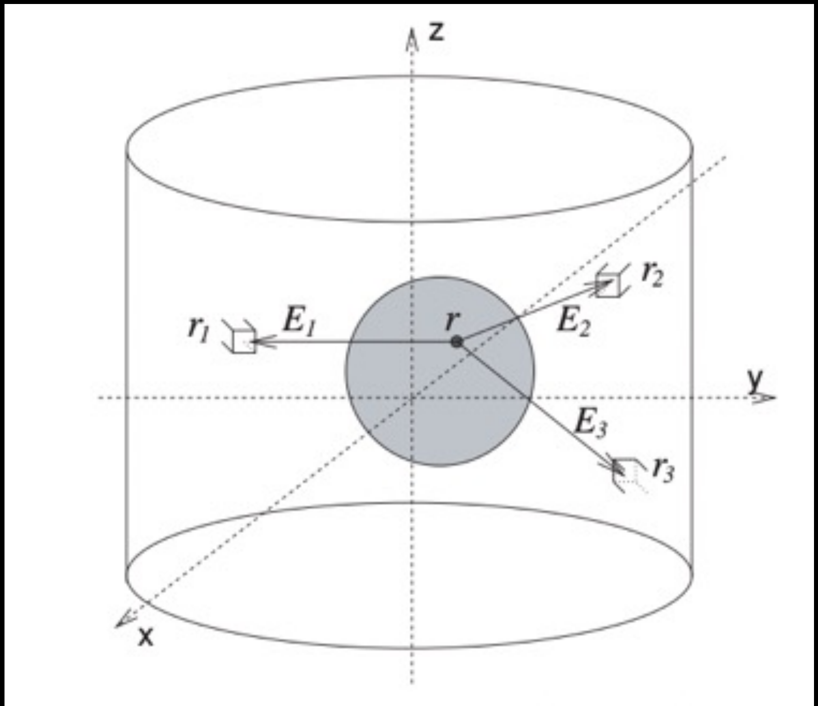

$$E_1 + E_2 + E_3 = m_e c^2 \approx 1022\ \text{keV}$$

3γ imaging is by no means an alternative to conventional PET, but rather an add-on, making use of the annihilation radiation which is currently wasted, it provides extra information. Dividing the 3γ image by the 2γ one, we obtain a map of 3γ /2γ decay probability ratio.

FBP Cost Reduction I

Vandenberghe et al. EJNMMI Physics (2020) 7:35
https://doi.org/10.1186/s40658-020-00290-2

Scintillator	Light output (photons/Mev)	Decay time (ns)	Density (g/cm^3)	Light attenuation length (cm)
LYSO	32000	41	7.1	20.9
BGO	8500	300	7.13	22.8
GSO	7600	30-60	6.71	22.2
$LaBr_3$	65000	15	5.29	16.0
BC-408 (plastic)	11000	2.1	1.023	380

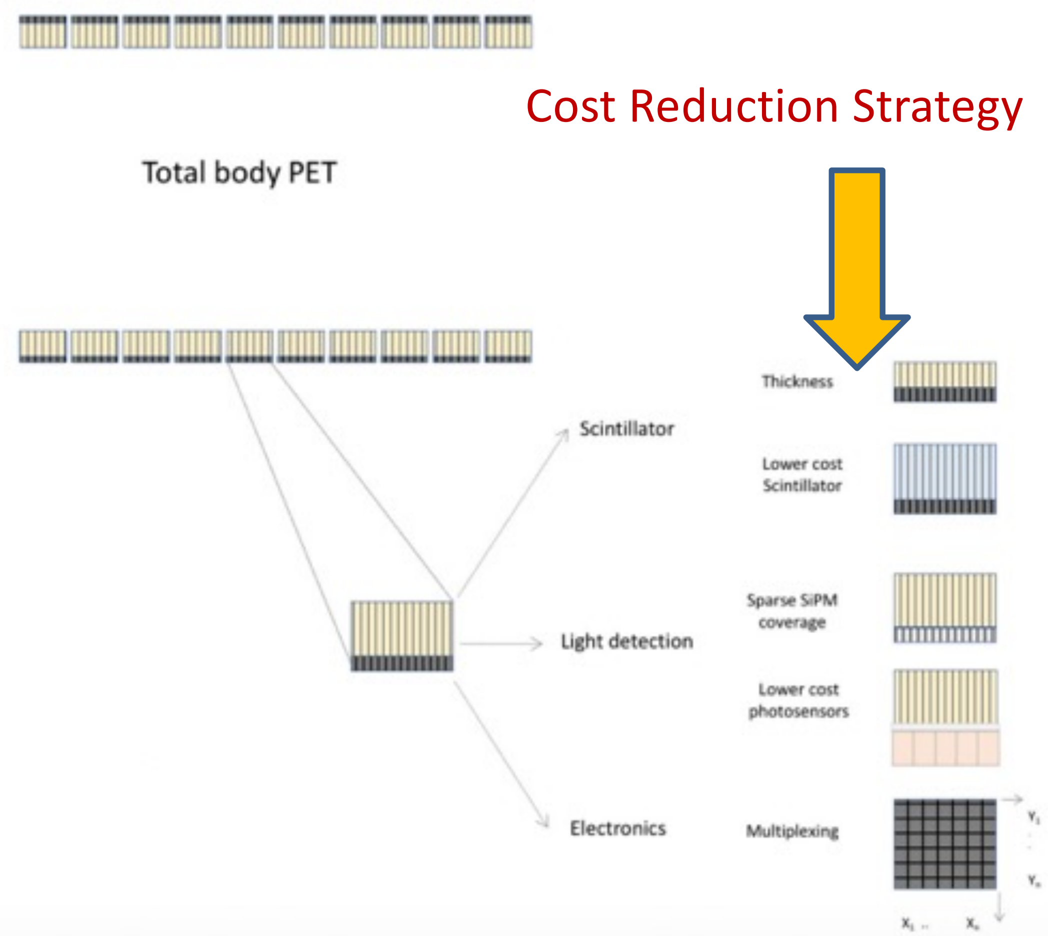

Materials also R&D with Large volume Gas and MCPs

But Also:

Reduction in Dose
→ ~10 times - 0.37 MBq/kg

Reduction in Scan Time
→ ~24 times – 5min total scan

Dynamical and multi-organ images

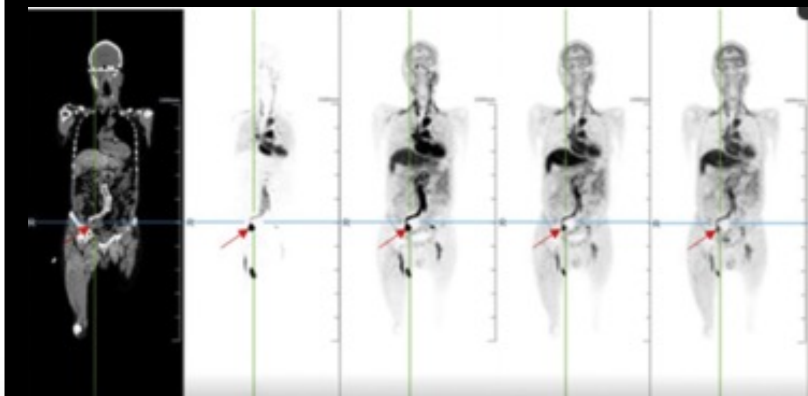

FBP Cost Reduction II

Cinzia Da Via, The University of Manchester, UK & SUNY USA– 2023

Same performance and FOV with a smaller detection area:

Geometrical and Organ Specific Systems

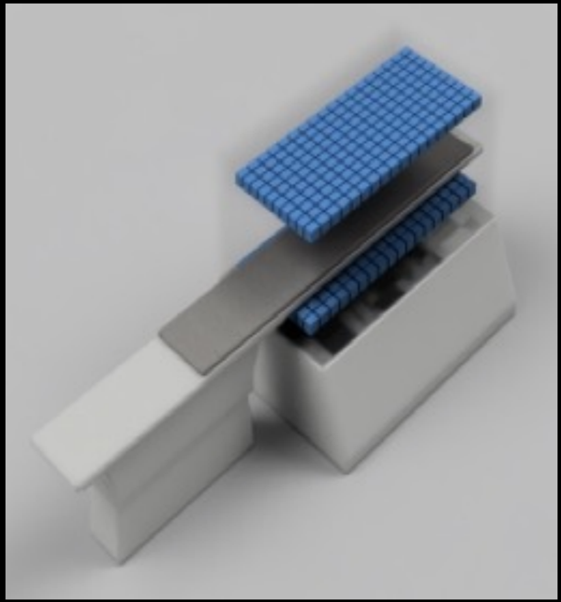

Total-Body System

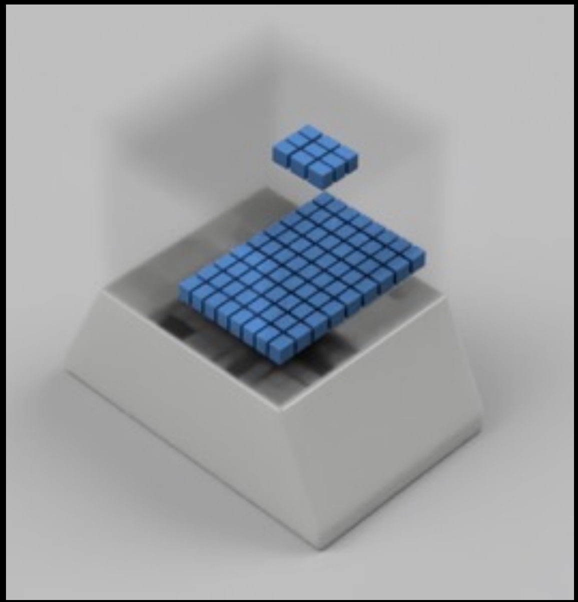

Brain Imaging System

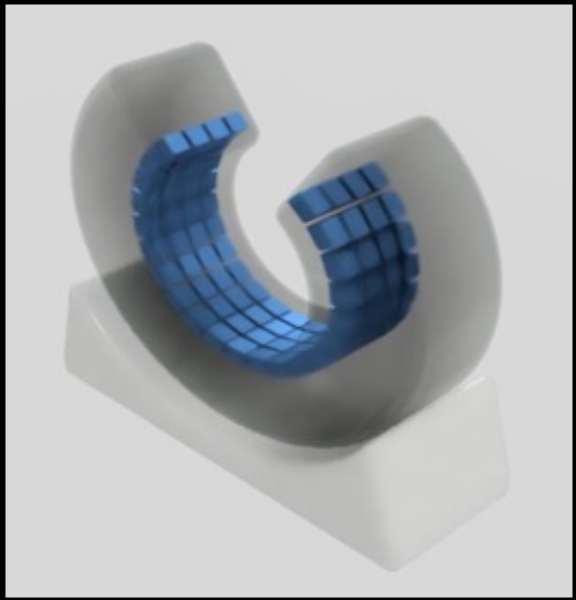

Cardiac or Breast Imaging System

Quantum Physics in Bio-Medical Imaging

•https://doi.org/10.1364/QIM.2014.QTu1A.1


nature > nature communications > articles > article

Article | Open Access | Published: 11 May 2021

Photon quantum entanglement in the MeV regime and its application in PET imaging

D. P. Watts, J. Bordes, J. R. Brown, A. Cherlin, R. Newton, J. Allison, M. Bashkanov, N. Efthimiou & N. A. Zachariou

Nature Communications 12, Article number: 2646 (2021) | Cite this article

7227 Accesses | 11 Citations | 16 Altmetric | Metrics

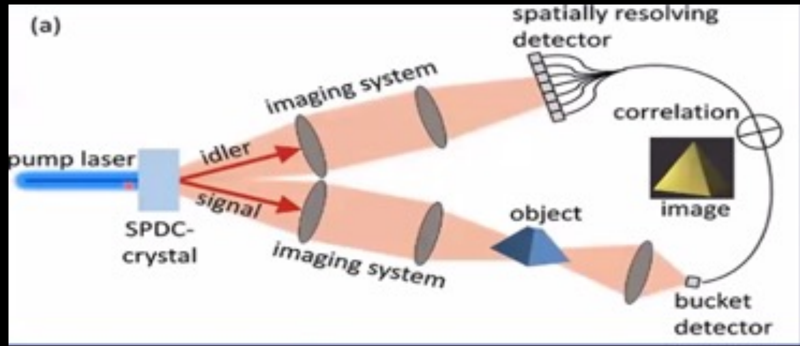

Suppression of BG due to Scattered events using photon entanglement correlations

Spontaneous Parametric Down Conversion SPDC Space and Intensity Correlations mediated by conservation of energy and momentum

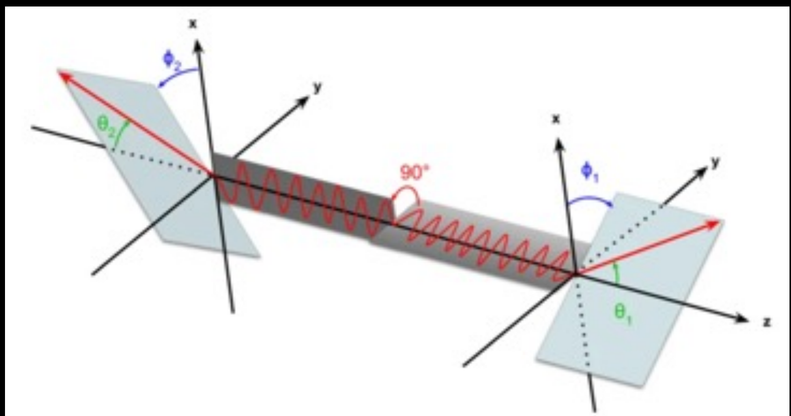

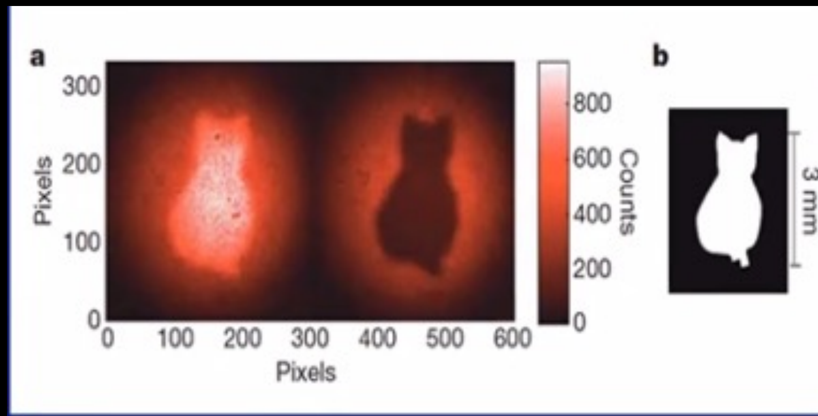

VISIBLE Infra RED – also works for X-Rays

PET Industrial Synergy

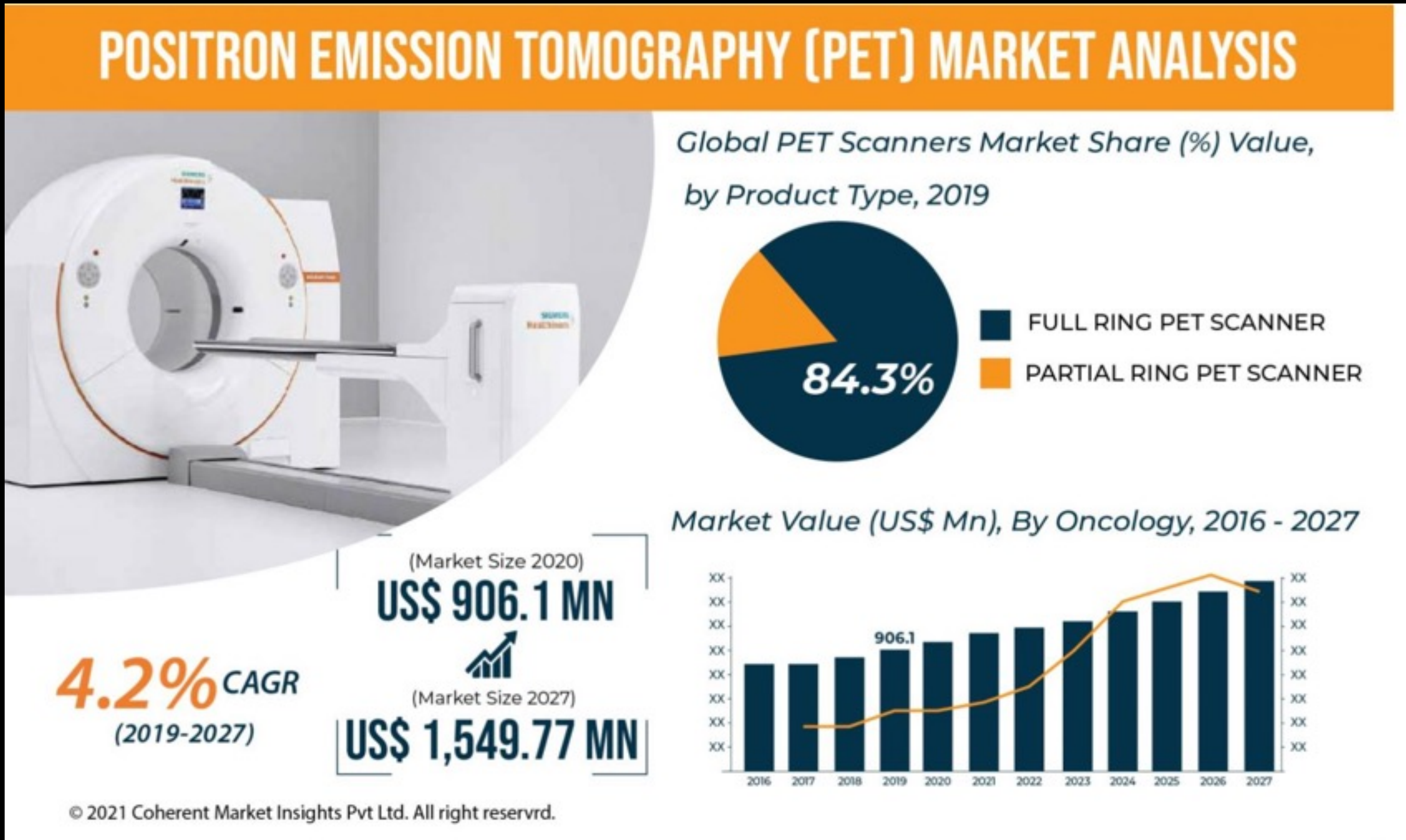

CASE STUDY: PERSONALESED CANCER THERAPHY

MANCHESTER 1824
The University of Manchester

Particle Dosimetry for Cancer Therapy using 3D printing and Geant4 simulation

Cinzia Da Vià, Francisca Munoz-Sanchez
Rebecca Heelis, Samuel Clarke, Jemma Goldstein, Mahfuza Ahmed
Rebecca Freestone, Stuart Morris, Jacob Heery, Paul Walmsley
The University of Manchester, UK

John Allison, Geant4 International

Adam Aitkenhead; Ranald MacKay, Christie's Hospital, Manchester UK

3D Cube

MANCHESTER
1824
The University of Manchester

Rationale

Personalized Treatment planning

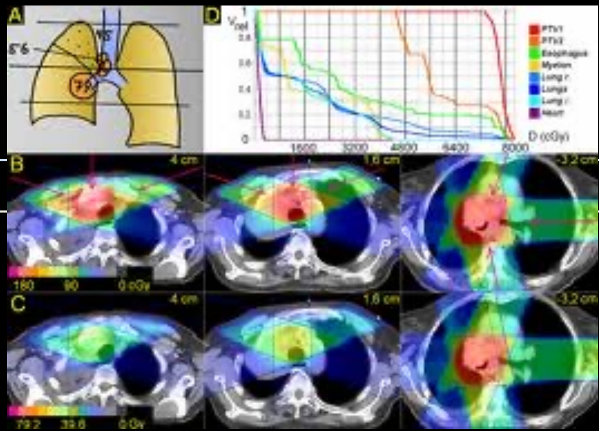

CT SCAN of the Patient

Digitized CT image
Transferred to G4

Experimental Data confronted to G4 into planning

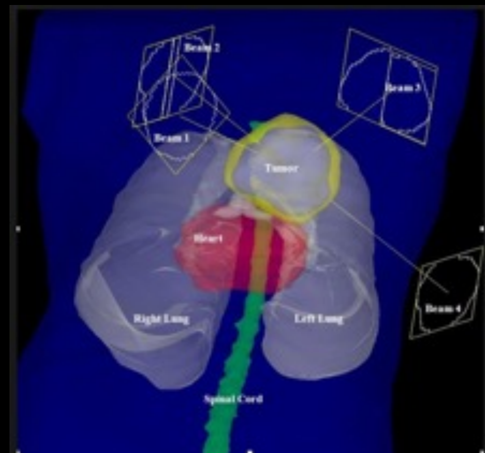

G4 simulation

Digitized CT image
Transferred to 3D printer

3D printed phantom

Cinzia Da Vià, April 2016

Cinzia Da Via, The University of Manchester, UK & SUNY USA– 2023

Cinzia Da Via, The University of Manchester, UK & SUNY USA– 2023

1-From CT image to 3D printing

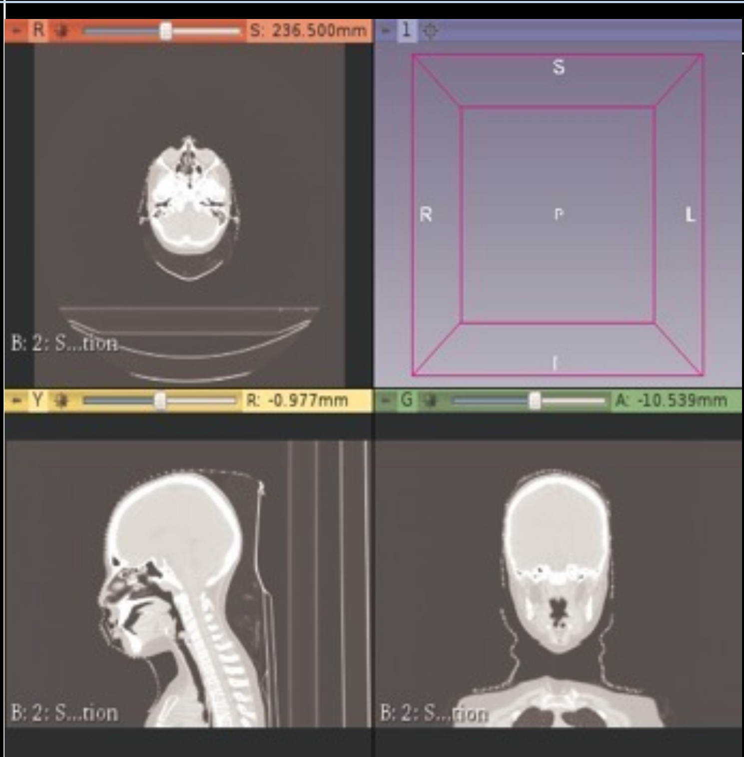

Converted DICOM files into NRRD files which could then be converted to STL files using a open source program called embodi3D.

Visualization of the DICOM file
Using the program 3D SLICER

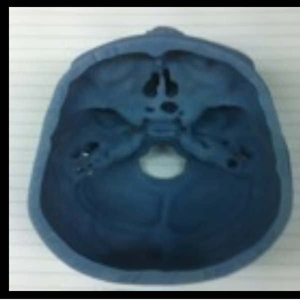

3D printed skull from
The original CT scan

From CT image to G4 simulation

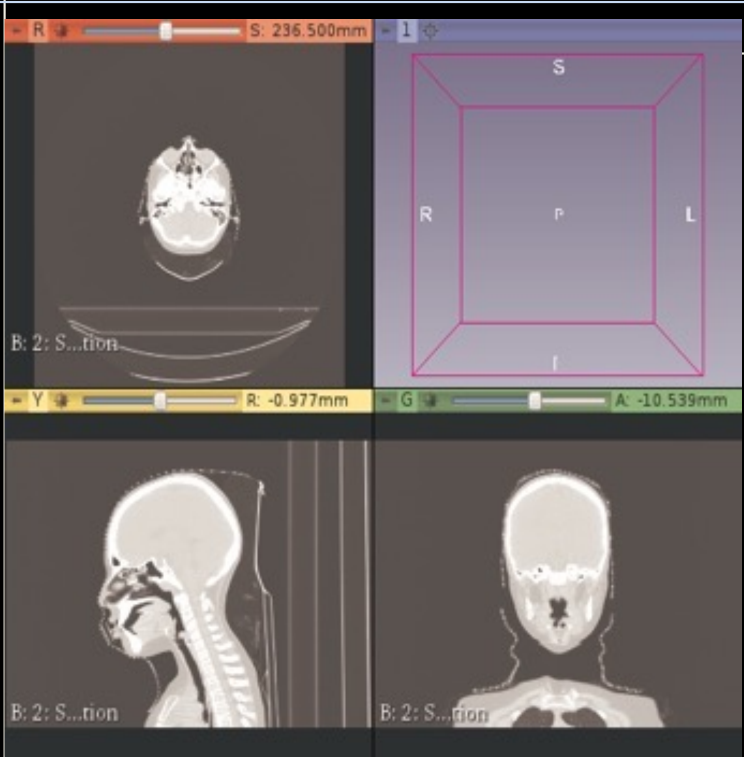

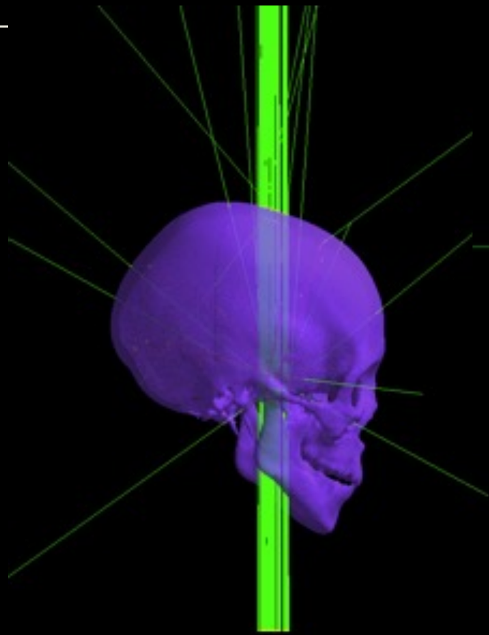

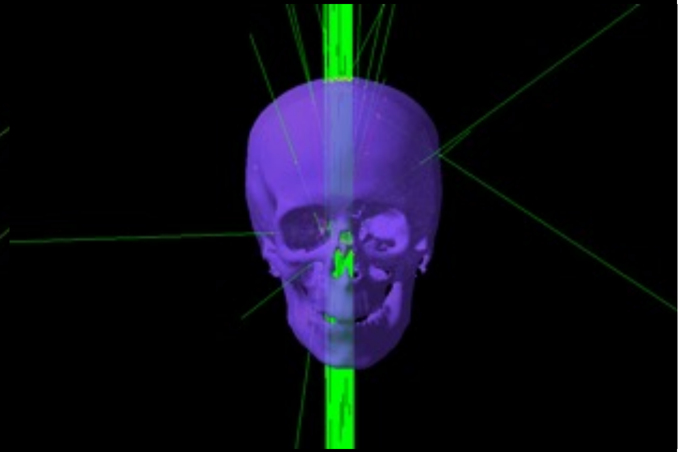

Visualization of the DICOM file
Using the program 3D SLICER

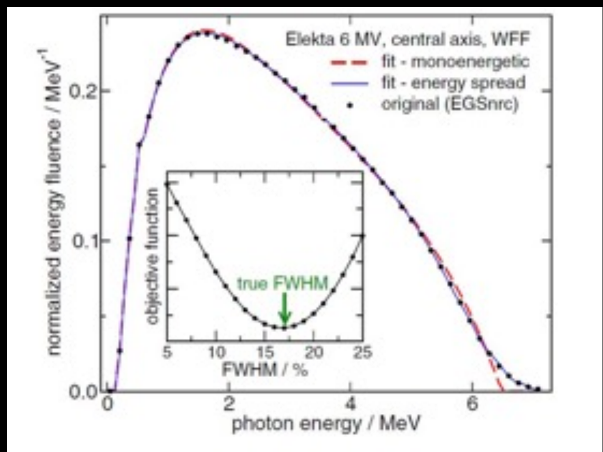

STL file imported into Geant4 using CADMesh. The skull was edited in the visualiser to have a slight translucency in order for the interacting X-ray photon beam to be seen more clearly.

The beam has a cross section of $2x2cm^2$ with an energy spectrum of the Elekta 6MeV system.

Cinzia Da Via, The University of Manchester, UK & SUNY USA– 2023

Synergy with Human Capital

- Inclusion
- Diversity
- Sociology
- Diplomacy in action

→ No political or religious barriers

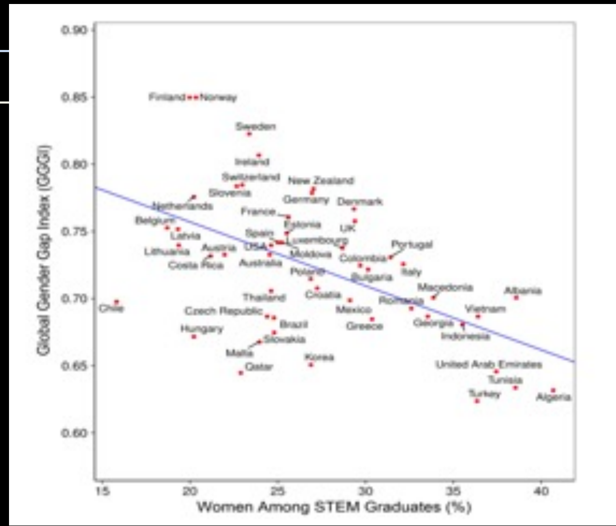

Women in STEM "Paradox"
The percentage of women with STEM degrees is lower in more gender-equal countries, as measured by the WEF [Gender Gap Index. Image from Stoet & Geary, 2018.]

Governance and management of large international Collaborations and Complex Structures

Knowledge transfer peer-to-peer industry

- Education (outreach)
- Networking
- Mentoring

→ The key role of Schools

- Analysis & Problem-Solving.
- Interpersonal & Leadership Skills.
- Project Management & Organization.
- Research & Information Management.
- Self-Management & Work Habits.
- Written & Oral Communication.

The Last Words

The Interface and synergies among scientific fields has always existed but today is even more evident since the overlap of the requirements among the various fields is more pronounced.

HEP and Bio-Medicine have always gone hand in hand

For instrumentation developers:

Always look beyond what you are doing!

Never stop being creative, in particular if someone tells you that what you imagined is not a good idea and is impossible!!!!

Thanks

I used material from several people and publications which are hopefully listed in the slides.

An extra special thanks goes to:

Patrick Le Du
Maurizio Vretener
RD51 Collaboration
Medipix Collaboration
3D Collaboration
Timespot Collaboration

For providing material directly or online, or for very useful discussions and insight